Majani, Ruby (2009) Gut construction: scaffolds for intestinal tissue engineering. PhD thesis, University of Nottingham.

Access from the University of Nottingham repository:
http://eprints.nottingham.ac.uk/29319/1/508228.pdf

GUT CONSTRUCTION:

SCAFFOLDS FOR INTESTINAL

TISSUE ENGINEERING

Ruby Majani, BSc

Thesis Submitted to the University of Nottingham for the

Degree of Doctor of Philosophy

July 2009

ABSTRACT

Forming tissues in the laboratory to replace diseased or dysfunctional tissue or act as models for drug treatment is the goal of tissue engineering. The large intestine epithelium (colon surface) is a tissue which could benefit from both diseased and non-diseased models for the purpose of tackling colon cancer causes and treatments. Scaffolds (cell supports) are a pivotal part in many tissue engineering strategies. This thesis describes the design and production of two separate scaffolds based on the degradable polymer poly(lactic-co-glycolic acid) (PLGA).

The first was a two dimensional scaffold to mimic the intestinal basement membrane which was modified with an oxygen plasma. The changes to the surface due to plasma and the degradation properties of the scaffold were extensively studied with SEM, XPS, AFM and GPC. The data showed that the oxygen plasma induced surface porosity and associated changes to surface roughness. The surface chemistry as detected by XPS was unchanged by both plasma treatment and degradation in buffered solution. The plasma treatment did lead to a dramatic loss in molecular weight but the degradation profile of both the untreated and etched films was similar. Extensive cell studies with SEM, live/dead, alamarBlue and Hoechst DNA assays showed that intestinal cells on the plasma treated scaffold was enhanced in terms of morphology, metabolic activity and proliferation. Finally, a two dimensional co-culture model using epithelial and myofibroblasts cell lines on the modified PLGA scaffold was achieved.

The second scaffold was a three dimensional scaffold bearing the crypt like architecture of the colon. An accurate mould produced through electron beam lithography using dimensions measured from mouse histological sections. PLGA particles were used to fill the mould and sintered to produce the scaffold. A unique cell seeding approach using cell sheets was used. The cell sheets were produced on plasma polymers of acrylic acid and the discharge power was shown to affect surface wettability, chemistry and cell viability. The cell sheet approach proved to enhance cell attachment to the scaffold compared to individual cell seeding. Finally, a bilayer scaffold with model protein to mimic Wnt protein presence in the lower half of the crypt was studied with ToF-SIMS.

"Imagination is more important than knowledge."

Albert Einstein

"Intelligent people pursue wisdom. Wisdom is the acknowledgement of the

intelligence of others."

Ruby 'I will not quote Einstein' Majani

ACKNOWLEDGEMENTS

To regurgitate the well known saying, this is probably the most read page in the entire thesis and so akin to a peacock, I will display my colourful personality in full splendour. I would still encourage you to read the rest of it as it is very interesting!!

I would like to start by thanking God, I am grateful for my life and I do not doubt your remarkable influence in it. My parents, Cyrilla and Ephraim, you let me be a star and twinkle with an unbridled sparkle. I love you both very much. To my sisters Yvonne and Lorraine, I will always love you both. A very special thanks to Yvonne, without you, we wouldn't have made it this far and the world would be a much less funnier place ('Can't touch this!'). It is cliché but true, you are a phenomenal woman and your legacy is inevitable and indelible.

Then, to the two special people I met at university, I would like to say thanks to Mischa and Chayanin. Without doubt, you are two of the most hardworking and intelligent people alive. More valuable, in my view, are the lessons I learned not from your brains but from your hearts. Mischa (hubby!), the magic touch of diplomacy that exudes naturally from you is something that I hold in awe. I am glad that I will continue to live and learn more every day with you. Chayanin, your nature of giving without expecting to receive is one that I aspire to. You are my chosen family, a link that will never be severed.

I would like to thank my supervisors Felicity Rose and Morgan Alexander. It goes without saying (but I will say it!) that I am grateful for your input, from selecting me to tackle this project and guidance through out it. Precision and accuracy - now that is a lesson!

PRESENTATIONS

MAJANI, R., ROSE, F., & ALEXANDER, M. R. (2007) Scaffolds not just for

buildings. Poster Presentation, UKGrad Regional Poster Competition, Warwick.

MAJANI, R., GADEGAARD, N., ROSE, F., & ALEXANDER, M. R. (2008) A micron

scale three dimensional scaffold for colon epithelial intestinal tissue engineering .

Oral and Poster Presentation, Society for Biomaterials Annual Conference, Atlanta.

MAJANI, R., ROSE, F., & ALEXANDER, M. R. (2008) Improving the porosity of poly

(D,L-lactic-co-glycolic acid) (PLGA) membranes through plasma etching. Poster

Presentation, Tissue Cell and Engineering Society Annual Meeting, Nottingham.

PUBLICATIONS

ZELZER, M., MAJANI, R., BRADLEY, J. W., ROSE, F., DAVIES, M. C. &
ALEXANDER, M. R. (2008) Investigation of cell-surface interactions using chemical
gradients formed from plasma polymers. *Biomaterials,* 29, 172-184.

CONTENTS

CONTENTS

CONTENTS

CONTENTS

CONTENTS

ABBREVIATIONS

Poly(lactic-co-glycolic acid)	PLGA
Total Parenteral Nutrition	TPN
Short Bowel Syndrome	SBS
Gastrointestinal	GI
Intestinal Epithelial Cell	IEC
Poly(lactic acid)	PLA
Poly(glycolic acid)	PGA
Poly(tetra fluoro ethene)	PTFE
Poly(ethyleneterephthalate)	PET
Extracellular matrix	ECM
Arginine Glycine Aspartic acid	RGD
Focal Adhesion Kinase	FAK
Forkhead Transcription Factor	FKHRL1
Untreated Poly(lactic-co-glycolic acid)	uPLGA
Etched Poly(lactic-co-glycolic acid)	ePLGA
High Performance Liquid Chromatography	HPLC
Plasma polymerised acrylic acid	ppAAc
X-ray photoelectron Spectroscopy	XPS
Kinetic Energy	KE
Binding Energy	BE
Water Contact Angle	WCA
Liquid Gas	LG
Solid Liquid	SL
Scanning Electron Microscopy	SEM
Gel Permeation Chromatography	GPC
Dulbecco's modified eagle medium	DMEM
Foetal Calf Serum	FCS
Ethylenediaminetetraacetic acid	EDTA
Hanks Buffered Salt Solution	HBSS
Analysis of Variance	ANOVA
Phosphate Buffered Solution	PBS
Tetrahydrofuran	THF
Two Dimensional	2D
Three Dimensional	3D

ABBREVIATIONS

Poly(ethyleneglycol)	PEG
Poly(caprolactone)	PCL
Transepithelial electrical resistance	TEER
Ultra Violet light	UV
4',6-diamidino-2-phenylindole	DAPI
Deoxyribonucleic acid	DNA
Time of flight secondary ion mass spectrometry	ToF-SIMS
Poly(olefin) plastomer	POP
Horse radish peroxidase	HRP
Poly(lactic-co-glycolic acid) particles with Horse radish peroxidase	PLGA-HRP

LIST OF FIGURES

LIST OF FIGURES

LIST OF TABLES

CHAPTER 1: AN INTRODUCTION TO INTESTINAL TISSUE ENGINEERING

1.1 INTRODUCTION TO TISSUE ENGINEERING

Langer and Vacanti perhaps provided the most quintessential definition of tissue engineering, describing it as, 'an interdisciplinary field that applies the principles of engineering and life sciences toward the development of biological substitutes that restore, maintain, or improve tissue function or a whole organ.' (Langer and Vacanti, 1993). Tissue engineering as a field has been successful in producing tissues such as bone, bladder and trachea (Atala *et al.*, 2006, Laurencin *et al.*, 1999, Macchiarini *et al.*, 2008). The underlying principle of this work has been the use of a suitable cell support (scaffold) to culture cells. Such success has driven research into engineering of more complex tissues comprised of different cell types which may be organised in niches (microenvironments) such as the intestinal epithelium.

1.2 INTESTINAL TISSUE ENGINEERING: ROLE IN MEDICINE

Most of the early work in intestinal tissue engineering focused on producing autologous tissue for the treatment of a debilitating condition known as SBS. This is a clinical condition largely associated with patients who have had large parts of the small intestine excised. Patients can suffer from severe malnutrition due to inability of the remaining intestine to absorb sufficient nutrients (Holterman *et al.*, 2003, Choi *et al.*, 1998).

Surgically, one of the options for treatment is lengthening of the intestine through bifurcation (splitting) of the remaining length. However, this procedure carries the possibility of ischaemia as the blood supply may prove to be insufficient (Benedetti *et al.*, 2003). Total parenteral nutrition (TPN – intravenous feeding) is usually recommended if intestine adaptation or surgical intervention do not correct SBS.

Patients with complications of TPN can undergo transplantation with donor tissue but concerns over tissue rejection and possible surgical complications with living donors make this procedure regarded as a trial. Transplantation lengthening has led to a 5 year survival rate of 70% in some surgical centres (Nishida *et al.*, 2002, Reyes *et al.*, 1998).

Tissue engineering was therefore proposed as a suitable alternative with the aim of creating and replacing the small intestine with autologous tissue developed for the patient (see section 1.8). This would circumvent the serious concerns raised by the bifurcation and/or transplantation approaches.

On the basis of this research on the small intestine, interest is now turning to the colon and the treatment of colorectal cancer. This is a condition that could potentially benefit from both non-diseased and diseased tissue models. Colorectal cancer is the second most common cause of cancer death in the UK (Kumar and Clark, 2002). Treatment traditionally involves resecting (removal of) part of the colon to ensure complete removal of the cancer. Although post-operative complications are rare, fewer than half of those who undergo operations survive more than 5 years (Kumar and Clark, 2002). This largely depends on the metastasis (spread) of the cancer and the extent of excision. Complete removal of the cancer is the primary objective of surgery and hypothetically, if larger sections of the large bowel could be taken out without comprising patient health, it may be possible to effectively increase this survival rate. Autologous *in vitro* tissue engineered intestine would perhaps offer a solution for those most severely affected allowing replacement of lost tissue.

However, it must be noted that specialists in the treatment of colorectal cancer are currently encouraging the prevention of the cancer by genetic counselling, early

diagnosis and treatment. A platform for this approach would be the production of diseased tissue models. Colorectal cancer occurs due to dysregulation of the mechanisms that limit the number of cells in the colon (see section 1.6). These models would be useful for simulating critical timepoints when carcinomas occur, hence aid early detection and would also serve as test models for potential cancer drugs. The next section explains in greater depth the structure and function of the colon as the tissue target. As mentioned earlier, the intestine is a complex tissue and successful engineering is very dependant on the integral grasp of the different cell types, niches and their function.

1.3 STRUCTURE OF THE INTESTINE

The gastrointestinal (GI) tract from the oesophagus to the anus (figure 1.1) is essentially a hollow tube with regional histological and functional differences (Kerr, 1999).
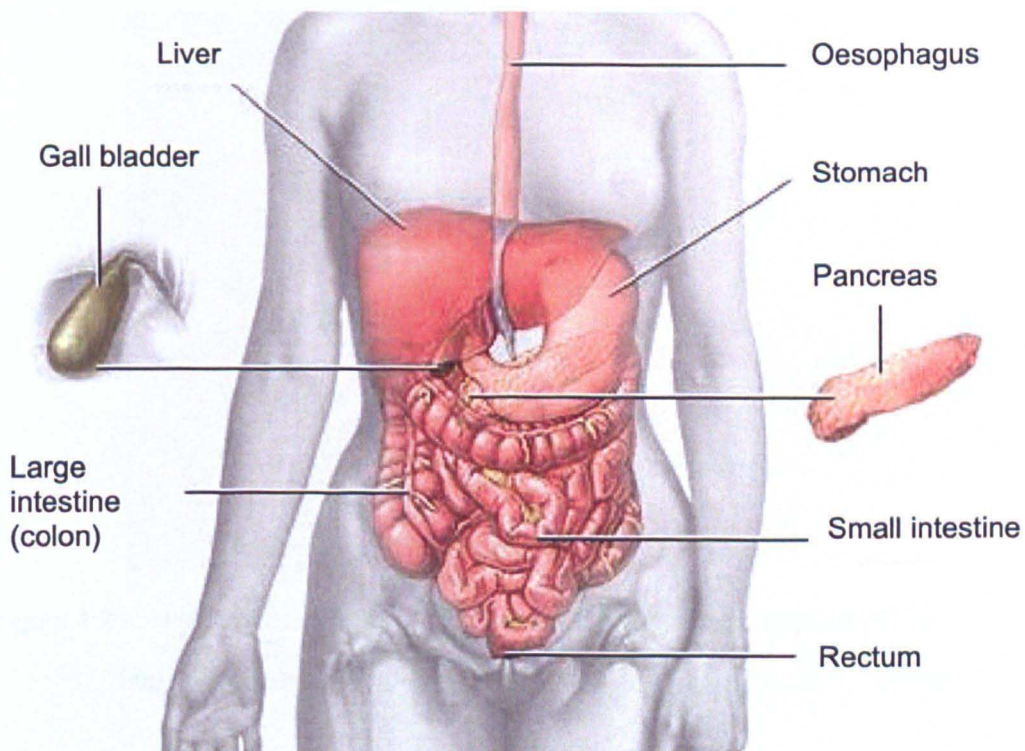
Figure 1.1: The gastrointestinal tract and its associated organs (Image from the National Library of Medicine).

These differences are crucial in tissue engineering as optimal function and morphology have to be retained. The large intestine (colon) is the lower part of the gut. As this part of the intestine is the focus of the main study, its detailed histology and function are discussed next.

1.4 HISTOLOGY OF THE COLON

The cells of the GI tract vary in phenotype and function. Isolating the focus of this review on the colon, histological studies show that its *mucosa* (the internal lining of the gut) consists of crypts (figure 1.2 a). These are short invaginations present on the mucosal epithelium (closely apposed cells without intervening connective tissue). In the large bowel, there are no villi (evaginations of the mucosal epithelium present in the small intestine). Crypts make up the epithelium and they are separated from mesenchymal cells by a porous basement membrane (Mahida *et al.*, 1997).
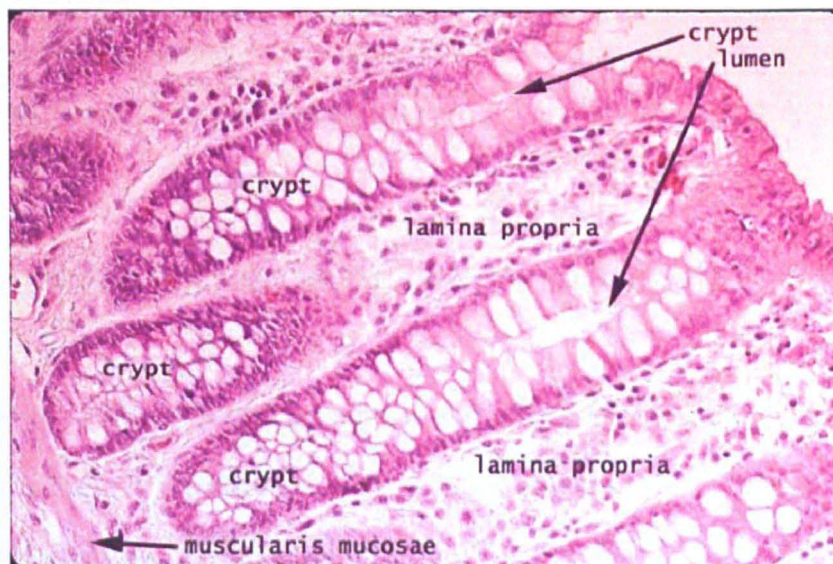
Figure 1.2 a: Histological staining of the human colon showing crypts cut in transverse (From David King Group – Southern Illinois University - http://www.siumed.edu/~dking2/erg/smallint.htm: accessed 07/08/2009)

Directly under the membrane are the subepithelial myofibroblasts and further below

lies the *lamina propria* (loose connective tissue comprised of individual cells within

an extracellular matrix) (Kerr, 1999).

Beneath this layer is the *muscularis mucosae* which is a thin layer of smooth muscle

and the *submucosa* (deeper connective tissue). Figure 1.2 a and b are histological

stainings of a human colon which clearly illustrate these layers.
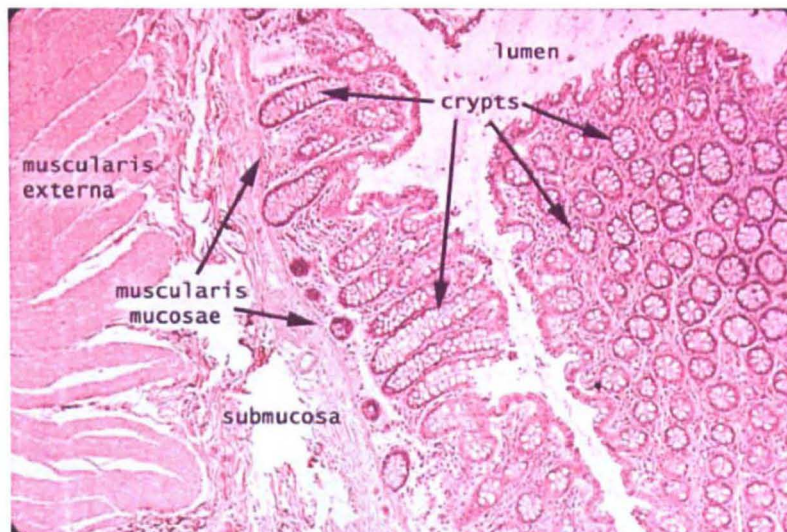
Figure 1.2 b: Histological staining of human colon showing crypts cut in cross section (From
David King Group – Southern Illinois University -
http://www.siumed.edu/~dking2/erg/smallint.htm: accessed 07/08/2009)

1.5 CELLS OF THE COLONIC EPITHELIUM: TYPES AND FUNCTION

The epithelium of the colon consists of several cell types and continuously

undergoes a cycle of proliferation, differentiation and apoptosis (Zhang *et al.*, 2003).

This cycle is illustrated in figure 1.3.

Progenitor or stem cells are thought to be located at the base of each crypt and they

divide every 12 to 16 hours producing 200 multipotent cells per crypt per day

(Sancho *et al.*, 2004). Distinguishing these stem cells from other epithelial cells is

difficult as until recently there was no specific biomarker for them (Marshman *et al.*, 2002, Willis *et al.*, 2008). The strongest evidence of their existence was demonstrated by the Clevers group with identification of lgr5 (leucine-rich-repeat-containing G-protein-coupled receptor 5) (Barker *et al.*, 2007). They demonstrated restricted expression of this Wnt sensitive receptor at the base of colonic crypts. Their argument that lgr5 does indeed mark the stem cells of the colon was strengthened by the observation that cells carrying this marker displayed two crucial stem cell characteristics, pluripotency and self renewal.
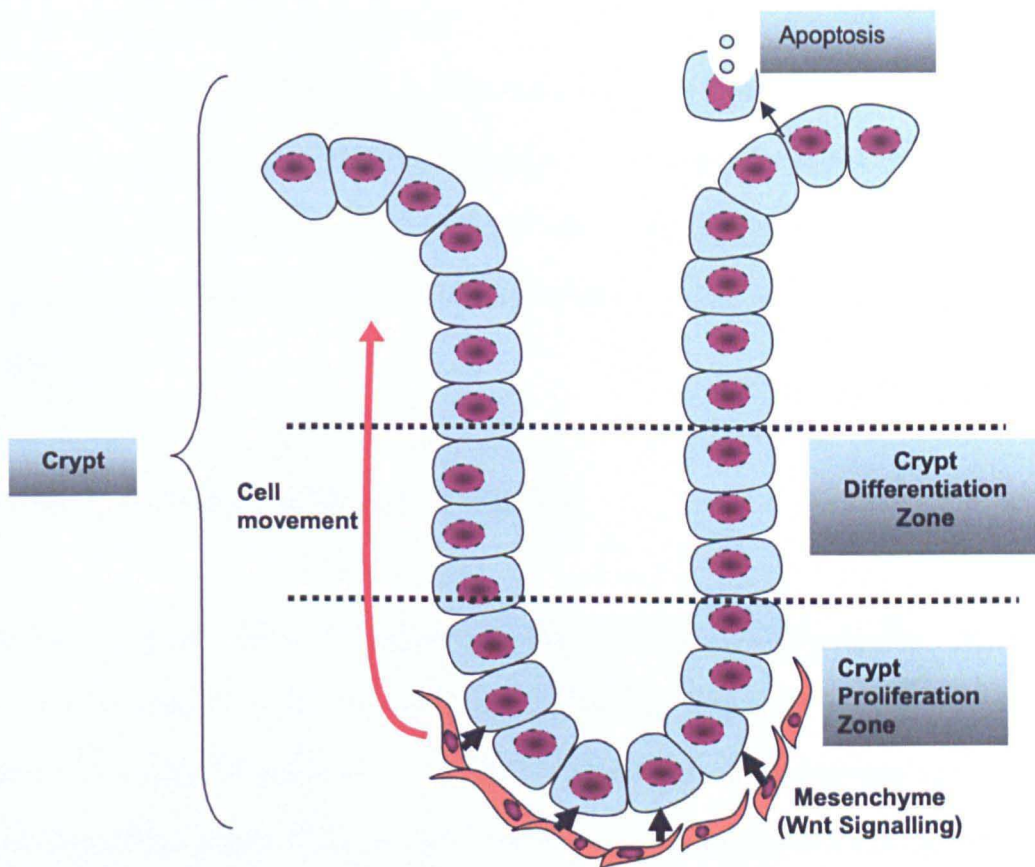
Figure 1.3: The epithelial crypt is under constant change. Cells proliferate at the bottom of the crypt due to Wnt signaling from the mesenchyme. These cells are then directed to move up the crypt and differentiation is triggered by a change in signaling. The differentiated cells are able to function as required (for example mucus production or absorptive function) before being triggered to detach from the basement membrane and undergo apoptosis.

The progeny of the stem cells are also known as transit amplifying cells. As these cells move up the crypt, they become committed, cease proliferation and differentiate into one of three phenotypes: colonocytes, goblet cells and enteroendocrine cells. A fourth cell type, the paneth cell, exists in the small intestine as well as a fifth type, the M cell which is produced in some crypts (Marshman *et al.*, 2002). Once the differentiated cells reach the apex of the crypt, they undergo apoptosis and are extruded into the lumen of the colon (Zhang *et al.* 2003).

Functionally, the large intestine is responsible for propulsion of contents from the caecum to the anorectal region (Kumar and Clark, 2002). Goblet cells secrete mucus into the lumen to aid this. Additionally, the colon has a crucial role in the absorption of water, electrolytes and organic anions (Cummings and Macfarlane, 1997). The absorptive cells or colonocytes are the predominant cell type of the colon epithelium demonstrating that the large intestine is specialized for absorption (Kerr, 1999).

1.6 'CROWD CONTROL' IN THE INTESTINE

As mentioned previously, each crypt can produce up to 200 cells per day. However the normal intestine remains under homeostasis. The migration and proliferation of the cells are not autonomous. These activities are finely controlled and directed through cell signalling from cells in the mesenchyme to cells in the epithelium. The process is intricate and involves multiple regulatory mechanisms (Sancho *et al.*, 2004). One key mechanism of interest is the Wnt protein pathway illustrated in figure 1.4.
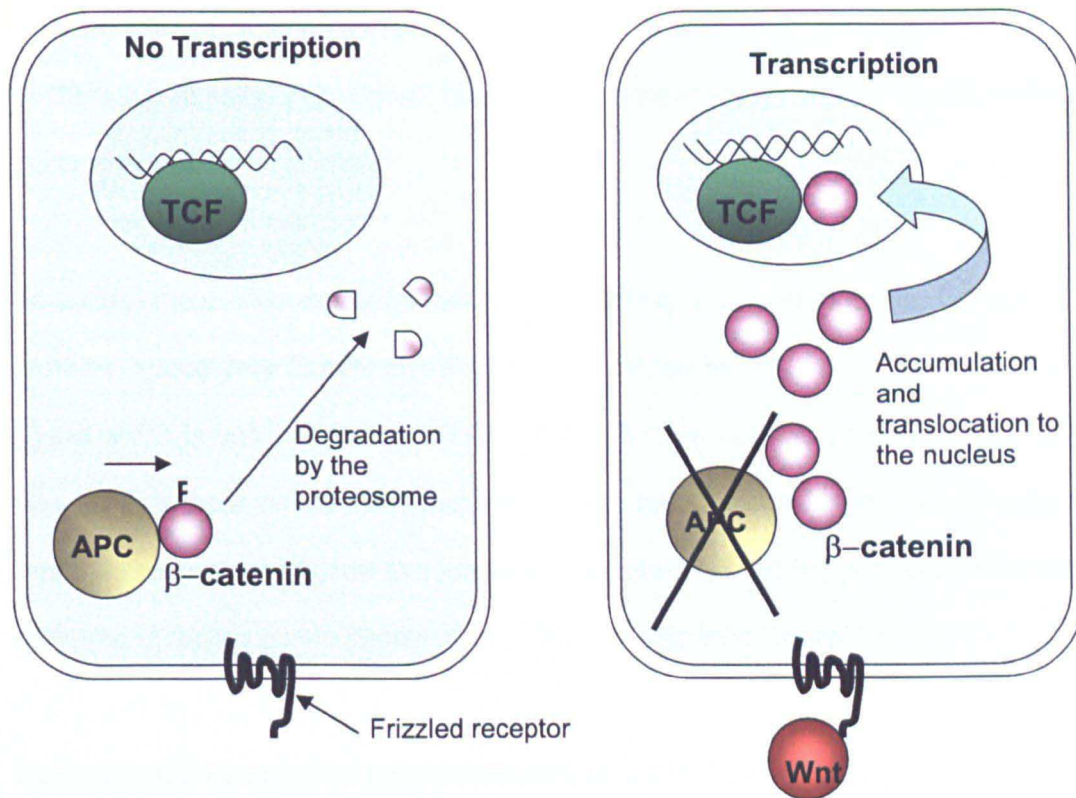
Figure 1.4: A simplified view of the canonical Wnt pathway. In the absence of Wnt protein, β–catenin is phosphorylated by the APC protein, ubiquitinated and degraded by the proteosome (left). However, when Wnt proteins bind to the frizzled receptor, the kinase action of APC is inhibited allowing β–catenin to accumulate in the cytoplasm and translocate to the nucleus (right). In the nucleus, the presence of β–catenin allows the DNA binding protein TCF to begin transcription.

Wnt proteins are thought to be released from the mesenchymal cells located below the epithelium. In the absence of Wnt proteins, the tumour suppressor protein adenomous polyposis coli (APC) phosporylates another protein, β–catenin, and this action targets β–catenin for ubiquitination and eventually destruction by the proteosome (figure 1.4). The APC protein therefore stops accumulation of β–catenin. In the presence of Wnt proteins, the kinase activity of the APC protein is suppressed and β–catenin accumulates in the cytoplasm before translocating to the nucleus where it binds to the T-Cell Factor (TCF) DNA binding protein (figure 1.4). The TCF- β–catenin complex upregulates 115 genes and downregulates 120 (van de Wetering et al., 2002). One of the upregulated genes is c-MYC which can

override G1 cell cycle arrest and repress the growth inhibitor p21, leading to proliferation of cells. This signal cascade is therefore what controls whether cells multiply or not.

To control the positioning of the cell, Wnt signalling again plays a role. Ephrin proteins, specifically EphB2 and B3 are upregulated by Wnt signalling while their ligand which is tethered to the cell membrane is downregulated (Batlle et al., 2002). This leads to cells on the basement membrane being separated out accordingly so that the receptor and ligand can interact consequently creating proliferation zones and differentiating zones (Batlle et al., 2002) as shown in figure 1.4.

Intuitively, failure of any of the components of the Wnt pathway implicates aberrant signalling in the colon. Hereditary colorectal cancers have provided evidence of this for example mutations in the tumour suppressor APC gene lead to sufferers expressing truncated APC protein. As a result regulation of the crypt is affected and abnormal cell proliferation leads to numerous polyps in the colon and colorectal cancer (Sancho et al., 2004). In summary, the Wnt pathway plays a substantial role in the regulation of the intestine and occurrence of colorectal cancer.

1.7 OBTAINING INTESTINAL EPITHELIAL CELLS: CHALLENGES OF ISOLATION

For in vitro tissue engineering, and specifically to form autologous tissue, it is necessary to obtain primary cells which can be amplified. However the colon has proved to be a uniquely difficult organ from which to obtain primary isolated epithelial cells. Anoikis refers to cell death induced by loss of adherence (figure 1.5). In vivo it is thought to be a protective mechanism, preventing detached cells from

growing dysplastically (Frisch and Ruoslahti, 1997). *In vitro*, anoikis occurs following

isolation of intestinal epithelial cells from the basement membrane, making it difficult

to maintain isolated cells (for example crypts) or obtain fully functional cells from the

human intestine (Strater *et al.*, 1996). Perreault and Beaulieu have reported *in vitro*

culturing of viable enterocytes from human foetal small intestine but the cells

obtained were non-proliferative (Perreault and Beaulieu, 1998).

Several studies carried out in an attempt to understand the biological pathway and

possible prevention of anoikis, concurred that the survival of crypt cells is dependent

on adhesion to extracellular matrix proteins and is mediated by the β_1 integrin

(Strater *et al.*, 1996, Frisch and Ruoslahti, 1997, Frisch and Screaton, 2001)

Another key finding was reported by Waterhouse *et al* who elucidated that

endogenous expression as well as exogenous addition of the cytokine interleukine-

1β rescued rat intestinal epithelial cell line IEC-18 cells from apoptosis (Waterhouse

et al., 2001).

Transformed cell lines offer a credible research tool as work continues to pursue a

conclusive method to prevent anoikis and obtain viable autologous cells from the

intestine. One cell line widely used in the pharmaceutical industry is the human

colon adenocarcinoma cell line (Caco-2). This cell line has proved useful for drug

permeability studies as it differentiates into small intestine-like cells at confluence

(Delie and Rubas, 1997). However it also retains some of its large intestinal

phenotype and has been described as a hybrid colonocyte/enterocyte (large

intestinal/small intestinal) cell line (Engle *et al.*, 1998, Fleet *et al.*, 2003).

Cancer cell surpresses programmed cell death and survives

Normal cell undergoes anoikis and cell death

← Epithelial cell layer
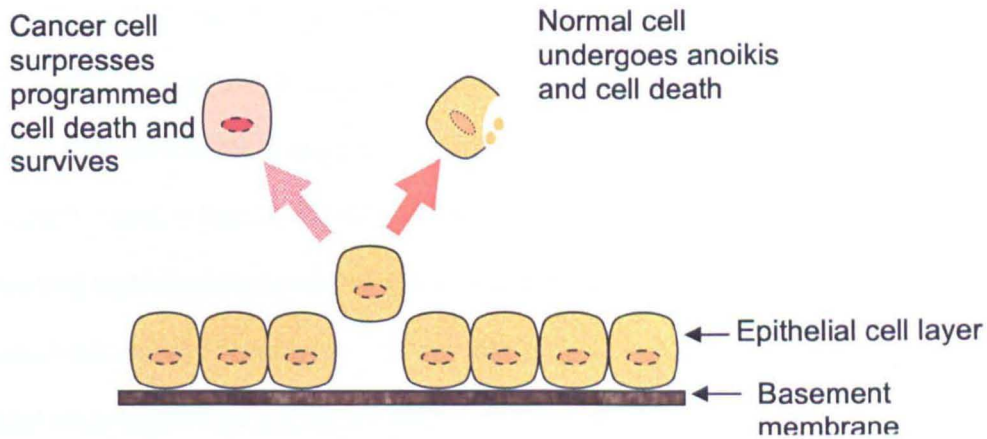
← Basement membrane

Figure 1.5: Anoikis occurs to ensure cells detached from the basement membrane of the intestine do not survive and grow dysplastically. Surpression of anoikis has been linked to cancerous cells. Image adapted from (Liotta and Kohn, 2004).

1.8 CURRENT REVIEW OF PROGRESS IN GASTROINTESTINAL TISSUE ENGINEERING

The complexity of the intestine in terms of cell types, niches and construction is clear. Tissue engineering has to account for this and researchers will generally isolate their focus on a specific part of the intestine. This section highlights the current literature in intestinal tissue engineering establishing past accomplishments, their benefits and disadvantages.

Generating small intestinal epithelium has dominated the field of research over the past few decades. Vacanti was one of the early pioneers seeding progenitor intestinal cells on a variety of biodegradable scaffolds (Vacanti et al., 1988). However, this resulted in a model with no cell-cell interaction between the epithelial and mesenchymal cells. Crypt cells are known to require mesenchymal interaction to survive, proliferate and differentiate (Rocha and Whang, 2004, Evans et al.,

1992). Vacanti's group therefore modified their technique to use epithelial organoid units which consisted of a villus structure, epithelium and mesenchymal core. Choi and Vacanti seeded these organoid units onto poly(glycolic acid) (PGA) scaffolds sprayed with poly(lactic acid) (PLA) then proceeded to implant the scaffolds *in vivo* into rats (Choi and Vacanti, 1997). Post-implantation the rats developed cysts containing neomucosa surrounded by vascular tissue containing degrading polymer, extracellular matrix, fibroblasts and smooth muscle like cells. The neointestine formed as a result had similar structure and function to native small intestine (Rocha and Whang, 2004, Choi *et al.*, 1998).

Recent work by Lloyd *et al*, was a modification of the early Vacanti method (Lloyd *et al.*, 2006). They implanted PLGA scaffolds in rats to stimulate vascularisation and several weeks later, they injected organoid units into the scaffold. This method allowed use of less tissue to generate the organoids and formation of mucosa and submucosa on the scaffold.

In an attempt to translate this experiment to a more controlled *in vitro* environment, Kim and colleagues seeded scaffolds with organoids and placed them in a bioreactor (Kim *et al.*, 2007). This had limited success with cells attaching onto the scaffold but no functional tests were undertaken to assess if the tissue would behave similarly to the *in vivo* experiment. Other efforts to engineer intestine include, Kawaguchi *et al* who designed poly(carbonate) membranes seeded with rat intestinal epithelial cells (Kawaguchi *et al.*, 1998). The cells survived *in vivo* when implanted in rats. However, similar to initial efforts by Vacanti *et al*, this method did not generate neomucosa.

Using an architectural point of view, Lee *et al* fabricated a three dimensional PLGA scaffold with villi-like structures. They seeded rat intestinal epithelial cells into the

scaffold but there was non-uniform distribution of cells within the scaffold. The interior of the scaffold had fewer cells than the exterior and this was postulated to be possibly due to diffusion limits of oxygen and nutrients and possible isolated voids within the scaffold (Lee *et al.*, 2005).

Overwhelmingly, the focus has been on the small intestine, however, tissue engineering within the large intestine has also been achieved. Grikscheit and Vacanti, developed tissue engineered colon using organoid units from the colon instead of the small intestine as described previously. The tissue generated had similar physiological functions to native large intestine (Grikscheit *et al.*, 2002).

Each of these studies has benefits and disadvantages. A primary emerging theme is that the greatest success in terms of cell seeding and function of construct was achieved with *in vivo* work and the use of organoid units. Theoretically, the reason for this may be that the cells are in a niche and are placed in an ideal area for stimulation by bowel growth factors (specifically for tissue engineered constructs implanted abnominally). The major disadvantage of the *in vivo* studies would be the inability to simulate the same effect in humans where surgery would be invasive and peritoneal scarring can create complications. However, the *in vitro* work by Lee showed non-uniform cell coverage of the scaffold and therefore in order to apply it as a potential solution, much more in depth study and experimentation would be necessary to achieve similar success to the *in vivo* work.

A second disadvantage of the *in vivo* work is the reliance on organoid units. It seems counterintuitive to use large parts of healthy tissue to generate engineered intestine. This method was nevertheless the only successful way of creating mucosa and hints at the fact that cells in a niche may have an advantage over isolated cells.

The arguable ideal would be to use cells which can perhaps proliferate and differentiate on their own similar to the intestinal progeny of stem cells.

Conclusively, plenty of knowledge regarding cell survival and the role of scaffolds has been gained from the studies mentioned above but there is a definite lack of successful *in vitro* tissue engineered intestine.

1.9 SUPPORT: SCAFFOLDS IN TISSUE ENGINEERING

In vivo cells within a tissue are supported by network known as the extracellular matrix (ECM). The ECM is composed of polysaccharide gels such as hyaluronan, proteoglycans such as chrondroitin sulphate and fibrillar proteins such as collagen and fibronectin (Giancotti and Ruoslahti, 1999, Laurent and Fraser, 1992, Kjellen and Lindahl, 1991). The extracellular matrix is produced by fibroblasts and while one of its key functions is support for the cells, it also has an integral role in the survival of cells through signalling which is further discussed in section 1.10.

With the aim of creating tissues from cells, one major task in tissue engineering is to ensure the cells have support prior to becoming established and able to create their own ECM. There are various considerations given to the scaffold selection depending on the location and type of tissue as well as eventual application. For example load bearing tissue such as articular cartilage and bone may require robust materials capable of withstanding large stresses when implanted *in vivo* (Hutmacher, 2000, Moutos *et al.*, 2007). Soft tissue on the other hand, lends itself to a myriad of material types ranging from hydrogels for ocular tissue to thixotropic gels for cell delivery to pliable foams for vascular and intestinal tissue engineering (Wake *et al.*, 1996, Pek *et al.*, 2008, Pratoomsoot *et al.*, 2008). With consideration to

intestinal tissue engineering, it is important to note that the scaffold architecture could dictate the ultimate shape of the tissue (Hutmacher, 2001).

Scaffold properties are, however, not limited to mechanical strength. Other desirable scaffold properties as described by Hutmacher can include:

- A three dimensional network of pores to facilitate transport of nutrients and metabolic waste from cells and developing tissue.
- Controllable degradation properties to match *in vivo* or *in vitro* cell behaviour allowing timely replacement of the scaffold by cells and matrix.
- Suitable surface properties such as chemistry and/or topography for cell attachment and proliferation.

The material choices and processing methods to produce scaffolds are numerous and diverse (Hutmacher, 2001). Natural materials such as collagen have found extensive use with good biocompatibility with a large number of different cell types including intestinal cells (Strater *et al.*, 1996). As a scaffold, collagen is restrictive in terms of strength (having a gel like formulation) and differences in batch to batch processing make it less versatile compared to synthetic materials (Marler *et al.*, 1998).

As seen in section 1.8, synthetic scaffolds in tissue engineering are dominated by the poly(α-hydroxy acids) of PLA, PGA and the copolymer PLGA. The polymer lends itself to a host of processing methods due to its ease of solubility in organic solvent. PLGA is an FDA approved material for biomedical use. To produce thin films suitable for intestinal tissue engineering, processing methods that can be used include solvent casting and electrospinning (Lu *et al.*, 1999, Li *et al.*, 2002).

An additional advantage of the poly(α-hydroxy acid) polymer is the ability to control degradation through manipulation of molecular weight and in the case of PLGA in terms of monomer ratio. In the present work, PLGA was used as the material of choice for the scaffold and further details of its properties and modification can be seen in Chapters 3 and 4.

1.10 THE CELL- MATERIAL INTERFACE

In tissue engineering, scaffolds provide the mechanical support for cell growth and subsequent tissue formation (Hutmacher, 2000). The interface between the material (scaffold) and the cells has drawn considerable attention especially as attachment dependent cells such as intestinal epithelial cells rely on close apposition to the material surface for survival (Chen *et al.*, 1997, Re *et al.*, 1994).

Extensive research shows that a material surface gains a layer of protein when immersed in serum. This is often referred to as a protein conditioned layer. Cells are attached indirectly to the material through binding to the proteins on the surface of the material (Pierschbacher and Ruoslahti, 1984). Upon attachment to the surface, a vast set of biomolecules are triggered and recruited to help maintain attachment and augment the survival and function of the cells on the surface of the material. The process by which this cascade happens is known as signal transduction and it plays a significant role in cell adhesion, focal contact formation and subsequent growth, matrix deposition and proliferation on the material (Giancotti and Ruoslahti, 1999, Basson *et al.*, 1996, Mann *et al.*, 1999).

Cell adhesion and signal transduction are explained next before turning attention to the material surface which also has an integral function in that it controls protein

adsoption. The material surface itself therefore plays a role in cell attachment and eventual survival. This is further reviewed in section 1.11.

1.10.1 Transmitting the Message: Cell Adhesion, Signal Transduction and Cell Survival

Cell adhesion to a surface induces signal transduction resulting in focal contact formation, regulation of gene expression as well as regulation of cell growth and proliferation (Desloges et al., 1998, Frisch and Ruoslahti, 1997). Cell adhesion is a complex process involving two main phases. The initial attachment phase involves rapid formation of physico-chemical linkages such as van der Waals forces and ionic forces between the cell and the material (Anselme, 2000). The cell adhesion phase is a longer process that involves cell-matrix and cell-cell interactions. These are mediated by biological molecules including ECM proteins, cell membrane proteins and cytoskeleton proteins (figure 1.6). Cell-matrix interactions are key in determining the success of a scaffold.
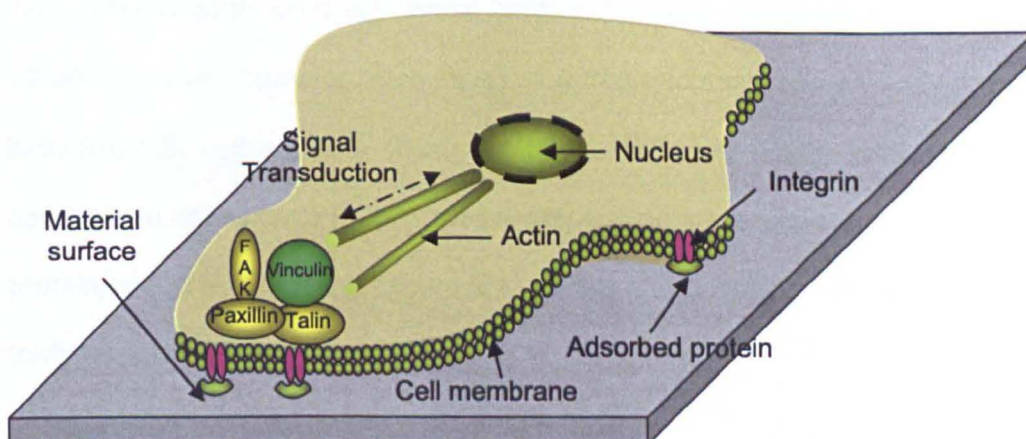
Figure 1.6: Cell adhesion to a material requires assembly of a multitude of receptors and proteins to facilitate signal transduction that determines the cell's fate.
In vivo epithelial cells of the intestine adhere to the basement membrane through

adhesion complexes (Balda and Matter, 2003, Stutzmann *et al.*, 2000). The

basement membrane as the attaching surface is comprised of ECM proteins

including laminin isoforms, nidogen, perlecan and collagenic proteins dominated by

type IV collagen (Simonassmann *et al.*, 1995, Timpl and Brown, 1996, Stutzmann *et

al.*, 2000)

Laminins present in the ECM are heterotrimeric glycoproteins composed of α, β and

γ chains. The α chain contains the Arginine-Glycine-Aspartic acid (RGD) amino

acid sequence which is involved in cell adhesion(Boateng *et al.*, 2005). This RGD

sequence has a role in initiating adhesion through interaction with receptor proteins

(mainly integrins) in the cell membrane (Pierschbacher and Ruoslahti, 1984,

Ruoslahti, 1996)

Integrins are present on the cell membrane and are the crucial link between the

extracellular matrix and the cytoskeleton. They are transmembrane heterodimeric

receptors consisting of two subunits α and β. An important integrin subtype involved

in *in vitro* cell adhesion is $\alpha_6\beta_1$ which binds exclusively to laminin (Desloges *et al.*,

1998). There are however more integrins with pronounced roles in cell adhesion

including $\alpha_v\beta_3$, $\alpha_2\beta_1$ and $\alpha_1\beta_1$ (Desloges *et al.*, 1998).The β_1 sub unit appears to be

dominant in adhesion to ECM proteins. Once integrins are bound to the extracellular

protein, signal transduction occurs to generate and/or activate proteins necessary to

form focal adhesions.

Focal adhesion kinase (FAK) is an important enzyme generated by this action. The

signal transduction pathway involves integrin clustering, interaction with the cell

cytoskeleton and multiple phosphorylations (Miyamoto *et al.*, 1995, Schlaepfer *et al.*,

1994). FAK is involved in focal adhesions where the cell membrane is in close

contact with the substrate at a separation of 10-15nm (Beckerle, 2002). Large

bundles of actin filaments terminate at these points and these have a structural role

in anchoring to the cell membrane and also take part in signal transduction

(Beckerle, 2002).

Talin, vinculin and FAK are three important proteins found at epithelial cell focal

adhesions (see figure 1.6). Talin and vinculin provide the binding site for the actin

cytoskeleton. Talin is also the site of attachment for FAK. FAK is a tyrosine kinase

and it activates other enzymes initiating a chain of subsequent phosphorylations,

which eventually lead to suppression of apoptosis. Bcl associated dimer and

caspase-9 are key apoptotic proteins that are eventually phosphorylated and

suppressed through the initial action of FAK (Gomperts B and Kramer I, 2003). The

forkhead transcription factor (FKHRL1) is also phosphorylated through the same

pathway and is consequently retained in the cytosol. This prevents it from activating

genes within the nucleus that promote cell death such as the Fas ligand. FAK

therefore helps to regulate signal transduction which is vital in prevention of

apoptosis (Gomperts B and Kramer I, 2003).

1.10.2 Shape Shifting: Morphology of Attachment Dependent Cells

In vitro, the preferred morphology of attachment dependent cells after adhesion is a

flattened shape (Beckerle, 2002). However, cell proliferation and differentiation are

thought to be dependent on the strength of attachment. For most epithelial cells to

survive they must be attached to a surface but in order to proliferate and function

they must not be too strongly adhered to the surface. Studies have found a

correlation between less cell adhesion and higher proliferation with osteoblasts

(Linez-Bataillon *et al.*, 2002). An additional observation from previous research on

osteoblasts again is the inverse relationship between cell spread area and motility

rate (Webb et al., 2000). This may perhaps be explained by later work which

revealed a link between strong adhesion to strong cell-ECM binding but less

remodelling of the cell cytoskeleton (Diener et al., 2005).

The cell shape is therefore crucial as it is likely affect adhesion, gene expression

and cellular differentiation (Lauffenburger and Horwitz, 1996, Benzeev et al., 1988,

Benzeev et al., 1980, Farmer et al., 1978, Folkman and Moscona, 1978).

1.11 INFLUENCE OF SURFACE PROPERTIES ON CELL ATTACHMENT

In tissue engineering where scaffolds are used, cells attach to material surfaces via

a layer of adsorbed protein. The surface of the material therefore presents a key

frontier in the cell-material interaction influencing the type, quantity and conformation

of this protein layer (Castner and Ratner, 2002). Protein adsorption therefore has a

wide ranging influence in determining the success or failure of a scaffold. This is

because subsequent steps in cell activity such as proliferation and adhesion rely on

cell attachment as a primary step. Anselme presented an extensive review relevant

to osteoblasts (bone cells) demonstrating that a myriad of surface properties

including chemistry, topography, crystallinity and wettability can be exploited to

control cell activity (Anselme, 2000). A pertinent question that arises is, how exactly

do these surface properties influence the behaviour of cells?

In answering this question, it is important to note that quite often cell behaviour can

be attributed to a convergence or interplay of several surface properties instead of a

solitary factor. This is perhaps best illustrated by two factors that have arguably

provoked the most interest, scrutiny and debate: surface chemistry and topography

(Curtis and Wilkinson, 1997). The surface chemistry of a material refers to the elements and chemical functionalities present on the surface. On the other hand, surface topography is the description of surface features of a material encompassing surface roughness but also includes features such as grooved or porous substrates. Both of these properties can affect the wettability of a material when probed with water droplets larger than the scale of the topography (Lee et al., 1994, Lampin et al., 1997).

1.11.1 Linking Surface Wettability to Cell behaviour

Wettability gives an indication as to how hydrophobic or hydrophilic a material is. Wettability is usually correlated with surface free energy, which is interpreted as a measure of adhesive energy (Dewez et al., 1996, Hench and Ethridge, 1983). It is known that surface wettability affects protein adsorption on the material surface and eventually affects cytoskeletal organisation within adhering cells (Sigal et al., 1998, Iuliano et al., 1993, Ruardy et al., 1995).

Succinctly, in vitro experiments have shown that a range of mammalian cells have low compatibility with hydrophobic surfaces often exhibiting low cell attachment and proliferation (Altankov et al., 1996, Webb et al., 1998, Groth and Altankov, 1996, Zelzer et al., 2008). Hydrophilic surfaces tend to be preferable, however, it must also be mentioned that moderately hydrophilic surfaces outperform highly hydrophilic surfaces (Webb et al., 1998).

One possible explanation for this observation was reported in a study by Groth and Altankov. They observed diminished tyrosine phosphorylation at focal adhesions of human fibroblasts cultured on hydrophobic surfaces (Groth and Altankov, 1995). This had a profound effect on the cell with more hydrophilic materials exhibiting

greater cell spreading, greater ability to form actin fibres, increased organisation of the fibronectin receptor and increased proliferation (Groth and Altankov, 1995, Groth and Altankov, 1996). However, studies by Tamada and Ikada, in part, contradicted these results (Tamada and Ikada, 1993). They demonstrated that on several hydrophilic materials, wettability was not as critical a factor in comparison to prior adsorption of proteins. In the presence of preadsorbed fibronectin, cell adhesion was enhanced regardless of wettability.

These studies emphasise the fact that wettability may in some cases, govern adsorption of proteins and hence determine whether or not adhesion will occur. The next section details research in surface chemistry and topography, highlighting potential reasons as to why these two key factors affect cell behaviour.

1.11.2 Surface Chemistry: Can Cells Sense Changes?

The functional groups of the material surface are of interest as they can significantly adjust the properties of the surface. The presence of polar or non polar groups will influence the surface wettability. Also, surface chemistry changes can be accompanied by surface topographical changes which must be considered. For tissue engineering applications the surface chemistry is generally regarded separately from the bulk material. The bulk material is generally modified to ensure adequate load bearing or degradation properties but the surface which is in direct contact with fluids and cells is adapted to ensure good attachment.

The influence of surface chemistry on the cell is initiated almost immediately. An intricate study by Keselowsky and colleagues demonstrated that adsorption of a key cell binding protein, fibronectin and its conformation can be modulated by the surface (Keselowsky *et al.*, 2003). Their conformation studies involved studying the

binding affinity of fibronectin to monoclonal antibodies and the use of self-assembled monolayers presenting terminal groups of varying chemical composition (charged and uncharged groups as well as polar and nonpolar groups). The results of this work showed that hydrophilic (OH terminus) surfaces exhibited cell adhesion at low fibronectin concentrations, similar levels of adhesion on hydrophobic (CH_3 terminus) surfaces could only be achieved at high concentrations of fibronectin. Citing previous work by others, the authors more explicitly suggested that this observation was related to conformational differences between hydrophilic surfaces which allow presentation of the integrin binding domain of the protein to the cell and strong denaturing of adsorbed protein on hydrophobic surfaces limiting protein unfolding.

The Keselowsky study shows an indirect effect of the surface chemistry with wettability playing a key role. The effect of surface chemistry can, however, be more direct with the functional groups on the surface affecting cell behaviour as shown by Webb and colleagues. In their study, cells did not follow the conventional wettability trend of hydrophilic surfaces exhibiting greater cell adhesion but instead demonstrated consistent spreading and migration on surfaces with different functional groups (Webb et al., 2000). The authors of this work did not propose a theory as to why certain functional groups elicited greater spreading than others but do critically point out that differences such as cell type and serum concentration can affect experimental observations. The work did show an inverse relationship between cell spreading and motility. This is an especially important observation for tissue engineering applications as the functional groups on the surface could potentially limit the movement (if required) of the cells on or into a scaffold.

In summary, it is important to consider that surface modification approaches such as self assembled monolayers and controlled deposition of plasma polymers (described later in section 1.12) can result in ideal surfaces to study surface

chemistry. However, when working with polymeric scaffolds as will be performed in this thesis, surface modifications can lead to topographical effects. Identifying chemical groups present on the surface of materials may help predict or explain cell behaviour but these observations should perhaps be taken with caution. The next section continues to expand further on this and also details more intricate surface topography studies.

1.11.3 Influence of Surface Topography on Cell Behaviour

Surface topography is well known to influence cell morphology and migration. This is reflected in two authoritative reviews by Singhvi *et al* and Curtis and Wilkinson, who examined these two areas in great depth (Curtis and Wilkinson, 1997, Singhvi *et al.*, 1994). The latter publication, crucially pointed out 'accidental topography' that can occur due to experimental procedure and therefore highlighted the need to carefully interpret data.

The surface of the material is vulnerable to change even when the intended change is to the bulk of the material. As an example, Washburn *et al* demonstrated that variations in crystallinity led to changes in nanometer roughness in poly(L-lactic acid) (PLLA) films. They produced gradients of crystallinity on PLLA films through annealing at different temperatures and subsequent analysis with atomic force microscopy showed that more amorphous films had lower nanoscale roughness (0.54 ±0 .17nm) compared to more crystalline films (13.00 ± 0.50nm) (Washburn *et al.*, 2004). In the same study it was observed that osteoblasts proliferated more on smoother surfaces than on rougher surfaces and that increase was attributed to the topographical differences.

More direct surface treatments such as polishing and chemical treatments are commonly used to adjust surface topography. A study on intraocular lenses made from poly(methylmethacrylate) showed that increased polishing led to smoother surfaces but decreased cell attachment (Yamakawa *et al.*, 2003). Separately, a study by Miller and colleagues treated PLGA with sodium hydroxide to create nanoscale topography which enhanced cell adhesion and proliferation of smooth muscle cells compared to conventional untreated PLGA (Miller *et al.*, 2004).

Cell adhesion and proliferation as illustrated by the previous examples are some of the most common effects of surface topography. Another, equally interesting effect is the ability of topography to guide cells. Berry *et al* created a patterned surface similar to a three dimensional network and noted that fibroblasts responded differently to the pit sizes on the surface of quartz. The cells within the smallest pits showed the highest proliferation though cells were more able to move into the larger pits. (Berry *et al.*, 2004). In a separate study, researchers suggested that epithelial cell migration can be influenced by pores on the surface (Steele *et al.*, 2000). There is also an array of papers demonstrating cell guidance by grooves reviewed by Curtis and Wilkinson (Curtis and Wilkinson, 1997).

More recently, the ability to exploit topography to induce differentiation was reported by Dalby and colleagues. Human mesenchymal stem cells were seen to express bone mineral and differentiate in the absence of osteogenic supplements. This occurred strongly when the cells were cultured on a disordered nanotopographical surface (Dalby *et al.*, 2007).

In conclusion, surface topography may affect many aspects of cell behaviour and is therefore a critical factor to consider when selecting or modifying materials for experimental use.

1.12 PLASMA INDUCED SURFACE MODIFICATION

Changes to the surface chemistry and topography of materials can be achieved in multiple ways but one method growing in popularity is the use of plasma due to its relative ease of application. A plasma is an ionised gas containing a mixture of electrons, neutral species, anions and cations (figure 1.7). It is sometimes referred to as the fourth state of matter as it contains greater energy than a solid, liquid or gas. The vast number of species in the plasma are generated largely by the electron avalanche. The small size and fast movement of the electrons leads to collisions with the gas molecules. This in turn leads to non radiative interactions such as ion formation and production of new electrons as well as radiative processes such as emission of photons in the ultraviolet and visible light range (Inagaki, 1996).
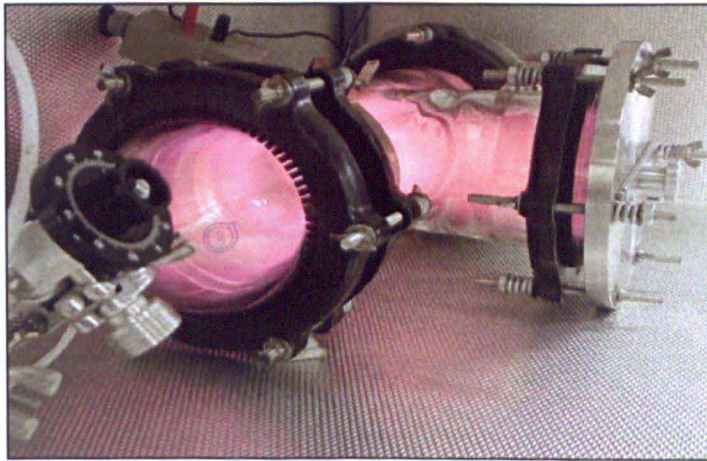
Figure 1.7: Characteristic glow associated with plasma in air.

Experimentally, plasmas are usually created by applying a voltage to a gas. An object placed within a plasma gains a negatively charged surface. This is because electrons are attracted first to the surface due again to their small size and fast acceleration compared to other charged and neutral species in the plasma. This negative charge then leads to the formation of a positive sheath around the object.

Interactions between the substrate and the plasma then take place and these are

dependant on a variety of factors but of key importance is the gas forming the

plasma (Lieberman and Lichtenberg, 2005, Inagaki, 1996, Biederman, 2004). Table

1.1 lists some of the various interactions that can occur between the substrate and

plasma.

Table 1.1: Plasma gases and substrate interactions (Adapted from (Inagaki, 1996)).

Plasma Type	Gas	Examples	Interactions
Non-polymer forming	Inorganic gas	Argon Oxygen Nitrogen	Etching Implantation Radical generation Chain scission Crosslinking Surface modification
Polymer forming	Organic gasses	Urea Allylamine Acrylic acid	Polymer deposition

The effect of plasma has been widely reported with great emphasis on changes to

the surface. Arguably, one of the most studied effects is the resulting surface

chemistry. Various plasmas have been shown to chemically alter the surface of

substrates by depositing controlled concentrations of functional groups at the

surface including oxygen, carbon and nitrogen based groups (Chan *et al.*, 1996).

This can occur through direct bonding with the surface or through formation of

plasma polymer films. These plasma polymer coatings differ from conventional

polymers as they consist of randomly branched highly crosslinked short chains as

opposed to the repeating monomer units found in conventional polymers

(Biederman, 2004). These thin film coatings have been used experimentally to study

and control cell behaviour (Zelzer *et al.*, 2008, France *et al.*, 1998, Barry *et al.*,

2006).

While surface chemistry effects due to plasmas are well studied, there is also evidence of topographical changes to the surface especially with polymeric substrates. This occurs especially with etching plasmas such as oxygen. For example Morra and colleagues reported topographical changes to poly(tetrafluoroethylene) (PTFE) with increasing time in an oxygen plasma (Morra *et al.*, 1990). A similar observation was reported by Wang *et al* with PLGA films increasing in roughness as oxygen plasma treatment time increased (Wang *et al.*, 2004).

For tissue engineering applications, plasma has been used for a wide variety of purposes. For example argon plasmas have been used to sterilize surfaces, plasma polymers of acrylic acid have been used to support keratinocytes (skin cells) and to aid in transfer of those cells to a wound bed and plasma polymers of varying wettability have been used to encourage cells to ingress into pores within a scaffold (Barry *et al.*, 2006, Holy *et al.*, 2001, Haddow *et al.*, 2006).

Plasmas create an atmosphere that can radically alter the surface of a material. Careful control of the plasma conditions and monitoring of surface chemistry and topography are necessary to create experimentally reproducible results.

1.13 AIMS OF THE THESIS

The overall aim of this thesis was to produce degradable scaffolds which could be used *in vitro* to mimic the human colonic epithelium. Intestinal tissue engineering has been successful *in vivo* with the use of small sections of the epithelium known as organoids. However, this approach requires large amounts of healthy intestine preferably from an autologous source. For patients suffering from colorectal cancer or short bowel syndrome (SBS), this may not be possible as large sections of the intestine may be diseased and would have to be removed surgically. Additionally, in an *in vitro* setting, the use of organoids would be difficult as they are very likely to disintegrate when cultured *in vitro*.

For this reason two model systems were proposed. The first system focused on creating a two dimensional degradable coculture model for the purpose of tissue engineering. The degradable material in this model was a thin film or membrane of poly(lactic-co-glycolic acid) - PLGA. The film was modified to create an ideal synthetic reconstruction of the *in vivo* basement membrane complete with internal conduits and surface porosity thereby enhancing its effectiveness. This modified scaffold was extensively studied to ensure no deleterious effects in terms of degradation or surface chemistry occur due to the modification process. Using established knowledge of surface and cell interactions, the material was then tested to ensure good cell attachment, activity and proliferation. Finally, the modified scaffold was compared to an established non-degradable model to determine its efficacy.

The second system described was a novel three dimensional scaffold to replicate the crypts (invaginations of the epithelium) seen in the colon which could not be produced in the proposed two dimensional model. The design of this scaffold

incorporated measurements from sections of *in vivo* intestine to create a suitable replica of the crypts of the epithelium. Electron beam photolithography was used to create an accurate mould from which the scaffold was produced. PLGA based submicron particles were used to fill the mould with a view to incorporating signalling molecules within the mould in future. A new cell sheet method for intestinal cells was used to seed the scaffold. As the method to produce the cell sheet was novel, the production process was studied and carefully controlled. Finally, a model protein was incorporated with the aim of demonstrating that signalling molecules which play a key role in maintaining the intestinal epithelium can in future be included into the three dimensional model.

Thus the aim of this thesis was to describe two novel scaffolds for colon tissue engineering.

CHAPTER 2: GENERAL

MATERIALS AND METHODS

This chapter lists the general materials and methods

that were used experimentally.

2.1 MATERIALS AND METHODS

A comprehensive list of materials and suppliers is provided in Appendix 1. Unless specified otherwise, all water used was ultrapure (18.2 mΩ resistivity at 25°C) and all incubation occurred at 37°C in a humidified, 5% CO_2 atmosphere. The methods used in this thesis follow.

2.2 TWO DIMENSIONAL SCAFFOLD FABRICATION

This is the description of the manufacture of untreated PLGA (uPLGA) membranes used in Chapter 3 and 4. The untreated PLGA membranes were oxygen plasma treated as described subsequently to produce the ePLGA films.

Poly (DL-lactide–co-glycolide) (PLGA; 75/25 140,000g/mol) was used to make films/membranes using a phase inversion technique. The polymer was dissolved in N-Methyl-2-pyrrolidone at a 20% w/w concentration. The solution was then rolled for 24-48 hours to equilibrate it and then heated briefly 40°C prior to use. Fifteen µL of the polymer solution was cast onto a glass slide (see figure 2.1). A second slide was used to compress the solution. The two slides with the compressed solution were then placed into a water bath. The top glass slide was then pulled back allowing the precipitation of solid polymer as the solvent leached into the water. N-Methyl-2-pyrrolidone is infinitely soluble in water. The polymer film was then immersed in water for 3 days. The water was changed three times daily and the films were allowed to dry in a desiccator and used within 2 days.

Samples for use in cell culture were sterilized with a PBS solution containing 100 units of penicillin/mL, 100µg streptomycin/mL and 60 µg amphotericin B/mL. The

samples were incubated for 24 hours and then rinsed three times in phosphate

buffered saline (PBS; pH = 7.4).

Polymer solution
Glass slide

Step 1: Application of polymer
solution and alignment of glass

Step 2: Compression and
immersion into water

ilm

Step 3: Separation of glass slides
and precipitation of film
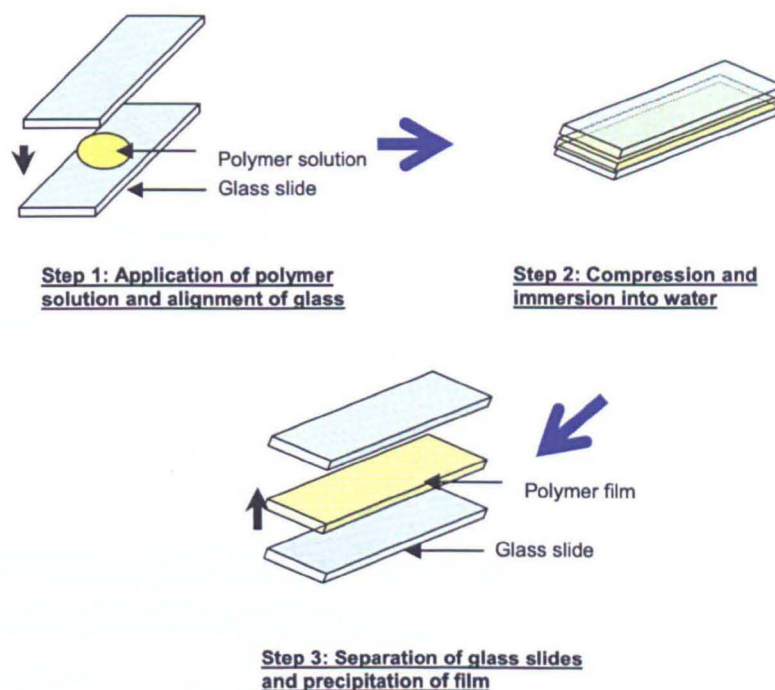
Figure 2.1: Illustration showing some of the key steps in preparation of the polymer films. The prepared polymer films were then soaked in water for 3 days to allow the solvent to escape fully. The films were then air-dried in a desiccator.

2.3 SURFACE MODIFICATION USING PLASMA

The set-up of the plasma machine is as shown in figure 2.2. A plasma was struck

using two external capacitively coupled copper electrodes connected to a

13.56 MHz radio frequency power source (Coaxial Power System Ltd). The reflected

power was externally controlled to <1 W. A pirani gauge (BOC Edwards) was used

to monitor the gas pressure. A quartz crystal microbalance located in the reaction

chamber was used to ensure depositions were carried out to a reproducible

thickness, although its inevitable physical separation from the point of deposition makes it an inaccurate measure of actual film thickness.
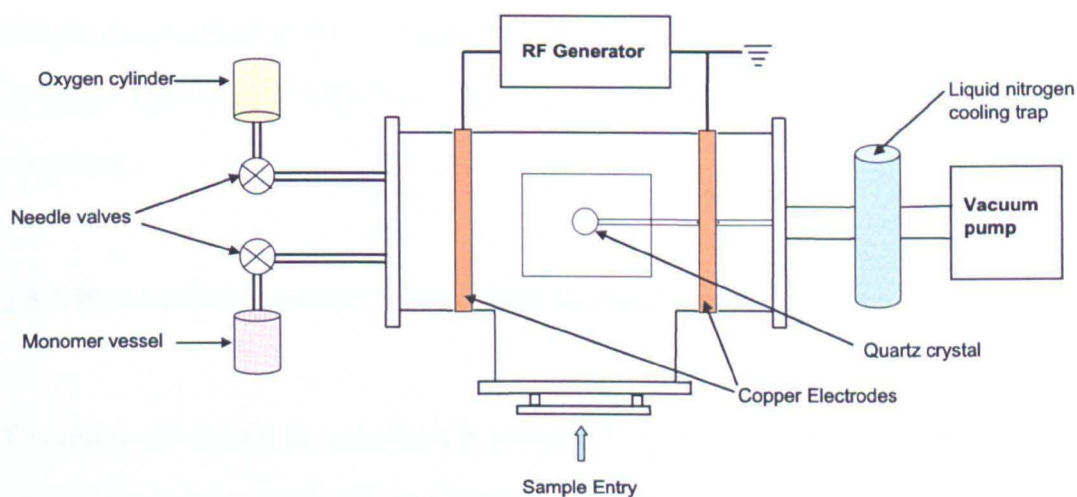
Figure 2.2: Illustration showing the plasma machine used to etch PLGA membranes, PET filters and deposit ppAAc coatings.

2.3.1 PLGA Scaffold Oxygen Plasma Treatment

uPLGA scaffolds (see section 2.2) were rinsed with ultra-pure ELGA water and allowed to dry in a desiccator for 3 days. They were then oxygen etched with a plasma struck at 20W at an oxygen pressure of 300mTorr. The plasma was allowed to run for varying durations (see chapter 3 and 4) not exceeding 2 minutes. The etched scaffolds (ePLGA) scaffolds used for cell work were etched for 90 seconds. Scaffolds were used immediately after plasma etching. No further sterilization was employed before cell culture. Pore dimensions of the ePLGA surfaces were determined from scanning electron microscope images using Image J (NIH,USA).

2.3.2 Oxygen Plasma Treatment of Coculture Supports

To sterilise the coculture supports (poly(ethylene terephthalate) - PET filters), were oxygen plasma treated for 5 minutes on each side. A plasma was struck at 20W at an oxygen pressure of 300mTorr. The filters were used within 24 hours of plasma treatment.

2.3.3 Plasma Polymerised Acrylic Acid for Cell Sheets

To create cell sheets as described in chapter 5, clean glass coverslips were coated with plasma polymerised acrylic acid (ppAAc). Prior to deposition, the acrylic acid monomer was degassed at least once using a freeze/thaw cycle. To clean the coverslips, they were placed in ultrapure water and sonicated for 15 minutes. This procedure was repeated 3 times. They were then rinsed in high performance liquid chromatography (HPLC) grade acetone (3 times) before being allowed to dry naturally. The dry coverslips were placed in the plasma chamber and oxygen etched at a power of 20 W, under a working pressure of 300 mTorr oxygen for 5 minutes. The coverslips were then ppAAc coated using a plasma struck at a power of 20 W, under a working pressure of 250 mTorr acrylic acid. Post deposition, the monomer was allowed to flow for three minutes prior to removal of the samples from the chamber. The entire procedure was repeated individually with power varying in increments upto 100W (see chapter 5). The deposition time varied from 3 to 12 minutes.

2.4 SURFACE ANALYSIS

2.4.1 X-Ray Photoelectron Spectroscopy (XPS)

XPS is a surface sensitive technique that allows analysis of the chemical functionalities present on a material surface. X-ray photons are used to bombard the material surface resulting in ejection of electrons from the inner shell of the atoms or molecules that comprise the material surface. The binding energy of these characteristic electrons can then be used to identify the chemical functionalities on the surface of the material. Mathematically, the simplified equation used to achieve this is

$$KE = h\nu - BE$$

Where KE is the energy of the photoelectron, $h\nu$ is the energy of the photon (h is Planck's constant and ν is the frequency of the photon) and BE is the binding energy of the photoelectron. The analysis depth with the X-ray beam at a right angle to the surface is approximately 10nm.

All samples were analysed using a Kratos Axis ULTRA spectrometer with monochromated Al Kα X-rays (1486.6eV) operated at 15mA emission current and 10kV anode potential. Pressure within the chamber was better than 10^{-9} Torr. A charge neutraliser filament placed above the sample surface gave a flux of low energy electrons to provide uniform charge neutralisation. A survey spectrum was recorded over a binding energy range of 0 to 1400 eV with a pass energy of 80eV. Detailed analysis of the C1s and O1s regions of each sample was performed using high resolutions scans with a pass energy of 20 eV. The take off angle for the photoelectron analyser in all cases was 90°.

Curve fitting was carried out using *Casa* XPS software (Casa Software Ltd, Cheshire, UK). Relative sensitivity factors were supplied by the manufacturer. A Gaussian-Lorentzian function with a 70% Gaussian component was applied to all data and found to give a satisfactory fit. No asymmetry component was introduced. Any constraints used are reported in the relevant results chapters.

To assess the surface chemistry of uPLGA and ePLGA films in a degraded state, samples were removed from degrading media and rinsed in water (3 times for 15 min each) then allowed to dry in a desiccator. For the starting value (day 0 of degradation), uPLGA and ePLGA samples were not immersed in degradation medium. They were analysed within 24 hours of preparation (see section 2.2 and 2.3). For ppAAc coated glass samples were analysed within 24 hours of acrylic acid plasma deposition. No further treatment was applied prior to XPS analysis.

2.4.2 Water Contact Angle (WCA)

Water contact angle (WCA) is a measure of the wettability of a material surface. It is described as the angle at which the liquid gas phase (LG) meets the solid liquid phase (SL). This is illustrated in figure 2.3 below.
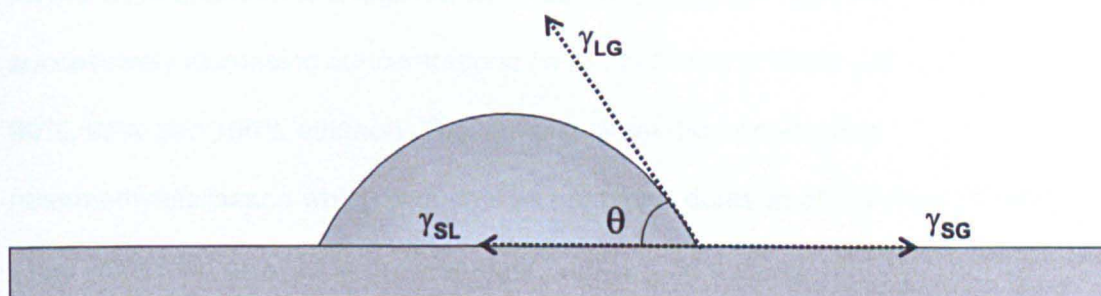
Figure 2.3: Water Contact angle θ is shown on a material surface.

The sessile droplet method using a CAM200 instrument (KSV Instruments, Ltd) was employed to obtain the water contact angle. An approximately 2-3µL sized droplet was dispensed onto each sample. Digital images of the droplet were taken at a shutter speed of 1 image per second for 20s. The images were then used to calculate the initial contact angle using the Young Laplace equation. For each sample at least 3 measurements were taken over different areas.

2.4.3 Scanning Electron Microscopy (SEM)

In Scanning Electron Microscopy (SEM), a beam of electrons is rastered over the surface of a conductive material yielding secondary electrons from the material surface. These electrons are then used to provide a topographical image of the material surface.

Samples with cells were fixed first to preserve the structural organization and appearance of the cells. To achieve this, the cells were soaked in 3% glutaraldehyde in PBS overnight. They were then rinsed in PBS (3 times) and coated with a conductive layer of osmium (1% osmium tetroxide in PBS). After two hours in this solution, the cells were rinsed in water (3 times for 15 minutes each). As the SEM chamber is a high vacuum, the cells were then dehydrated gently in successively increasing concentrations (v/ v) of ethanol in water (25%, 50%, 70%, 90%, 95% and 100% ethanol). The samples were then dried using hexamethyldisilazane which was applied neat for a duration of 5 minutes (twice). They were then allowed to dry overnight prior to gold coating.

All polymer samples (with or without cells) were gold coated to introduce a conductive layer for SEM. The samples were coated in using a sputter coater (Pelco Sputter Coater 91000) set at 20 mA for a total time of 3 minutes. Topographical

images were captured using a JEOL JSM-6060LV Scanning Microscope operated at

10 -12 kV at varying magnifications as shown on individual images.

2.4.4 ATOMIC FORCE MICROSCOPY (AFM)

Topographical images of a surface can be captured using atomic force microscopy.

Typically a tip attached to a cantilever (figure 2.4) scans the material surface. A

laser is used to track its position allowing topographical images in the nanoscale

range to be captured.
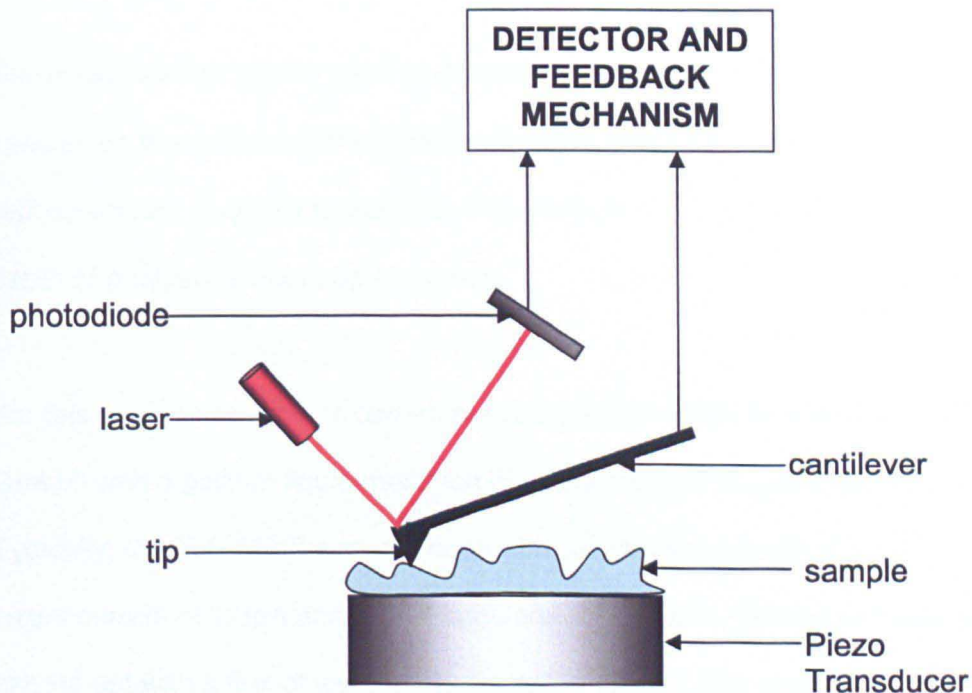
Figure 2.4: Key components of the AFM

In this work, a Dimension 3000 AFM with a NanoScope IIIa controller (Veeco

Instruments, CA) was used in tapping mode to obtain images of uPLGA and ePLGA

samples (matt and shiny sides). Surface roughness and images of the surfaces

were processed using The Scanning Probe Image Processor (SPIP, Version

3.3.6.0,2005, Image Metrology). Appropriate plane corrections were used prior to determining surface roughness.

2.4.5 Time of Flight Secondary Ion Mass Spectrometry (ToF SIMS)

ToF SIMS is an analytical technique that allows chemical characterisation of a surface. A primary ion beam is directed at a surface enabling the release of several species including electrons, photons and secondary ions. The secondary ions are accelerated into a mass spectrometer where their mass is analysed by measuring their time of flight from the sample surface to the detector.

The mass spectra can be used to determine the elemental and molecular chemical species on the surface of the material. Images or ion fragment maps can be retrospectively acquired to visualize the distribution of species on the surface. The depth of analysis is approximately 1nm.

For this work, analysis was carried out using a ToF-SIMS IV instrument (ION-TOF GmbH) with a gallium liquid metal ion gun and a single stage reflection analyser. Typically, the ToF SIMS was operated at a primary ion energy of 15-20kV, pulsed target current of 1.3pA and a post acceleration of 10KV. Charge compensation was carried out with a flux of low energy electrons (20eV). The primary ion dose was kept below the static limit with a maximum dose of 10^{12} ions per cm^2 (Marletta *et al.*, 1990).

ToF SIMS negative spectra were acquired over a mass range of m/z=0-200 and the area of analysis was 500μm x500μm. The raw data was analysed using Ion Spec ToF SIMS software (ION-TOF GmbH). Ion fragment maps were constructed using this data.

From published literature, selected peaks due to the peptide backbone present in horseradish peroxidase were highlighted in the negative spectra (Wagner and Castner, 2001, Wuhrer *et al.*, 2004). These are the CN⁻ (m/z= 26) and CNO⁻ (m/z = 42). For comparison purposes, these peaks were normalized to the sum of their intensity to ensure correction due to variations in the total secondary ion yield.

2.5 GEL PERMEATION CHROMATOGRAPHY (GPC)

Gel permeation chromatography allows measurement of the molecular weight of various polymers. This technique relies on size exclusion allowing larger molecules to be eluted first from a column before smaller fragments. The pathway for the smaller fragments is slower as they can access pores within the column, creating a more tortuous path prior to elution.

The molecular weights and polydispersity indices of the uPLGA and ePLGA films including degraded samples were determined by GPC (Polymer Labs GPC-120). This was performed using a K-501 HPLC pump with two phenogel 5 µm MIXED-C columns (300×7.5 mm^2, particle size 5 µm, with its linear calibration range of M_w 200–2,000,000 g/mol), 1 phenogel 5 µm Guard column (50×7.5 mm^2, particle size 5 µm) and refractive index detector. For analysis, the polymer was dissolved into tetrahydrofuran (THF) in toluene at a concentration of 3mg per mL.

2.6 MAMMALIAN CELL CULTURE

In cell culture human colonic epithelial and myofibroblast intestinal cell lines were used. The epithelial cell line selected was the human caucasian adeno-carcinoma

cell line (Caco-2) obtained from ECACC and the cells were used between passage 42 and 48. The human colonic myofibroblasts cell line (CCD-18Co) was obtained from ATCC and used between passage 7 and 9. Caco-2 cells were cultured in Dulbecco's Modified Eagle's Medium (DMEM), supplemented with 1% antibiotic/antimycotic solution, 10% foetal calf serum (FCS) and 1% non-essential amino acids. Complete media for CCD-18Co cells was similar to Caco-2 cells without non-essential amino acids.

The cells were incubated at 37°C in a humidified, 5% CO_2 atmosphere. Post confluence, the cells were removed from the tissue culture flasks using 0.25% trypsin/ 0.02% ethyl amine tetra acetic acid (EDTA) in PBS.

Where relevant, images of the cells were captured using a Leica DM IRB microscope. For light microscopy, cells were illuminated with a 12V, 100W Halogen lamp. Images were captured using a QICAM Fast 1394 camera (QImaging, Canada). Image analysis was carried out using QCapture Pro software version 6.0 (QImaging, Canada).

2.6.1 Monoculture, Coculture and Transepithelial Resistance

For monoculture, myofibroblast cells (CCD-18Co from American Type Culture Collection - ATCC) were seeded at a concentration of 2 x10^5 cells/cm^2 per filter (see figure 2.5). For epithelial cells (Caco-2 from European Collection of Cell Cultures - ECACC) in monoculture, cells were added in a similar manner and concentration into separate filters (BD Biosciences, 1μm pores). These are filter shaped inserts for tissue culture with a porous PET surface to act as a scaffold for cell support). Cells were cultured in the incubator for 14 days during which time media was changed daily .

In coculture, cells were set up as shown and described in figure 2.5. Filters were inverted as shown in figure 2.5 and CCD-18Co cells were seeded and incubated for 18 hours to allow the cells to attach. The filters were then reverted, transferred into a new well with fresh media added to both sides of the filter. The cells were cultured in the same manner and duration as the monoculture filters (upto 14 days).

Monoculture

Filter

Cells

Media filled well

Coculture

Myofibroblasts

Filter

Epithelial cells
Myofibroblasts
Media filled well
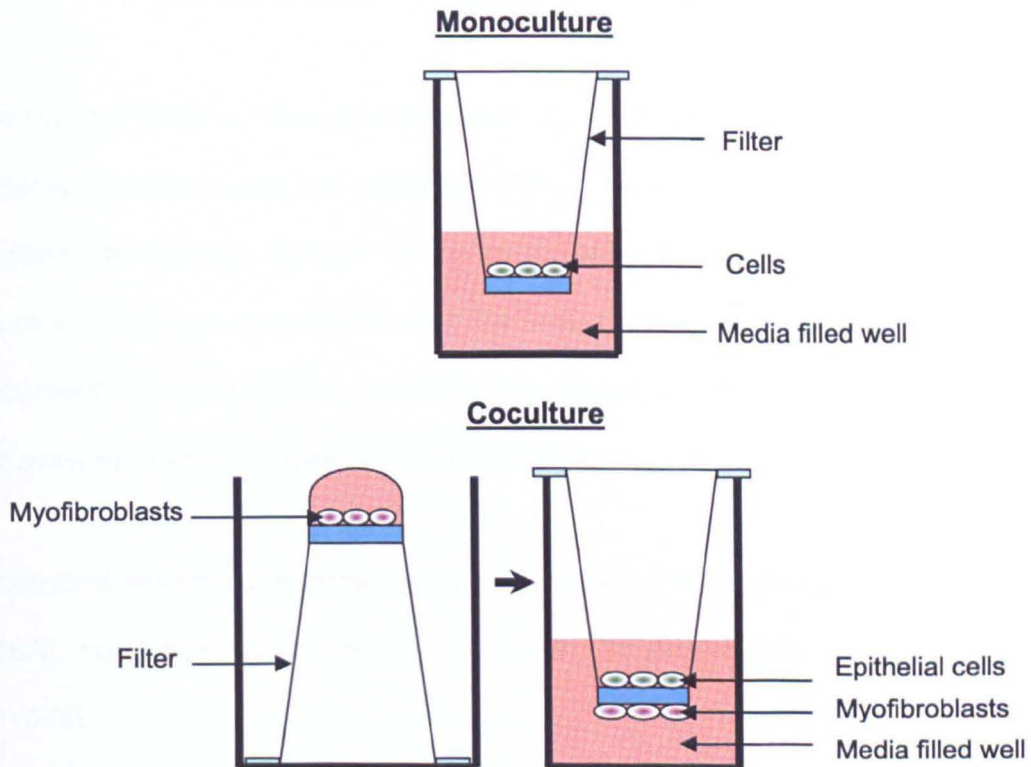
Figure 2.5: Monoculture and coculture experimental setup. In monoculture, cells were seeded directly onto a filter and cultured (top). In coculture, myofibroblasts were seeded on an inverted filter and allowed to attach. After 18 hours, the filters were inverted and epithelial cells were seeded onto the luminal side of the filter.

For the ePLGA membrane, an oxygen plasma treated membrane (as described in chapter 3), was held in place as seen in figure 2.6 with a cell culture insert (scaffdex, Finland). Cells were cultured in monoculture and coculture in exactly the same manner as the filters.
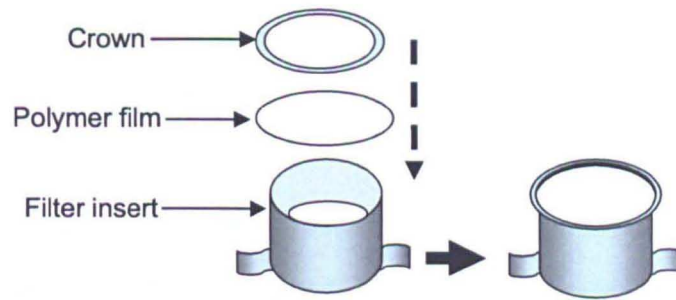
Figure 2.6: Schematic of inserts for PLGA based polymer films.

To monitor TEER as described previously (Lo *et al.*, 1999, Neuhaus *et al.*, 2006), at appropriate time points, the resistance of the cells was measured using an epithelial voltohmeter (EVOM, World Precision Instruments). The TEER was calculated by subtracting the resistance of a blank filter/insert from the resistance of the appropriate monoculture or coculture. The result was multiplied by the area of the filter/insert ($0.9cm^2$) to express the TEER in Ωcm^2.

Statistical analysis was carried out using GraphPad Prism (GraphPad Software, USA). Two tailed unpaired t-tests were used. Statistical significance was set at $P<0.05$.

2.7 CELL FUNCTION ASSAYS

2.7.1 Alamar Blue Assay

The metabolic activity of the cells was measured using the Alamar Blue assay. This assay is based on the non-fluorescent blue dye resazurin which undergoes reduction in the presence of metabolically active cells and is converted to a pink fluorescent product, resorufin.

Cells were seeded at a concentration of $2x10^4$ cells/cm^2 onto the PLGA films and also onto tissue culture plastic. They were cultured for and tested at fixed time points. One mL of stock Alamar Blue solution was diluted in 9mL of Hanks Balanced Salts Solution (HBSS) without phenol red. This was used to replace cell culture media and incubated for 90 minutes. One hundred μL of the post incubation Alamar Blue solution was then used to measure fluorescence with an MFX fluorometer (Dynex technologies). Ultraviolet light at an excitation of 355nm and emission of 460nm was used.

Statistical analysis was carried out using Graph Pad Prism (Graph Pad software Inc, San Diego, California). Group comparisons were assessed by analysis of variance (ANOVA) using the repeated measures test followed by Tukey's multiple comparison post test. Statistical significance was set at $p < 0.05$.

2.7.2 Hoechst Assay

Hoechst 33258 (bisbenzimide) is a fluorescent dye that intercalates double stranded DNA at adenine and thymine rich regions. The action of this dye allows quantification of the DNA contained in a sample relative to the fluorescence intensity.

A series of solutions were prepared as detailed in appendix 2. One hundred μl of the working solution was added to 100 μL cell lysate in a 96 well plate. Fluorescence intensity was then measured using an MFX fluorometer with excitation set at 355nm and emission at 460nm.

Statistical analysis was carried out using GraphPad Prism (GraphPad Software, USA). Analysis of variance (ANOVA) was used with statistical significance set at $P < 0.05$. A Tukey's multiple comparison post test was used.

2.7.3 CellTracker Assay

CellTracker™ is a commercial live cell staining product based on chloromethyl derivatives. It permeates the membrane of live cells and is converted in the cytosol to produce membrane impermeable fluorescent adducts.

Cell sheets were seeded onto 3D scaffolds (see chapter 5). After 3 days in culture, cell culture media was removed and substituted with a solution containing CellTracker™ Green CMFDA (5-chloromethylfluorescein diacetate). This solution was prepared according to manufacturer standards. In brief, 1 vial of CellTracker™ Green CMFDA was dissolved in 10μL of dimethylsulphoxide and added to 10mL of supplemented media without foetal calf serum. The cells on the surface were then incubated in this solution for 45 minutes. After this time period, the CellTracker™ containing media was aspirated and substituted with supplemented media without foetal calf serum. The cells were then cultured for another 45 minutes. At this point the cells were then washed in PBS and imaged using a Leica DM IRB microscope. The fluorophore was excited by a ultra violet light through a band pass filter (I3 blue 450-490nm)

2.7.4 Live/dead Assay

The live/dead cell viability assay is a commercial fluorescence based kit. There are two components in the kit, calcein AM and ethidium homodimer-1. Calcein AM is hydrolysed to a green-fluorescent product (calcein); indicating that the cells have

esterase activity and an intact membrane, therefore, alive. Ethidium homodimer-1 is a red-fluorescent nucleic acid stain that can only enter compromised membranes of dead cells.

A live/dead solution was prepared by mixing 20 μL of 2 mM ethidium homodimer-1 to 10 mL PBS. After vortexing this mixture, 5 μL of 4 mM Calcein AM was added and the solution was vortexed again.

Cell media from test samples was aspirated and the cells were washed 3 times in PBS. The prepared live/dead solution was then added to the samples and incubated at room temperature for 40 minutes. The solution was then aspirated off and the cells were washed with PBS (3 times for 15 minutes at each time). The samples were then imaged using a Leica DM IRB microscope. The fluorophores were excited by a ultra violet light through band pass filters (N2.1 green 515-560nm for ethidium homodimer-1 and I3 blue 450-490nm for calcein AM).

2.8 HISTOLOGY

2.8.1 Immunostaining

Solutions were prepared as listed in appendix 2. For each sample, culture medium was removed and cells were rinsed with PBS (repeated 3 times for 15 minutes each time). The cells were fixed at room temperature for 20 minutes in 4% PFA. The fixative was removed and the cells were rinsed with PBS as described previously. The cell membranes were then made permeable (porous) by covering the surface of the cells in permeabilising solution as detailed below.

Permeabilising Solution

HEPES	0.48g	Magnesium chloride	0.06g
Sucrose	10.27g	Triton X-100	0.5mL
Sodium Chloride	0.29g	Distilled Water	100mL

The samples were then transferred to a freezer at 0°C for 10 minutes (the solution was not allowed to freeze). The permeabilising solution was then removed and the cells were rinsed in PBS again as described previously

Prior to immunostaining, a sufficient amount of a solution of 1% (by weight) bovine serum albumin (BSA) in PBS was used to cover the cells. This solution was used to block non-specific binding of the antibody and was removed after 30 minutes at room temperature.

Primary antibodies were dissolved in a solution of 1% (by weight) BSA in PBS. Final concentrations of the antibodies are shown below. The prepared antibody solutions were added to cells and allowed to bind at room temperature for 60 minutes. Please note that each antibody was used separately on an individual sample

Primary Antibody

Monoclonal mouse anti human smooth Muscle Actin IgG2A   700ng/mL

Monoclonal mouse anti human E-Cadherin IgG_1 1460ng/mL

The primary antibody was removed and the cells were washed in a solution of 1% (by weight) BSA in PBS (3 times for 15 minutes each time). A secondary antibody fluorescein isothiocyanate - FITC anti mouse IgG (Fab specific) (Sigma Aldrich, UK, Catalogue number F5262) was then added. This antibody was diluted from stock at a volume ratio of 1 part antibody to 128 parts of a solution of 1% (by weight) BSA in

PBS. The antibody in solution was allowed to bind at room temperature for 60 minutes. The cells were then washed in a solution of 1% (by weight) BSA in PBS as described previously and mounted in ProLong Gold antifade reagent with 4',6-diamidino-2-phenylindole (DAPI). Cells were then viewed using a Leica DM IRB microscope with ultra violet light through a band pass filter (I3 blue 450-490nm).

2.8.2 Haematoxylin and Eosin Staining

Paraffin embedding

Sections of tissue were paraffin embedded using an automated processor (Leica TP1020). The tissue was dehydrated gently using a sequence of solvents where solvent dilution was necessary a volume by volume mixture in distilled water was used. The sequence used was 25% ethanol -1hour; 50% ethanol – 1 hour; 70% ethanol – 1 hour; 95% ethanol – 1hour; 100% ethanol – 1 hour (repeated with a change of ethanol) and finally 100% xylene – 1 hour (repeated with a change of xylene). The dehydrated tissue was then dipped in molten paraffin wax at 62°C (Repeated twice for a duration of 2 hours each). The tissue was removed from the automated processor and transferred to a wax embedder (Leica EG1160). The tissue was correctly oriented, coated in molten wax and allowed to cool. A microtome (Leica RM2165) was used to section the tissue into 10 micron thick samples.

Staining

Paraffin embedded section were rehydrated using the following sequence of solvents (solvent dilution as described above): xylene - 3 x 1 minute; 100% industrial methylated spirit (IMS) - 5 minutes; 90% IMS (volume by volume in water) - 5 minutes; 70% IMS - 5 minutes; 50% IMS - 5 minutes; tap water- 5 minutes.

The sections were then placed in Gill's haematoxylin for 10 minutes and washed in tap water to remove excess stain (between 5 and 30 minutes). The samples were then placed in Scott's tap water for 2 minutes before a second wash in tap water. The samples were dehydrated through a sequence of solvents each for a period of 5 minutes, 50% IMS, 70% IMS and 90% IMS - 1 minute.

The sections were then dipped 3 times in 1% alcoholic eosin before further dehydration by dipping in 100% IMS (2 times) and xylene (2 dips) The sections were allowed to air dry to the touch before mounting with distyrene, plasticizer and xylene (DPX) and being allowed to dry overnight.

2.9 METHODS FOR THE THREE DIMENSIONAL PLGA PARTICLE BASED SCAFFOLD

2.9.1 POP Block for Electron Beam Lithography

Polyolefin plastomer (POP) pellets were placed between metal plates and melted at 190 °C for 1 hour under a weight of 25 kg. The melted pellets were allowed to cool to room temperature to form a solid POP block. A set of release films were placed between the metal plates to ease removal of the POP block. The POP block was then rinsed with ethanol and allowed to dry.

2.9.2 Electron Beam Lithography

It was proposed that the scaffold would be formed from a mould bearing imprints of the desired dimensions of the colon (figure 2.7).

Electron beam lithography performed by Nikolaj Gadegaard was used to create the mould . The technique has been described previously (Gadegaard *et al.*, 2003). Silicon substrates were coated with ZEP 520A resist. They were then baked for a few hours at 180 °C and afterwards exposed in a Leica LBPG 5-HR100 beamwriter at 50 kV. A 1 cm^2 area was patterned with pits using spot sizes as desired (see Chapter 5). The silicon substrate was then heated and pressed against a POP block to transfer the pattern.
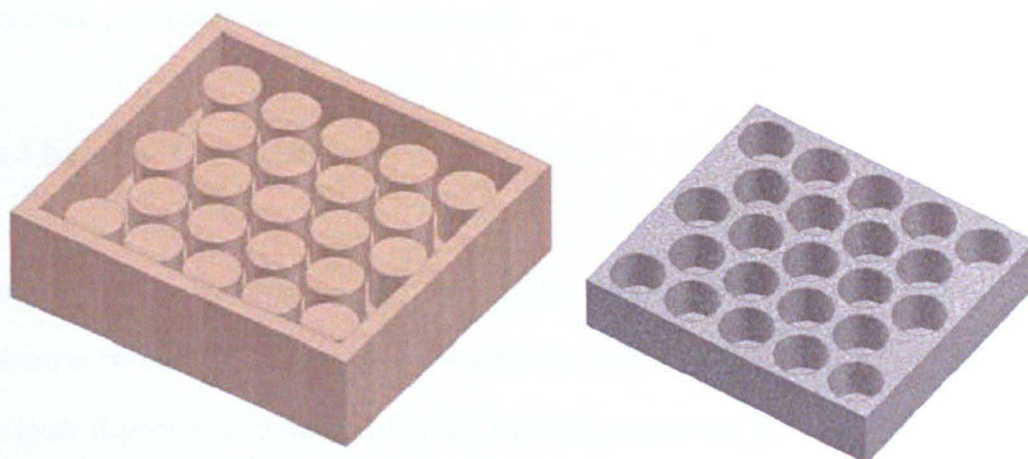
Figure 2.7: Computer Aided Design (CAD) model of the mould (left in brown) and scaffold (right in grey)

2.9.3 PLGA and PLGA-HRP Particles

PLGA particles were prepared by an emulsion method. PLGA 85/15 Mw 35000 (Lakeshore biomaterials) was added to dichloromethane to form a 3% w/w solution. Separately a 10% solution of PVA in distilled water was made and filtered. Equal volumes (4 mL each) of the 3% PLGA solution and the 10% PVA solution were mixed and homogenized at 12400 rpm for 5 minutes. The emulsion was then added to 1L of 0.3% PVA in water under constant stirring allowing the particles to form. The dichloromethane was allowed to evaporate overnight before the particles were

separated from the liquid removed through centrifugation. The particles were freeze dried for 3 days and stored in the freezer.

To incorporate the model protein horseradish peroxidase (HRP), a solution of this protein (10mg in 250μL of water) was added to the PLGA/dichloromethane solution. The PLGA-HRP particles were then formed as described previously by mixing the PLGA/dichloromethane - HRP solution with an equal volume of a 1% PVA solution and homogenizing at 12400 rpm for 5 minutes. All other subsequent steps as described previously were then performed.

2.9.4 Dynamic Light Scattering

Particle size was determined by dynamic light scattering (DLS) using a Malvern Zetasizer Nano 4700 instrument with vertically polarised light supplied by an argon-ion laser (Cyonics) operated at 40 mW. For DLS experiments, the particles were suspended in ultrapure water at a concentration of 1mg/mL mixed for 5 min and transferred to a disposable cuvette. The measuring angle was 90^0 to the incident beam. All experiments were performed at room temperature and an average of 30 readings per sample was undertaken.

2.9.5 Enzyme Activity Test

3,3',5,5'-Tetramethylbenzidine (TMB) is a substrate for the HRP enzyme with a sensitivity of 0.15ng/ml. TMB undergoes a colour change from colourless to blue or blue-green in the presence of HRP. To test the activity of the PLGA-HRP particles, 500μL of TMB were added to the particles and digital images were taken to record the colour change. Experiments were performed at room temperature and the colour change was instantaneous.

2.9.6 Particle Scaffold

To prepare scaffolds for cell culture, PLGA particles were suspended in a 0.01%
Tween in PBS solution to form a slurry, placed on the mould and allowed to air dry
for 2 hours. The three dimensional scaffold was formed by sintering the particles on
the mould for 1.5 hours at 60°C. The scaffold was then allowed to cool overnight
before being separated from the mould.

To prepare the bilayer scaffold, the PLGA layer was set first using PLGA particles
suspended in 0.01% Tween in PBS. 1µL of this solution was applied to the mould
and allowed to dry. PLGA-HRP particles were then suspended in 0.01% Tween in
PBS and added to the scaffold. This was also allowed to dry before sintering the
particles as described previously.

2.9.7 Production of Cell Sheets for Scaffold Seeding

Human caucasian colonic adenocarcinoma (Caco-2) cells were maintained in cell
culture flasks as described in section 2.6. At 80% confluence, the cells were
removed with trypsin and seeded at a concentration of 1.4×10^4 cells per cm^2 onto
ppAAc coated glass coverslips (discharge power for ppAAc = 20W). For initial
comparison testing, a positive control of tissue culture plastic and a negative control
of clean glass coverslips were also seeded with cells at the same time. Images
($1mm^2$) were captured using a Leica DM IRB microscope and ImageJ (NIH, USA)
was used to determine the area of the image which was covered by cells. Statistical
analysis was carried out using Graph Pad Prism (Graph Pad software Inc, San
Diego, California). Group comparisons were assessed by analysis of variance
(ANOVA) using the repeated measures test followed by Tukey's multiple
comparison post test. Statistical significance was set at $p < 0.05$

For the cells seeded on ppAAc coverslips, after 5 days in culture when the cells had reached confluence, gentle agitation was used to lift the cells off the coverslips as cell sheets. The cell sheets were then transferred to a scaffold. The sheet was held in place by a clean coverslip overnight. The scaffold was then left in culture for 5 days.

CHAPTER 3: CHARACTERISING THE DEGRADATION OF PLGA BASED SCAFFOLDS

As described in chapter 1, scaffolds often play an integral role in tissue engineering. This Chapter describes the manufacture of a PLGA based scaffold and subsequent modification for eventual use as an intestinal cell support. The degradation properties of both the unmodified and modified scaffolds were investigated. Key differences emerged, establishing the need to study scaffold degradation characteristics in tissue engineering.

3.1 INTRODUCTION

Poly (D,L-lactic-*co*-glycolic acid) is a copolymer based on aliphatic polyesters that

has had extensive use in tissue engineering as a temporary scaffold to organise

cells prior to tissue regeneration (Cima *et al.*, 1991, Giordano *et al.*, 1997). This

polymer is attractive for a variety of reasons. It is synthetic, therefore, can be

produced relatively uniformly and importantly possesses quantifiable, controllable

and replicable mechanical and degradation properties (Lu *et al.*, 1999). Its chemical

structure is shown in figure 3.1 below.
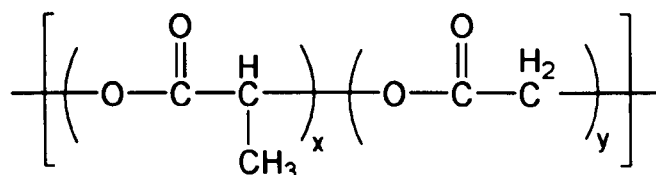
Figure 3.1: Chemical structure of PLGA

PLGA scaffolds as prepared tend to be intrinsically hydrophobic, a property which

can limit cell attachment as described in chapter 1 (Pang *et al.*, 2007, Khang *et al.*,

2002, Safinia *et al.*, 2008). Appreciably, as cell attachment is a prerequisite property

for future cell behaviour such as proliferation, the scaffold surface has to be tailored

for tissue engineering applications. Researchers can achieve this goal by several

methods but focus was drawn to plasma modification due to the fact that it is a

relatively simple process which can be monitored adequately during modification,

does not rely on line of sight and can sterilize surfaces (Holy *et al.*, 2001, Chu *et al.*,

2002).

The modification of the material through plasma could potentially affect several

intrinsic properties; perhaps, the most apparent being surface chemistry and

degradation. Degradation principally could be further exacerbated when the material is placed in an aqueous environment at a higher temperature as would happen should the material be placed *in vitro* in an incubator or *in vivo*. Intuitively, the mechanical stability of the scaffold would be affected as degradation proceeds and as the degradation products are acidic, there is some concern about the effect of localized low pH at implant sites specifically on cell and host response (Griffith, 2000). As the intestine is not a load bearing tissue, mechanical strength is of less concern in comparison to potential cell response.

Various studies have concluded that the biological response is affected by the degradation rate specifically in respect to cell viability, cell growth and host response. This is reflected by Sung *et al* who observed that cell viability was inversely related to degradation rate (Sung *et al.*, 2004). This study was carried out on primary mouse aortic smooth muscle cells cultured on either PLGA or poly(caprolactone) PCL scaffolds. The PLGA scaffolds were described as a fast degrading polymer in comparison to PCL scaffolds. Differences in surface chemistry of the two polymers were not explored as a potential reason for the observation. In a separate study on osteoblasts, Ignatius and Claes further stress the importance of studying degradation as they found that high concentrations of degradation products from PLGA can be toxic to cells in *in vitro* culture (Ignatius and Claes, 1996). Finally an extensive review by Babensee *et al* reflected on host response to PLGA as well as other biodegradable scaffolds (Babensee *et al.*, 1998). The effect was varied ranging from mild to severe inflammatory reaction by the host in some cases to slow or impaired cell function in other cases.

For these reasons, studying the degradation of PLGA is of high interest. This chapter exclusively describes the degradation of the selected polymer in unmodified

and modified states. Linking the degradation behaviour to any detrimental or deleterious effects to cells is discussed further in chapter 4.

As PLGA is a well established material, there has already been extensive research into understanding the process and mechanism of degradation. It is known that PLGA degrades through the hydrolysis of the ester linkages into lactic and glycolic acid (Park, 1995). The ester bond is cleaved first to produce a carboxyl and hydroxyl end group. The carboxyl group then catalyses further cleavage of other ester bonds within the polymer. This is illustrated in the schematic figure 3.2.
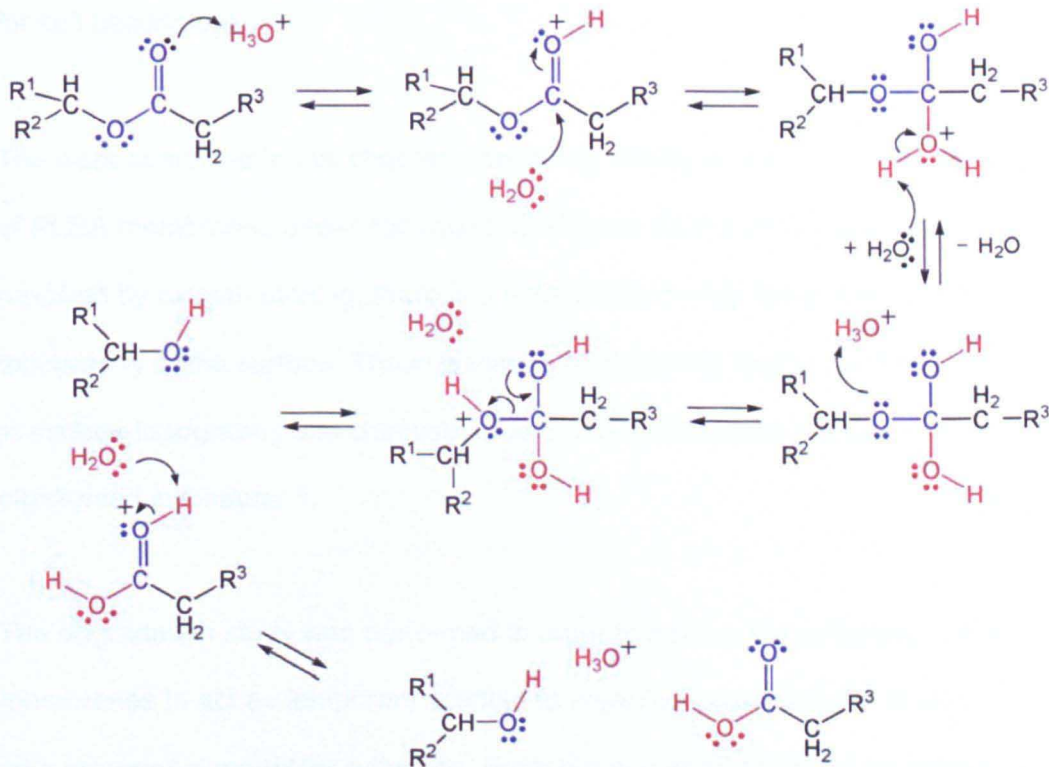
Figure 3.2: Schematic of PLGA degradation. Adapted from (Ma and Elisseeff, 2005)

In vivo, the acids produced from this degradation are eliminated from the body through the Krebs cycle. *In vitro,* degradation products can be eliminated by regular changes of fluid. Previous studies on PLGA based scaffolds have analysed the influence of a number of factors on degradation including copolymer composition, molecular weight, crystallinity, specimen size, fluid flow and environmental effects such as enzymes, temperature and pH (Cai *et al.,* 2003, Agrawal *et al.,* 2000, Griffith, 2000, Lu *et al.,* 1999, Ignatius and Claes, 1996, Grizzi *et al.,* 1995). However, to the best of my knowledge, no study has looked at surface chemistry changes during degradation. Deducing the surface polymer composition and any changes over time is essential as this part of the material presents the initial frontier for cell attachment.

The work described in this chapter extensively characterises the *in vitro* degradation of PLGA membranes under controlled conditions. As the PLGA scaffold was modified by oxygen etching, there is a potential to modify the surface chemistry and topography of the surface. The importance of observing and characterising changes in surface topography and chemistry due to the modification process was highlighted in Chapter 1.

The degradation study was performed in order to assess the suitability of the membranes to act as temporary scaffold to organise intestinal cells *in vitro* and act as a provisional matrix for adhesion. From a material perspective, an ideal surface for intestinal tissue engineering would not fluctuate greatly in surface composition in order to maintain consistent cell attachment through proteins adhered onto the surface. It would also maintain its bulk structure for a sufficiently long period to ensure time for the cells to deposit their own extra cellular matrix. This work is the first to study the surface composition of the degrading polymer.

3.2 EXPERIMENTAL

Details on the film/scaffold preparation and subsequent modification can be found in Chapter 2. Experimental procedures used within this chapter are also detailed extensively in Chapter 2.

For the degradation experiment, films were cut into 4 cm^2 pieces and placed in 6 well tissue culture plates with each well containing 7 mL of PBS. The well plates were then transferred to a plate shaker (~ 40 rotations per minute) within a humidified incubator (37°C, 5% CO_2) for periods up to 60 days. During this time period the degrading media was replaced every 2 days for the first 3 weeks and thereafter every 7 days.

The experiment was carried out such that the samples were all removed at the same time. To achieve this, samples with the longest time point initiated the experiment. Each week new samples representing the next time point in reverse chronological order would be placed into the incubator.

At the end of the experiment samples were analysed by SEM, XPS and GPC to study surface structure and composition as well as bulk degradation. After 42 days in degradation media, the samples became easily friable, making it difficult to distinguish the matt and shiny side of the films. GPC was therefore the only experimental technique employed after 42 days.

3.3 RESULTS

3.3.1 Surface Topography

The films as prepared were characterized for use as a tissue engineering scaffold. On preparation, the untreated uPLGA films, were observed to have a shiny side (side exposed to water first) and a matt side. SEM and AFM techniques were used to discern the reasons for the differences. SEM revealed that the surface of the uPLGA films as prepared was non porous (figure 3.3a). The matt side of the film had a large number of indentations on its surface compared to the shiny side. A cross sectional view of the membranes revealed a series of porous conduits across the film thickness (figure 3.3b). The film thickness was verified to be $15\mu m \pm 3\mu m$ (Average$\pm$ SD for 10 samples)

Shiny

Matt
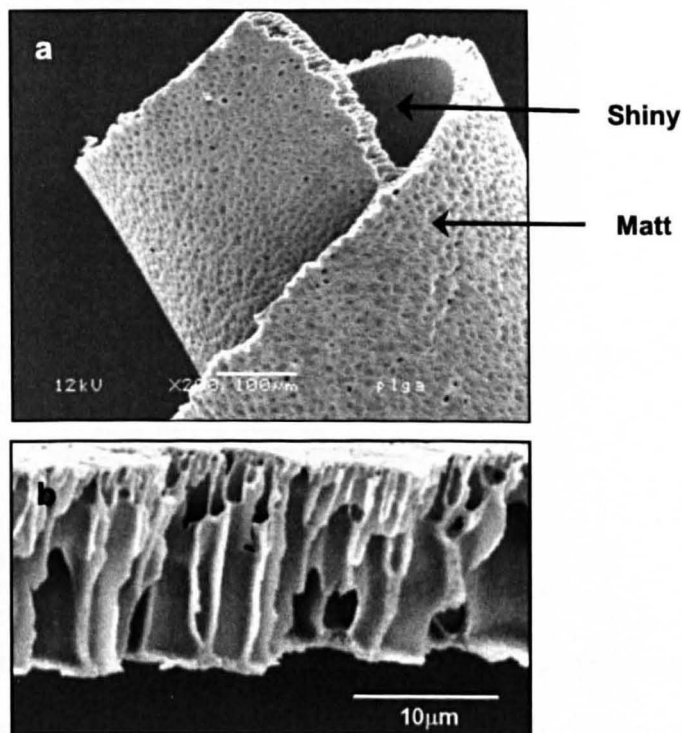
Figure 3.3: Representative images of the uPLGA films as prepared. SEM revealed indentations in the film surface (a) and porosity across the film thickness (b)

The uPLGA films were assessed by AFM (figure 3.4). The surface of the film was seen to be non porous and minor differences in roughness were noted. The root mean square roughness of the matt side of the film was measured at 137nm (z range=150nm) while that of the shiny side was measured at 32nm (z range=160nm)

Height Image

Matt Side

Shiny Side
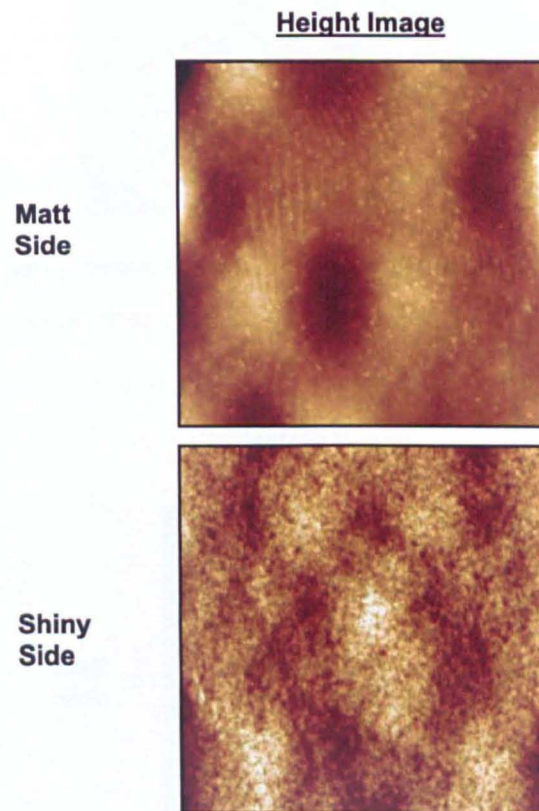
Figure 3.4: Representative AFM images of the uPLGA films. The area shown is 50μm x 50μm.

3.3.2 Changes to the Film due to Etching

As the surface of the uPLGA film was non porous, oxygen plasma treatment was employed to etch pores into the surface of the thin films. These pores are essential for the transport of nutrients and mediators across the membrane during cell culture. Scanning electron microscope studies confirmed that oxygen plasma etching did result in the production of pores on both the matt side and shiny side of the films referred to as ePLGA films after modification (figure 3.5). Visually the matt and shiny

side were still distinct. AFM imaging equally confirmed that there were pores on both sides of the ePLGA film (figure 3.6)

Matt side

Shiny side
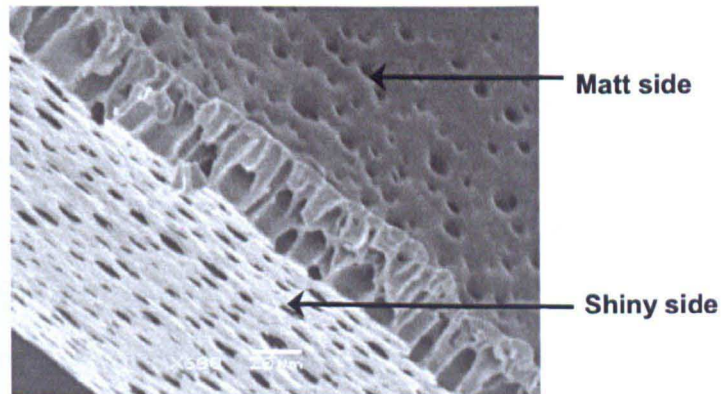
Figure 3.5: Oxygen plasma treatment induced porosity in the films. Representative image above shows a cross section through an ePLGA film.

Height Image

Matt
Side

Shiny
Side
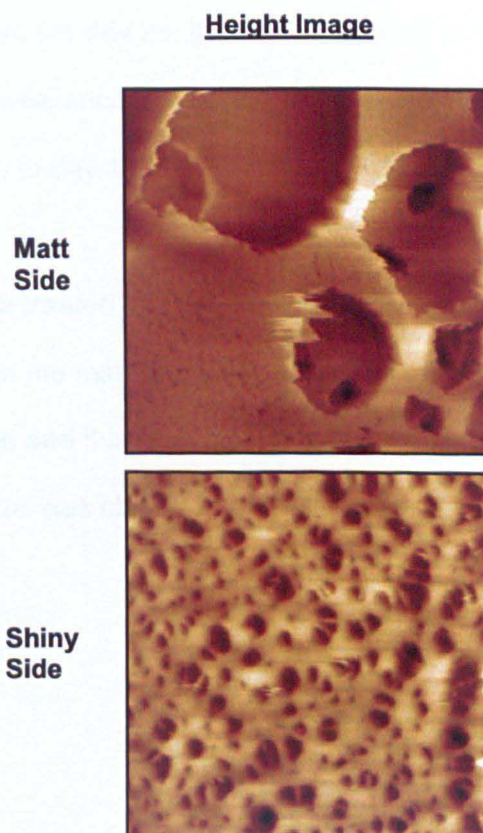
Figure 3.6: Representative AFM images of the ePLGA films. The area shown is 50μm x 50μm

3.3.3 Changes to Topography due to Degradation

As PLGA is biodegradable, observations of any alteration to the material surface appearance in terms of porosity due to culture conditions during the degradation experiments were necessary. An SEM study was carried out and revealed that the untreated uPLGA films as prepared initially had a non-porous surface prior to exposure to degradation media (figure 3.7). As degradation proceeded, the matt side of the film became increasingly porous. Around day 28 there was a significant change to the material surface (figure 3.7). The films began to exhibit a wrinkled appearance and pores were less visible. This appearance was observed through to day 42. Contrarily, the shiny side of the untreated films did not become porous through degradation. On day 28, there was similarly a change to the material surface with the appearance of indentations in the surface (figure 3.7). This was maintained through to day 42.

The oxygen plasma treated ePLGA films retained their induced porosity throughout the 42 days on both the matt and shiny side. The pore size, however, decreased with increasing time and this observation was consistent from day 0 to day 42. The decreasing pore size was observed on both the matt and shiny sides of the ePLGA films.

	Untreated uPLGA		Oxygen plasma treated ePLGA	
	Matt side	Shiny side	Matt side	Shiny side

50µm
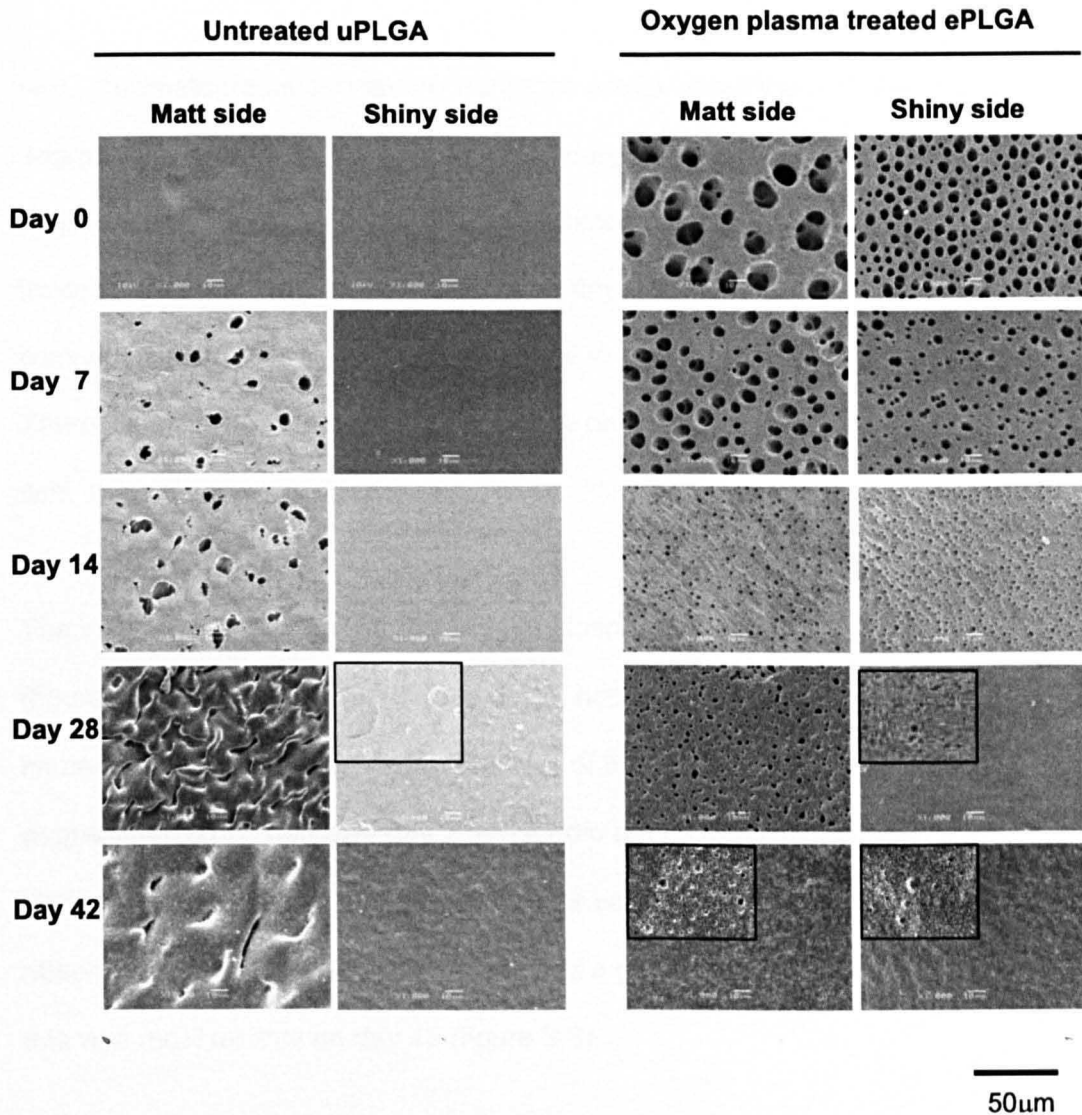
Figure 3.7: The topographical appearance of the PLGA films changed during degradation. This was monitored using SEM. Representative images of the matt and shiny side of the PLGA membrane as prepared and the oxygen plasma treated films are shown as labelled above. The images above show key points where structural changes to the material were notable (Scale bar applies to the main images, inset images magnification scale x10 relative to displayed image).

3.3.4 GPC Study of Degradation

GPC chromatograms can reveal important details about the polymer and its degradation state such as whether it is undergoing homogeneous or heterogeneous degradation. The peaks of the uPLGA samples demonstrated increasing elution times as degradation proceeded between day 0 to day 60 (figure 3.8). The elution time increase can be related to a decrease in molecular weight of the polymer. There were only single peaks noted on the chromatograms of the untreated uPLGA film.

The initial chromatogram for the oxygen plasma treated ePLGA films had two peaks (figure 3.8). These films marked as day 0, had been oxygen etched but not yet immersed into degrading media. The rest of the ePLGA films representing degradation times between day 7 and 42 did not have these bimodal peaks. A similar trend with regards to elution time as seen with the uPLGA scaffolds was observed with the ePLGA films. There was a gradual increase in elution time and this was most distinct on day 42 (figure 3.8).
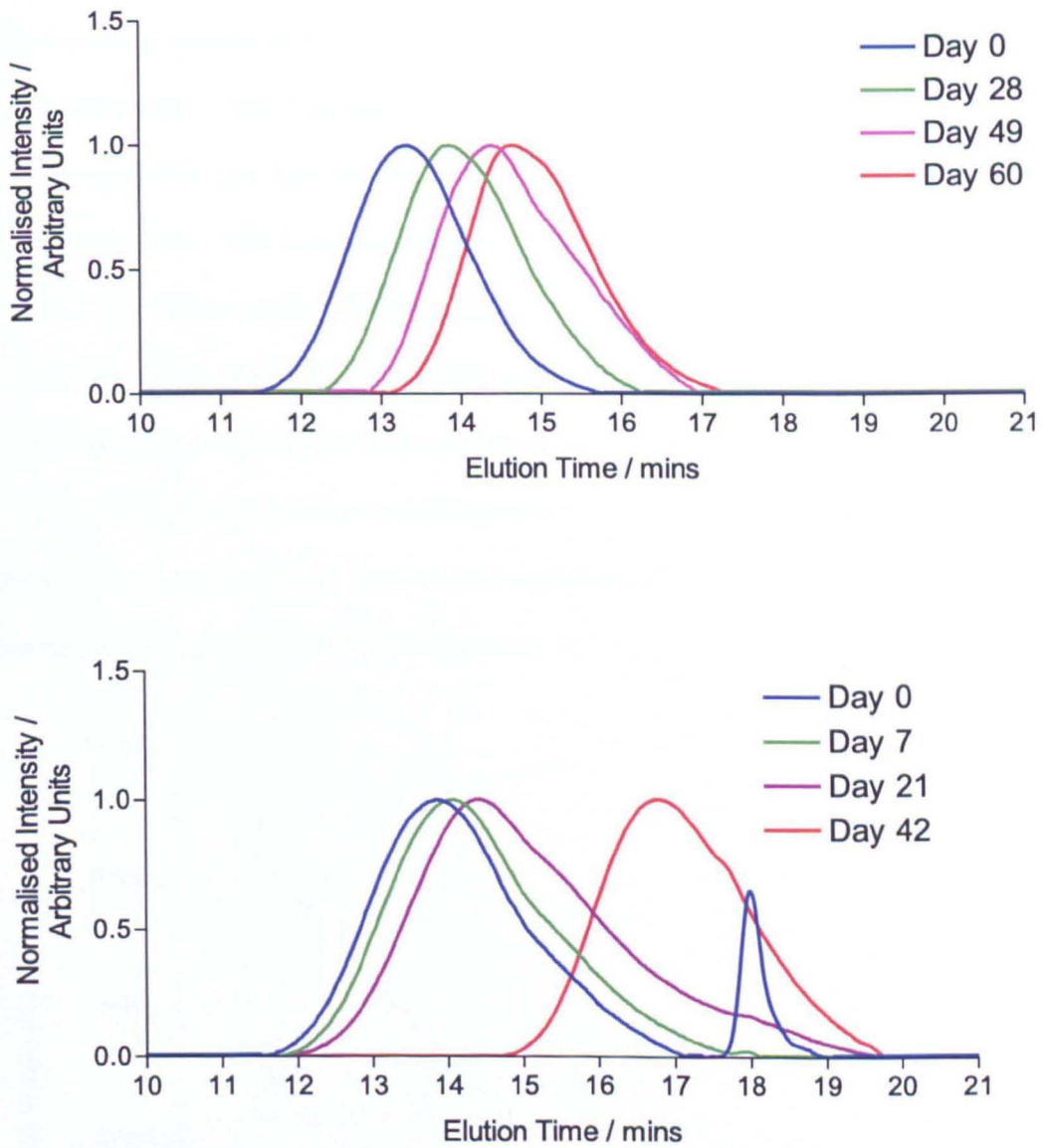
Figure 3.8: GPC chromatograms showing representative peaks of the PLGA films when untreated (top) and oxygen plasma treated (bottom).

3.3.5 Molecular Weight Changes During Degradation

The molecular weight of a polymer is predicted to decrease as degradation occurs due to breakage of the chemical bonds and related shortening chain length. Patterning its change is therefore a direct measure of degradation. In this experiment, the PLGA films decreased in molecular weight throughout degradation (figure 3.8). For the untreated film, there was a rapid loss of weight over the first 42 days, after which, the molecular weight did continue to decrease but at a much lower rate as denoted by the change of gradient (figure 3.9). The etched film on the other hand degraded rapidly throughout the course of 42 days. The final molecular weight of the etched film on day 42 was significantly less than that of the untreated membrane on day 60 (***P =0.0004 t-test).
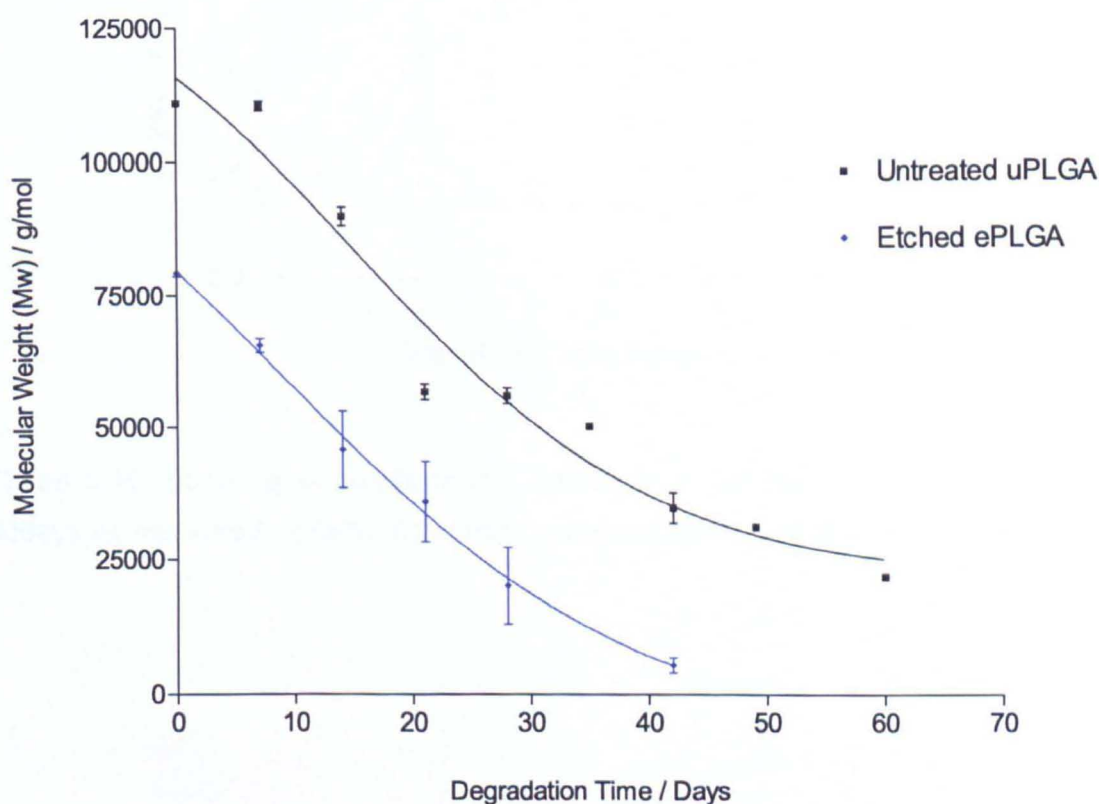
Figure 3.9: The molecular weight of the PLGA films decreased as time increased. Changes were monitored over the course of 60 days in the case of the untreated membrane and over 42 days for the etched film. Error bars represent mean ± SEM for n=3 (in some cases error bars are not visible).

3.3.6 Polydispersity Index

The PDI is the ratio of weight average molecular weight and number average molecular weight. A polymer of uniform chain length would have a PDI of 1 while a polymer composed of chains of different lengths would have PDI greater than 1. The untreated PLGA showed minimal variation ranging from 1.65 to 1.97 (figure 3.10). The etched films on the other hand, displayed a rapid increase in polydispersity between day 7 and 21 before reaching a maximum and then decreasing once more between day 28 and 42 (figure 3.10).
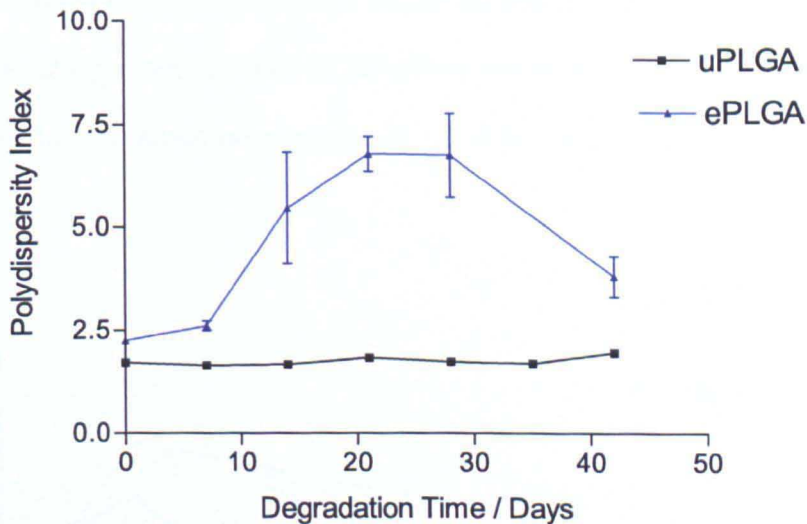
Figure 3.10: Variation in polydispersity indices of PLGA films over the course of 60days as measured by GPC. Error bars represent mean ± SEM for n=3.

3.3.7 Variation in pH During Degradation

During degradation, the media was changed frequently (see section 3.2) as PLGA is known to produce acidic by-products which can compromise cell behaviour. The pH of the media was measured weekly over the course of degradation to monitor any changes and ensure that the pH was maintained at a neutral level. The precision of the pH meter was ± 0.1.

The media containing the untreated uPLGA films was initially slightly acidic at pH 6.6 but within 2 weeks, a near neutral pH between 7.1 and 7.3 was achieved (figure 3.11). The etched ePLGA films equally began degradation at a slightly acidic pH of 6.7 before reaching a neutral level of 7.0 within two weeks. However after that point, the pH varied but remained near neutral at 7.0 or just slightly acidic at 6.8.
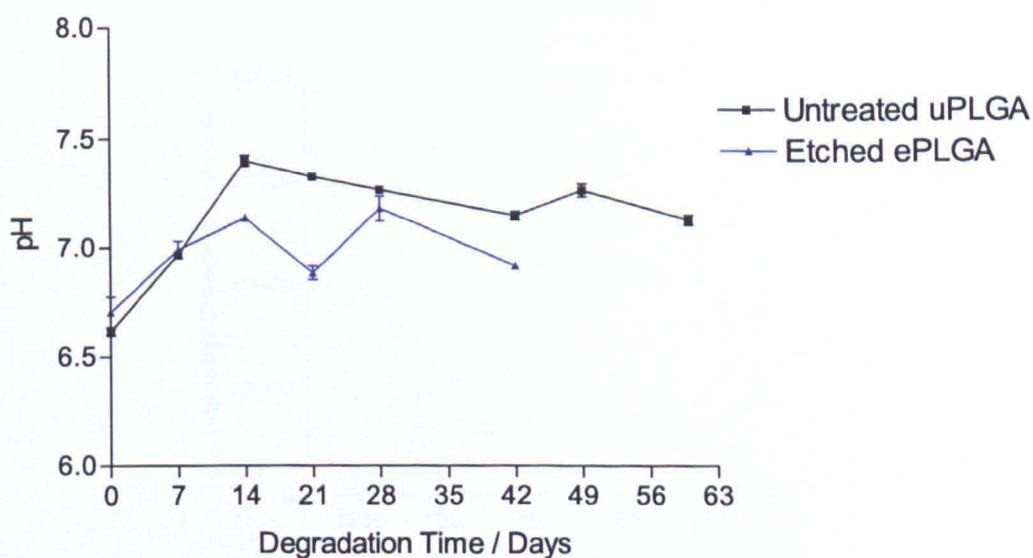
Figure 3.11: As degradation proceeded, the variation in pH was monitored. Slight differences were noted between the untreated and etched PLGA films. Error bars represent mean ± SEM for n=3.

3.3.8 Surface Chemical Analysis with XPS

The elements and functionalities present on a surface comprise the surface chemistry of the material. XPS was used to monitor the surface chemistry of the untreated and etched PLGA films during the degradation study. A representative XPS spectrum is shown in figure 3.12. Spectra recorded the presence of oxygen (O1s 533 eV) and carbon (corrected to C1s 285 eV) (figure 3.12)..
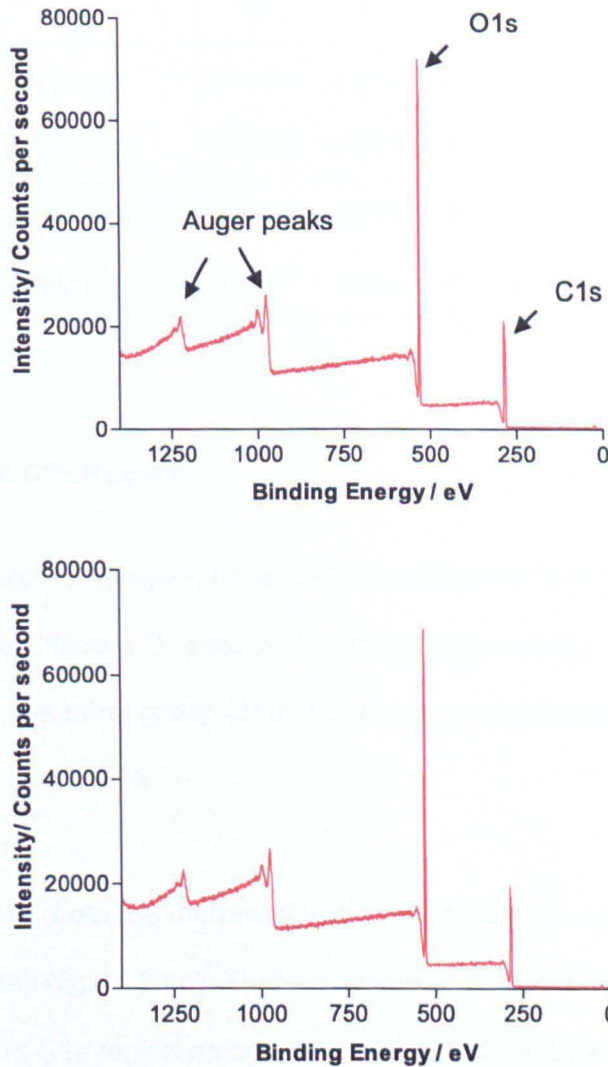
Figure 3.12 : Representative XPS wide spectrum of PLGA samples and showing oxygen (O1s 533 eV) and carbon (C1s 285 eV) peaks. Auger peaks for these elements are also shown but were not used for analysis. The top spectrum is a representative untreated sample while to the bottom is an oxygen plasma treated sample.

Samples after day 42 were friable making it difficult to discern the matt and shiny side for XPS analysis and they were therefore eliminated. The percentages of the elemental carbon and oxygen are shown in table 3.1.

Table 3.1: Elemental composition of carbon and oxygen in PLGA films. Figures shown represent the mean of 6 samples. In all cases the standard error of the mean was below ± 2%.

Carbon and Oxygen/ Atomic Percentage						
Day	0	7	14	21	28	42
Untreated uPLGA (Matt)	41/59	43/57	43/57	42/58	44/56	43/57
Etched ePLGA (Matt)	39/61	43/57	41/59	44/56	41/59	45/55
Untreated uPLGA (Shiny)	40/60	42/58	42/58	42/58	44/56	40/60
Etched ePLGA (Shiny)	43/57	43/57	41/59	42/58	41/59	43/57

3.3.9 Analysis of C1s Region

For further quantitative analysis, three carbon environments were identified from curve fitting of the C1s and O1s region for PLGA (figure 3.13). These were the methyl group (1), the ether group (2) and the ester group (3) as labelled in the PLGA structure inset in figure 3.13.

During degradation, both the untreated and oxygen plasma treated PLGA films had very similar profiles (figure 3.14). There were minor fluctuations within the chemical components of the C1s region on both the matt and shiny sides. The fluctuations generally remained within 3% of each other. There was not a systematic change in composition from day 1 to day 42.
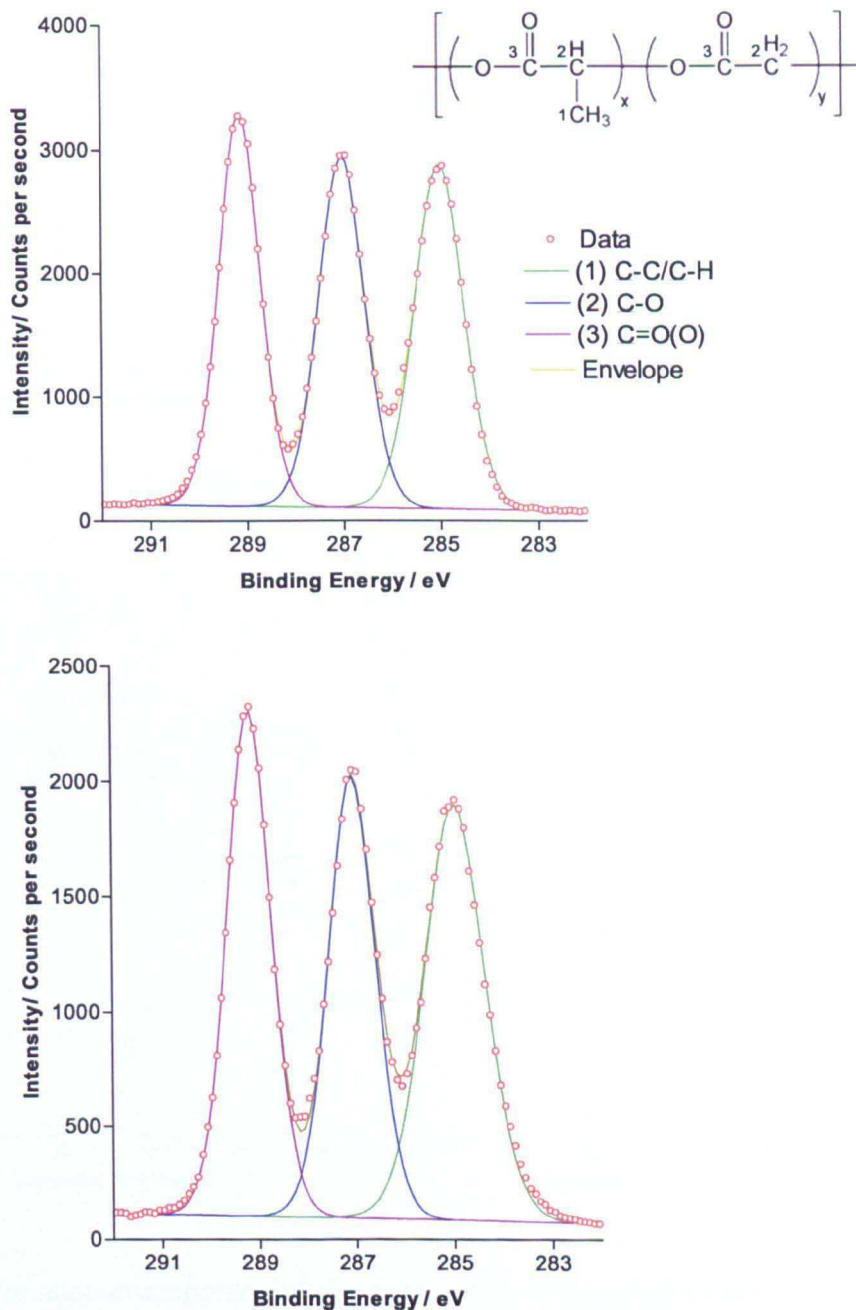
Figure 3.13 : Representative High resolution spectrum of PLGA C1s region showing carbon functionalities. At the top is a representative spectrum of an untreated uPLGA film while the lower spectrum is an etched ePLGA film. The samples shown are freshly prepared samples which were not immersed in degradation media (day 0).
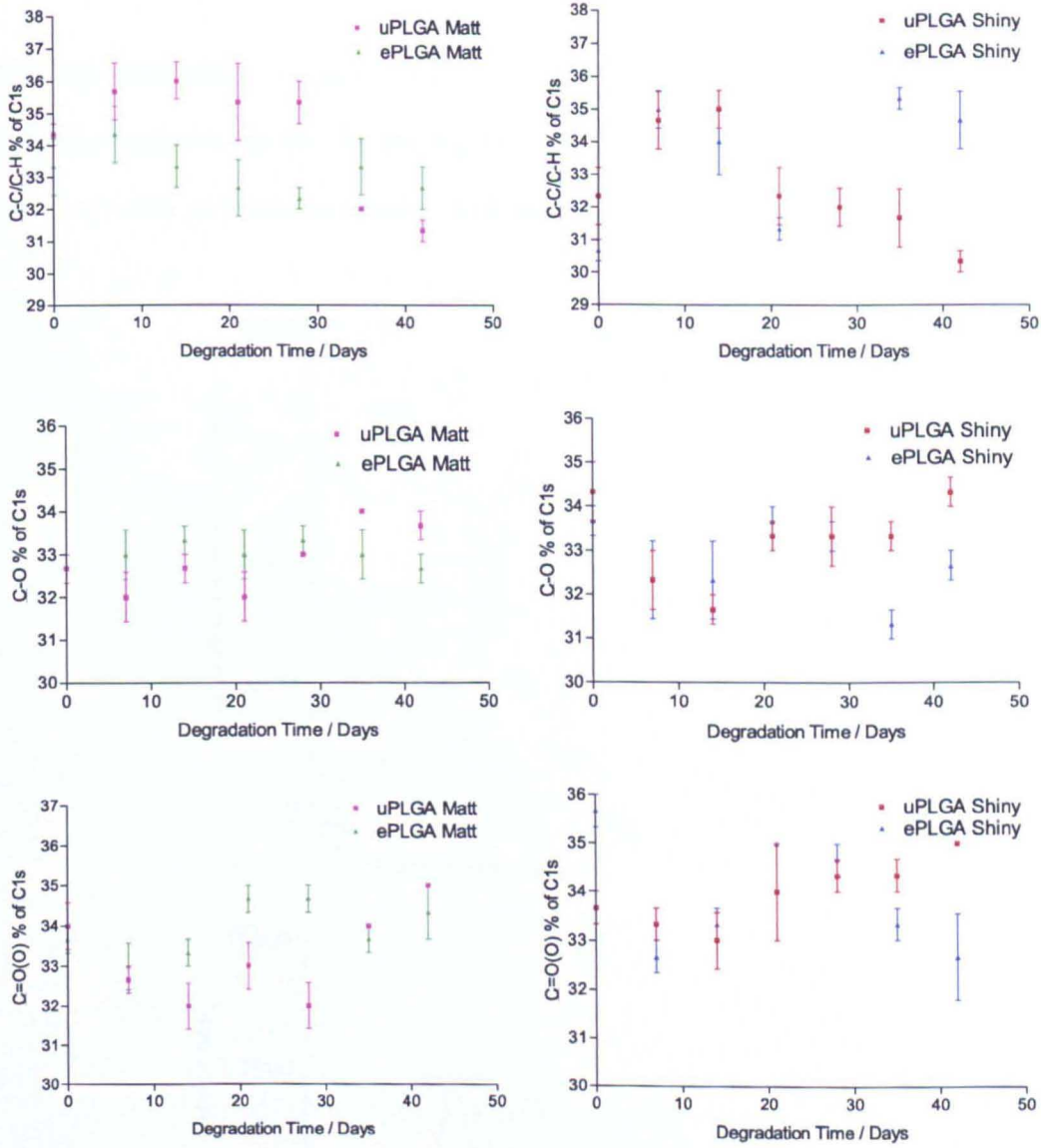
Figure 3.14: Variation in proportion of environments in C1s region for the matt side of the PLGA film. Error bars represent mean ± SEM for n=3.

3.3.10 Analysis of O1s Region

The high resolution O1s peak could be deconvoluted into two peaks as labelled in the representative spectra below (figure 3.15). As degradation proceeded several samples were analysed to monitor changes to these peaks.
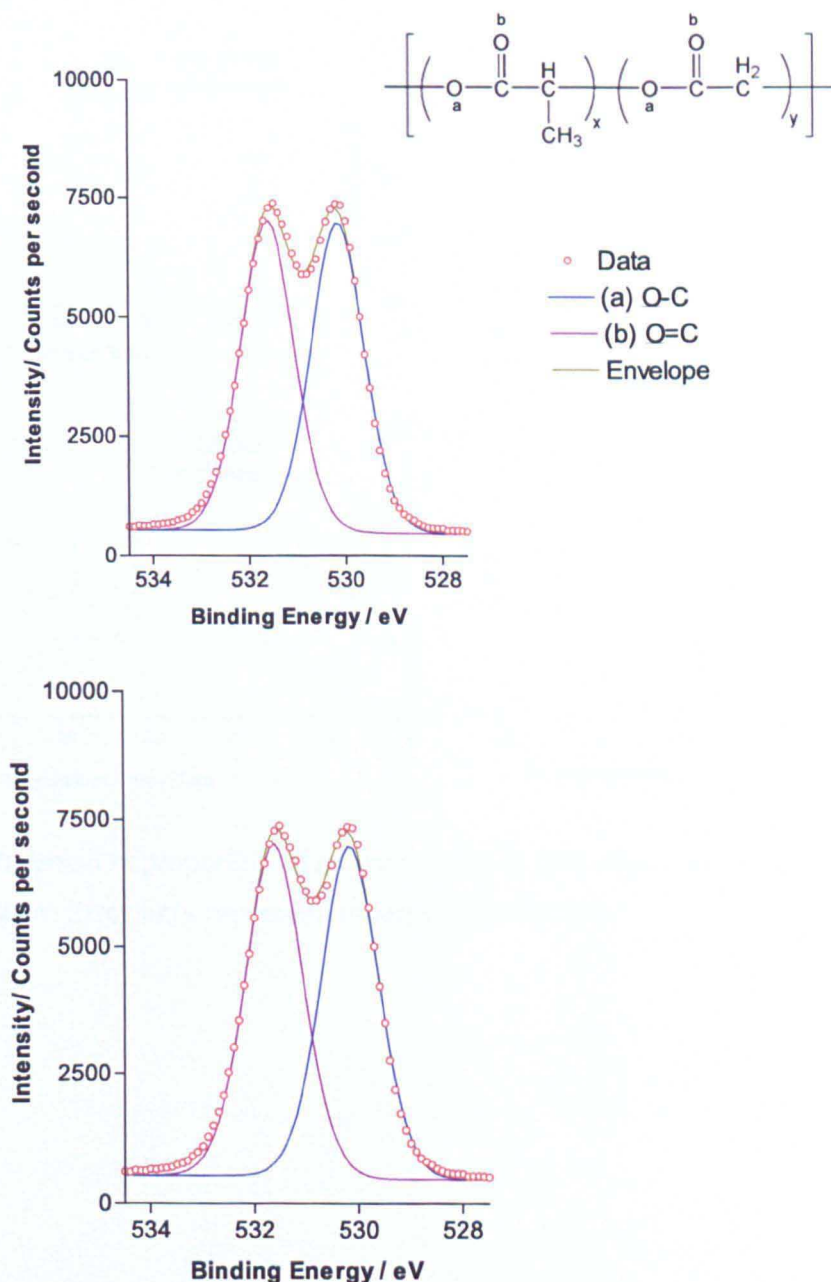
Figure 3.15: Representative High resolution spectrum of PLGA O1s region showing carbon functionalities as labelled. The top image is a representative untreated uPLGA film while the bottom spectrum is an oxygen plasma treated ePLGA film.

A very similar chemical pattern to the C1s region emerged with very little change to the functionalities of the O1s region of the films as degradation proceeded (figure 3.16). This was true for both the uPLGA and the ePLGA films and for both the matt and shiny sides.
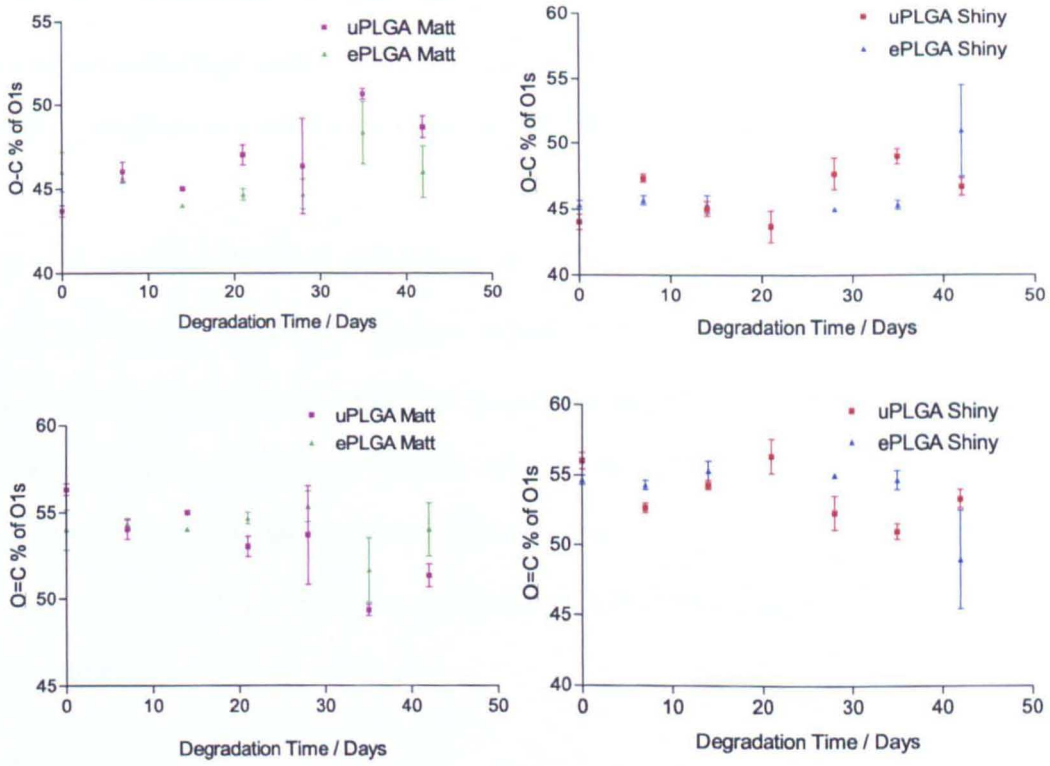
Figure 3.16: Variation in proportion of environments in O1s region for the shiny side of the PLGA films. Error bars represent mean ± SEM for n=3.

3.4 DISCUSSION

3.4.1 Changes to Surface Topography due to Etching

The PLGA films as prepared were observed to have a non porous matt and shiny side and a porous internal structure. Differences in nanoscale roughness were noted with the matt side being rougher than the shiny side. Etching these films resulted in a desired surface porosity for tissue engineering purposes being produced while the porous conduits previously seen on the untreated films were preserved.

There is existing literature that shows that PLGA substrates undergo substantial changes to roughness when oxygen etched (Wang et al., 2004). Separately PTFE substrates have also been reported to undergo etching and topographical change when exposed to an oxygen plasma over a prolonged period (15 minutes) (Morra et al., 1990). The changes to the PLGA films after oxygen etching was not limited to the material surface and some key differences in morphology were observed during degradation.

3.4.2 Changes to Surface Morphology due to Degradation

First, as the uPLGA films degraded, pores developed on the matt side only while the shiny side remained non-porous (figure 3.17). On day 28, the matt surface had a wrinkled appearance while the shiny surface had indentations. This appearance may correspond to the collapse of internal pores as degradation proceeded. In contrast, the oxygen plasma treated ePLGA surface remained porous during the degradation period. The pores did decrease in size as degradation proceeded possibly due to erosion of the surface and bulk.

uPLGA   ePLGA

Day 0

Day 7
to 21

Day 28
to 42

Matt

Shiny
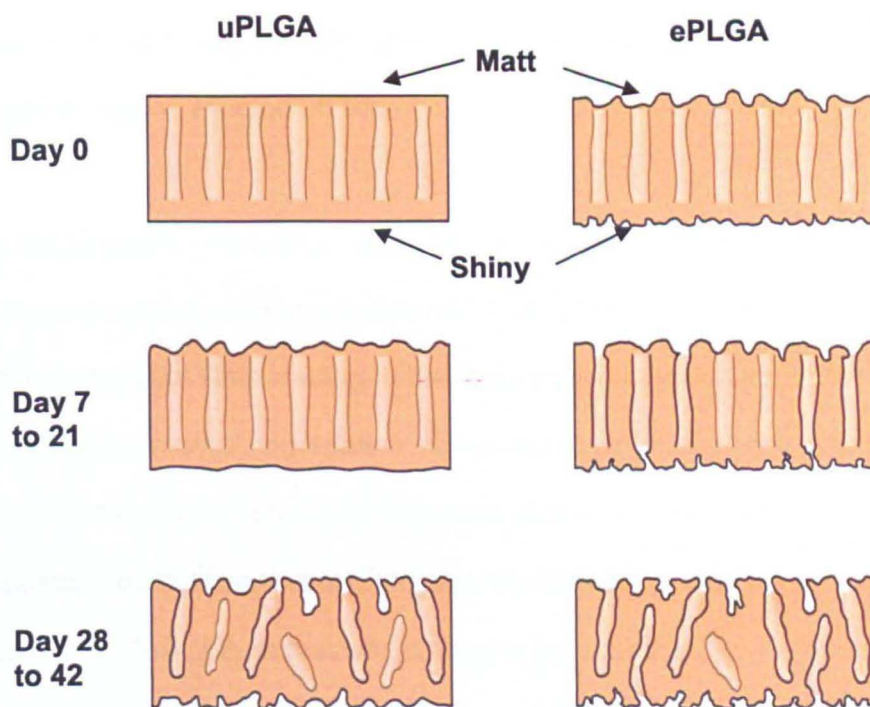
Figure 3.17: Schematic showing the morphological changes to the surface of uPLGA and ePLGA scaffolds due to etching in plasma and subsequent degradation in media.

3.4.3 GPC: Chromatograms and Molecular Weight

An interesting observation was that the GPC spectra of the degrading materials were all single peaks though the ePLGA peaks were broader indicating possible greater dispersity in terms of molecular weight. Only the ePLGA chromatogram at day 0 displayed a clear bimodal peak. This is likely due to the effect of the plasma on the surface, breaking the polymer chain and reducing the molecular weight in comparison to the bulk of the material. The bulk material appears as a larger molecular weight fraction (75000 g/mol) while the surface which would have experienced extensive degradation appears as a second much smaller peak of a lower molecular weight (750 g/mol). The effect does appear to be transient and disappears after day 0. This could perhaps be because the affected material surface

becomes more susceptible to degradation due to weakening of the polymer and therefore may be washed off easily.

The single peaks of the degrading uPLGA and ePLGA scaffolds do point towards a homogeneous degradation mechanism. Internal autocatalytic degradation is common in PLGA films leading to heterogeneous degradation, where there is a distinct faster internal degradation, compared to external degradation(Lu *et al.*, 1999). This is often seen on GPC spectra as bimodal peaks. A study by Grizzi *et al* proposed a qualitative model of degradation that concluded that there was a critical thickness of 200-300µm that would need to be exceeded for PLA microspheres to degrade heterogeneously (Grizzi *et al.*, 1995). This led to the conclusion that PLA and PLGA films of small dimensions would degrade homogenously. While the GPC results of this current study supports Grizzi's conclusion, it is notable that not all thin PLGA films degrade homogenously. Lu *et al* found that PLGA films of 10µm thickness experienced heterogeneous degradation (Lu *et al.*, 1999).

Another dramatic difference was seen with the molecular weight. The etched PLGA films exhibited a reduction in weight by just over 25% immediately after plasma treatment but before being placed into degradation media. This was a clear indication that oxygen etching did not just create porosity and in fact played a role in enhancing the degradation of PLGA. During degradation the molecular weight of the untreated and etched PLGA followed a relatively similar decreasing trend. In spite of a shorter period in degradation, the etched PLGA did reach a much lower molecular weight after 42 days compared to the untreated PLGA which was degraded for 60 days

A possible explanation for this lies in the initial observation that the molecular weight of the PLGA film after etching was lower. The UV light formed during the plasma

process is very likely to have broken the polymer chains making it possible for the etched PLGA to contain smaller polymer chains than the untreated PLGA film. This is evidenced by the initial bimodal peak seen on the etched PLGA chromatogram. A small region of very low molecular weight was seen corresponding to a highly degraded region of the polymer which was not observed on any of the untreated films. Photodegradation by UV light in plasma has been reported previously for polymeric substrates such as poly(methylmethacrylate) and poly(styrene) (Chan *et al.*, 1996). The opposite effect, photocrosslinking of PLGA by an argon plasma, has also been reported (Holy *et al.*, 2001). As stated in the introduction the gas used in the plasma is of importance; the oxygen plasma as described is now demonstrated to cause degradation of PLGA and could be used in future to tune degradation by controlling exposure time.

The final part of the GPC analysis was the polydispersity index variation over time as the films degraded. The untreated films showed little change in PDI unlike the ePLGA films which showed great variation initially increasing before decreasing once more. The pattern exhibited by the ePLGA is typical of rapidly degrading films with the increase in PDI indicating the polymer was degrading and becoming more disperse in terms of chain length. The degradation of the untreated PLGA films may be more controlled compared to the etched films. Etching the film induced immediate degradation with a clear decrease in molecular weight as explained previously. In theory, the chain length of the polymer may have become more disperse due to oxygen etching and this was simply further exacerbated by degradation conditions (immersion in liquid and temperature increase to 37°C).

3.4.4 Surface Chemistry Changes Due to Etching and Degradation

From a surface chemical point of view, XPS analysis of the PLGA films, both untreated and oxygen plasma treated, showed typical peaks characteristic of the lactic and glycolic acid chemical composition. Interestingly, oxygen etching did not substantially increase the oxygen content of the PLGA film unlike previous observations with oxygen treated PLGA films (Qu et al., 2007, Wang et al., 2004). This was consistently observed with the wide spectra and deconvoluted C1s and O1s peaks. In considering why this happens, it is important to understand that oxygen plasmas produce two simultaneous competitive interactions with polymer surfaces. The first is an etching process with reactions creating volatile products and the second, a surface modification process with incorporation of oxygen functional groups (Chan et al., 1996). Morra and colleagues suggest that increasing the etching time of an oxygen plasma can drive the plasma equilibrium away from incorporation of oxygen and in favour etching of the surface. The result of this would be volatile products at the surface that were essentially dissipated leaving the oxygen plasma treated surface similar chemically to the untreated (Morra et al., 1990).

XPS showed that there was minimal fluctuation (below 3% in most cases) in the oxygen and carbon groups including the functionalities as the scaffolds (both uPLGA and ePLGA) underwent degradation. This is in contrast to bulk degradation studies which have shown loss of the glycolic acid group prior to the lactic acid group (Alexis, 2005). However the studies in the review by Alexis were bulk studies with NMR and not surface studies.

This current study indicates that there was a general maintenance of the overall polymer composition at the surface of the films on both the matt and shiny sides of

the uPLGA and ePLGA scaffolds over the 60 days. This is also further evidence that

degradation as happened during plasma treatment may not result in a surface

chemical change detectable by XPS.

3.5 SUMMARY

In summary this chapter described the production and modification of a thin film

made from degradable PLGA. As an artefact of the production method, the film had

varying roughness on either side. Plasma oxygen treatment etched the film

producing porosity across the membrane. Plasma treatment also initiated the

degradation process with the molecular weight of the treated film decreasing sharply

and the appearance of low molecular weight polymer chains.

The untreated and plasma treated films degraded at a similar rate with one distinct

difference being that the etched films were able to degrade to a much lower

molecular weight than the untreated films. The etched films also demonstrated

greater polydispersity and broader peaks in the GPC spectra.

Surface chemical analysis of the uPLGA and ePLGA films revealed that the two had

very similar compositions. This was explained by the shift in the balance of etching

and incorporation processes that occur during the oxygen plasma and the

dominance of the etching process.

Finally degradation of the films revealed that there was little surface chemical

variance detectable by XPS on both the uPLGA and ePLGA films. This was

sustained over the 42 days in degradation.

CHAPTER 4: A two dimensional Intestinal Epithelial Tissue Engineered Model

This chapter describes the material characterisation and design considerations undertaken to form a novel two dimensional intestinal epithelial model. The introduction highlights the key requirements for the tissue engineered model (in comparison to in vivo tissue) before expounding on the experimental work done to achieve a desirable model.

4.1 INTRODUCTION

The epithelial cells of the *in vivo* intestine are separated from the underlying

mesenchymal cells by a porous basement membrane (Mahida *et al.*, 1997b). The

epithelial cells rely on the cells in the mesenchyme to provide signals to allow

proliferation (Evans *et al.*, 1992). These three layers: the epithelial cells, basement

membrane and myofibroblasts directly underlying the basement membrane

therefore comprise the intestinal epithelial tissue (figure 4.1).
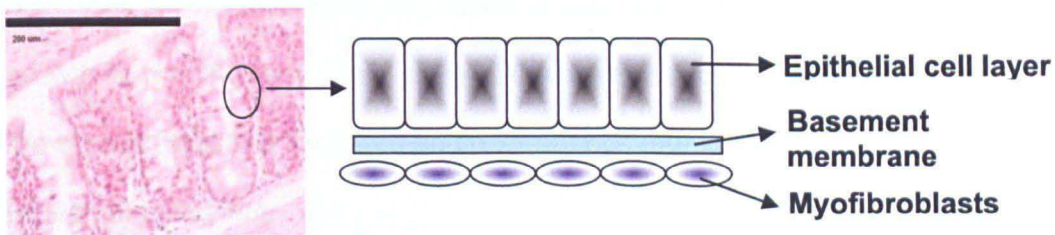
Figure 4.1: The intestinal epithelial tissue is comprised of epithelial cells, the basement membrane and myofibroblasts. Histology image from own work.

The epithelial cells that populate the luminal side of the basement membrane have

essential digestive functions (see chapter 1). They do also have another

pronounced role, forming a monolayer with tight junctions which effectively acts a

barrier separating the contents of the lumen and the lamina propria (McKaig *et al.*,

1999, Anderson and Vanitallie, 1995). In many senses this barrier function is

indispensable as the luminal contents can contain many micro-organisms and toxic

molecules that could create systemic infection to the whole body (Madara, 1989,

Madara, 1998, De-Souza and Greene, 2005).

Directly under the epithelial cells lies the basement membrane. At first glance, the

membrane's most apparent function is to serve as a support for the epithelial cells

but its capabilities are far more wide ranging. The basement membrane itself is

thought to modulate the proliferation and differentiation of intestinal cells (Louvard *et al.*, 1992). Its pores act as conduits facilitating transportation of immune cells and mediators from the underlying tissue which is enhanced when the epithelial cells are denuded (Mahida *et al.*, 1997b). It is therefore a very important structural and functional part of the epithelial layer.

The final layer of the epithelium is comprised of myofibroblasts that flank the basement membrane adjacent to the lamina propria. The myofibroblasts have a pronounced role from proliferation to angiogenesis (Shao *et al.*, 2006). They have also been shown to enhance the repair of wounded epithelial cells by secreting growth factors (McKaig *et al.*, 1999). The interaction between the epithelial cells and the myofibroblasts is therefore an important communication pathway for the intestinal epithelium.

The epithelial model as presented in figure 4.1 has been constructed for *in vitro* use predominantly for transport studies, predicting the flow of proteins or drugs. Intestinal cells are routinely cultured on semi-permeable filters and experiments can be performed in coculture as presented or as a monolayer. The Caco-2 cell line, a colonic carcinoma epithelial cell line, once confluent, can differentiate into a hybrid model containing both colonic and small intestinal cells. This cell line has therefore been used for transport studies of the small intestine and the colon mimicking the *in vivo* effect of the tight barrier formed by tight junctions of epithelial intestinal cells (Yee, 1997, Artursson, 1991, Rubas *et al.*, 1996). Measuring the extent of tight junctions is often done by calculating the transepithelial electrical resistance (TEER). TEER has previously been shown to rise with increasing formation of tight junctions in Caco-2 cells and decrease when tight junctions were few or absent for example due to cells being cultured in serum free conditions (Hidalgo *et al.*, 1989).

The porous semi permeable filters used as the cell supporting scaffold are often made of non degradable or moderately degradable material including but not limited to cellulose, poly(carbonate) and poly(ethyleneterephtalate) - PET (Hidalgo *et al.*, 1989, Hubatsch *et al.*, 2007). While these filters are useful for *in vitro* work, for the purpose of creating an *in vitro* tissue engineering model, it would be essential to obtain a biodegradable alternative to ease the transfer of this work from an *in vitro* experiment to an *in vivo* setting. PLGA is a US Food and Drug Administration approved material that can act as a temporary support allowing the cells to establish themselves. As it is biodegradable and non toxic there would be less concern over potential material failure or interference to normal host function.

The work described in this chapter addresses the question of a biodegradable scaffold to support intestinal cells (see Chapter 3 for degradation behaviour of this scaffold). Herein, the design and modification of the scaffold to mimic the *in vivo* basement membrane is proposed and discussed. The function of the novel degradable model is tested in *in vitro* monoculture and coculture.

4.2 MATERIALS

PLGA scaffolds as prepared in Chapter 2 (uPLGA and ePLGA) were used as a basement membrane substitute. Appendix 1 lists all the materials and suppliers used within this chapter. Appendix 2 lists the solutions used within this chapter.

4.3 EXPERIMENTAL

Due to the enhanced surface porosity of the ePLGA scaffolds, they were selected a support for intestinal cells. Therefore, uPLGA scaffolds were modified by oxygen etching and observed under SEM to allow selection of a suitable scaffold with pores similar to those found on the *in vivo* basement membrane. Intestinal epithelial cell attachment (Caco-2 cells) to the ePLGA and uPLGA scaffolds was compared and tested. This was performed using live/dead staining for viability, Alamar Blue assays for cell metabolic activity and Hoechst DNA assays for proliferation. Additionally SEM was used to compare the morphology of the cells on ePLGA and uPLGA scaffolds.

The ePLGA scaffold was then employed as a basement membrane substitute in an intestinal epithelial monoculture model consisting of epithelial cells (Caco-2) as well as a coculture model with Caco-2 and myofibroblasts cells (CCD-18Co cells). A positive control consisting of the same cells cultured on a PET surface was used for comparison purposes. Transepithelial electrical resistance (TEER) measurements were recorded over a period of 14 days. TEER measurements are used to infer the formation of tight junctions and hence development of a monolayer of closely packed cells required to ensure the intestinal epithelium acts as a barrier.

4.4 RESULTS

4.4.1. Analysis of surface porosity induced by oxygen plasma treatment

As the basement membrane of the *in vivo* intestine is porous, it would be essential for an *in vitro* model to also mimic this property. The surface of the untreated uPLGA membranes as prepared by phase inversion was non-porous (Chapter 3). The degradation study had revealed that oxygen plasma treatment resulted in creation of surface porosity. SEM images of the plasma etched scaffold showed porosity on both the matt and shiny side of the scaffolds (figure 4.2). The matt side possessed larger pores which appeared to increase as etching time increased. The pores on the shiny side appeared smaller and did not appear to follow the incremental trend. A series of images from several etched scaffolds was used to quantitatively assess the pore diameter and percentage surface coverage by pores.

The pore size of the *in vivo* basement membrane of the colon has been previously published as 0.2-3.3μm in diameter (Mahida *et al.*, 1997b). The surface porosity of the ePLGA scaffolds quantitatively reflected the qualitative observation and first revealed that the pores on the shiny side did not vary significantly in size (fig 4.3) and were small averaging 1.07μm (range = 0.63 to 1.74 μm). Secondly, the pores on the matt side exhibited a gradual increase in pore diameter relative to etching time. The closest value to the *in vivo* basement pore diameter was achieved with etching times of 30s, 60s and 90s.

Matt Side   **Shiny Side**

30 seconds

60 seconds

90 seconds

120 seconds

50μm
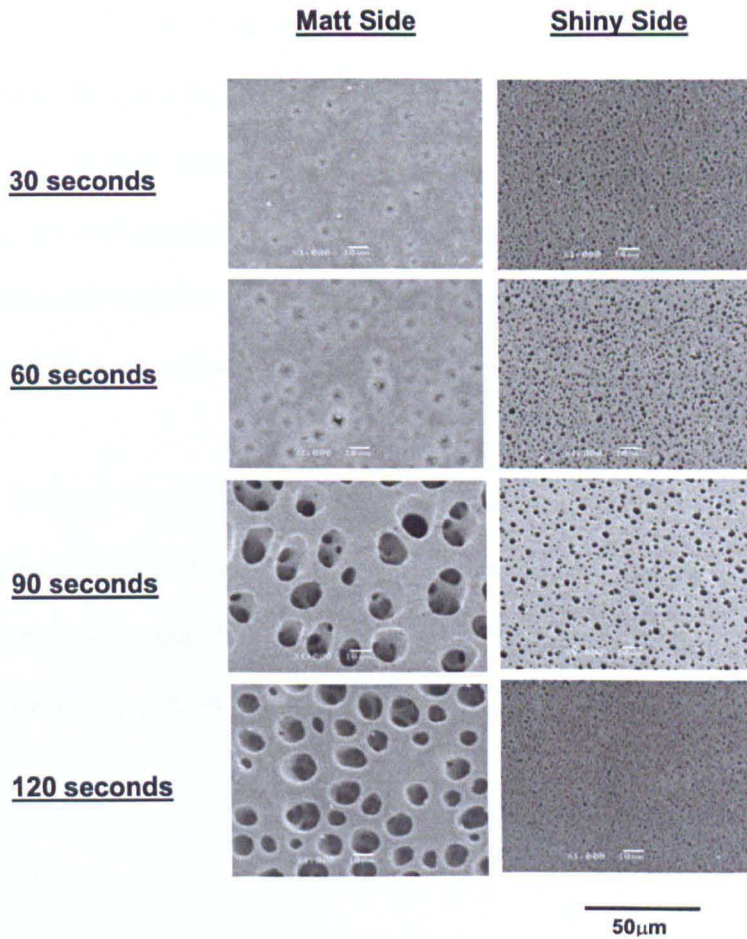
Figure 4.2: Etching the PLGA membrane induced pores of varying size on the matt and shiny surfaces. This was dependent on the etching time.
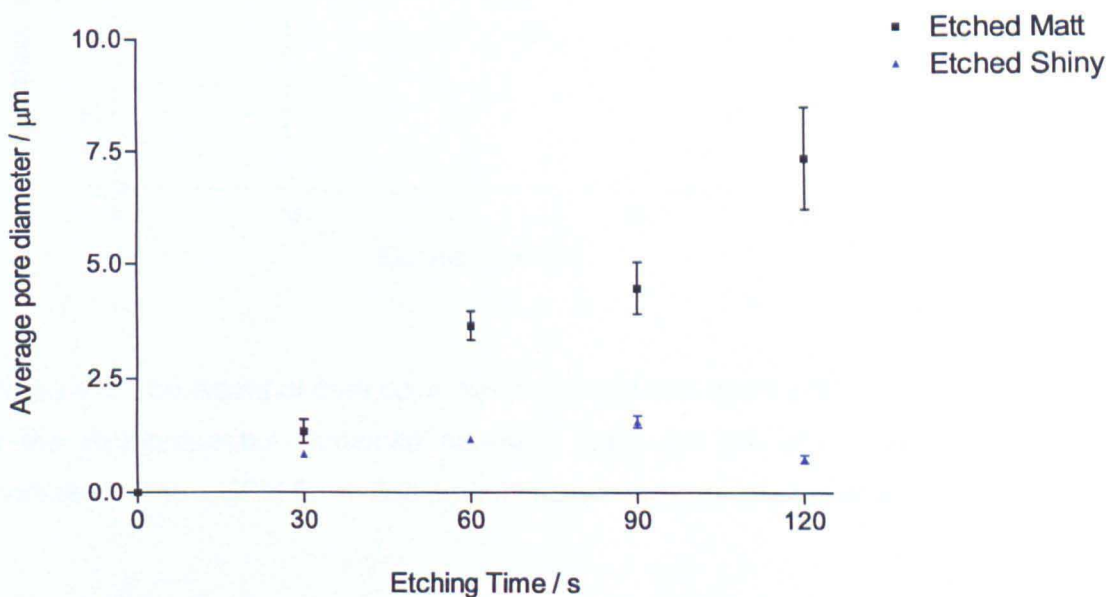
Figure 4.3: Pore diameter increased with etching time. Error bars represent mean ± SEM for n=6 (in some cases error bars are not visible).

Quantitative analysis of the percentage surface coverage by pores was also

undertaken (figure 4.4). This allowed selection of an ideally modified scaffold

accounting for both pore size and coverage. The data collected showed that the

shiny side of the scaffold again remained relatively stable. The matt side exhibited

an incremental trend in extent of surface coverage by pores as oxygen etching time

increased, but this peaked at 90s.

On the basis of these observations, the 90s time point was selected as the ideal

etching time to create pore size and coverage similar to that found in the *in vivo*

basement membrane. All results presented next describing an etched ePLGA

scaffold were based on oxygen etching the phase inversion membrane for 90s.
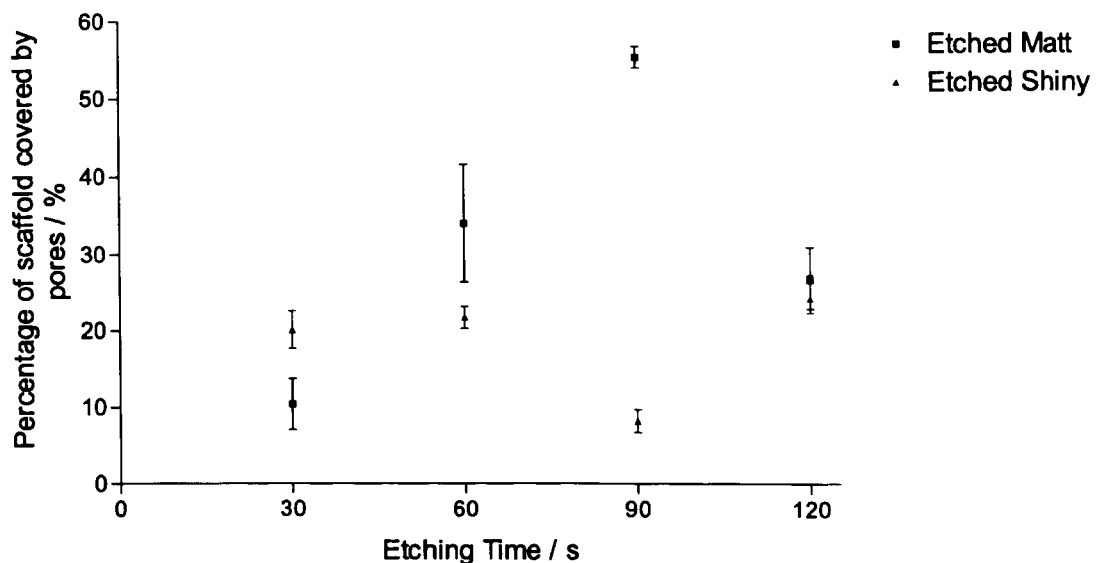
Figure 4.4: The extent of pore coverage increased with etching time on the matt side of the membrane but remained relatively stable on the shiny side. Error bars represent mean ± SEM for n=6 (in some cases error bars are not visible).

4.4.2 Cell Viability on PLGA Surfaces

Oxygen etching of the films induced surface porosity but did not impact surface chemistry (See Chapter 3). As stated in the introduction, surface changes can lead to differences in cell behaviour which is especially important for epithelial cells which are attachment dependent. It was therefore important to assess if the plasma treatment to create the porosity of the ePLGA surface would impact cell activity.

Caco-2 Cells were therefore seeded on uPLGA and ePLGA surfaces and cultured for two days as described in Chapter 2. Subsequently a simple qualitative live/dead assay was used to examine cell attachment to the PLGA surfaces. Green fluorescence indicating live cells was observed on both the etched and untreated surfaces (figure 4.5 and 4.6). Red fluorescence indicating dead cells was observed more distinctly on the uPLGA surfaces (figure 4.5 a and 4.6 a).

4.4.3 Morphology of Cells on the Surface

For epithelial cells, the cell shape or morphology can dictate a multitude of processes including but not limited to cell survival, migration and proliferation. For this reason, an SEM comparison study of the morphology of the cells on the untreated PLGA surfaces and the modified etched PLGA films was undertaken. Several images were taken of the Caco-2 cells after incubation, three days post seeding. Representative images show that the untreated surface had few cells or a large number of rounded cells while the etched surface predominantly displayed flattened cells (fig 4.7 and 4.8).
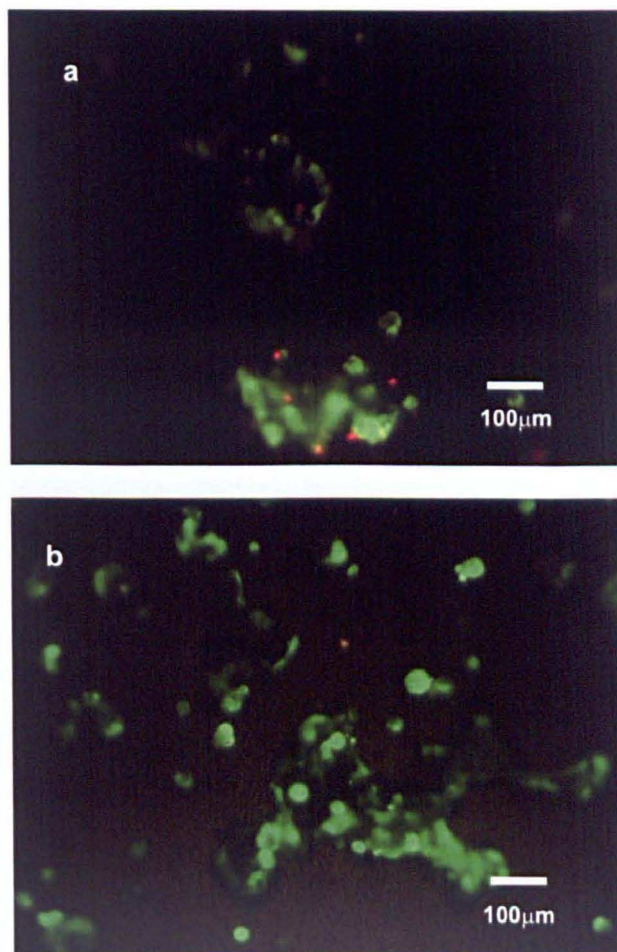
Figure 4.5: Representative images of Live/Dead fluorescent cell staining on the uPLGA surface (a) and the ePLGA surface (b). Cells were stained after 3 days in culture. Green fluorescence indicates live cells and red fluorescence denotes dead cells. The matt side of the films is shown above.
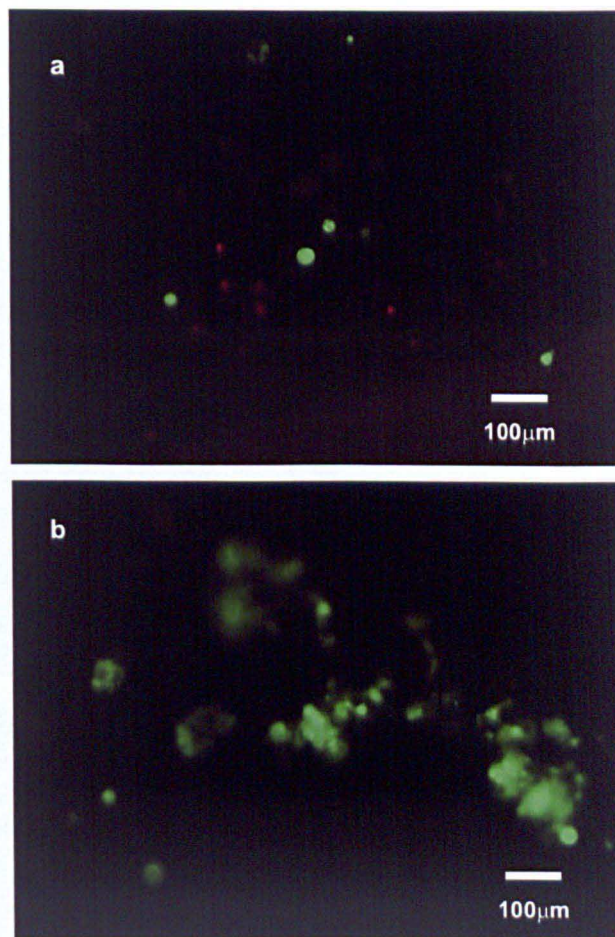
Figure 4.6: Representative images of Live/Dead fluorescent cell staining on the uPLGA surface (a) and the ePLGA surface (b). Cells were stained after 3 days in culture. The shiny side of the films is shown above.
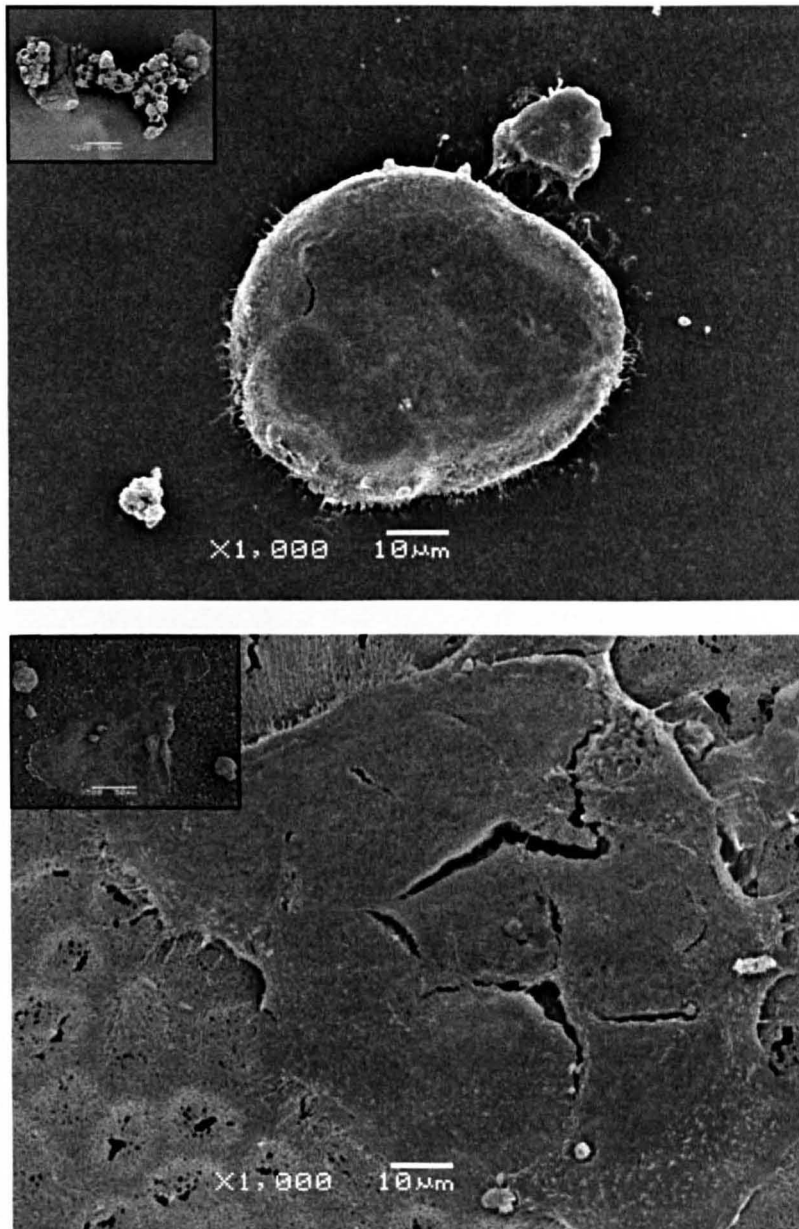
Figure 4.7: Representative SEM images show that cells attached on the uPLGA were visibly more rounded (top) compared to those on the ePLGA surface which were spread out (bottom). In both cases the matt side of the surface is shown.
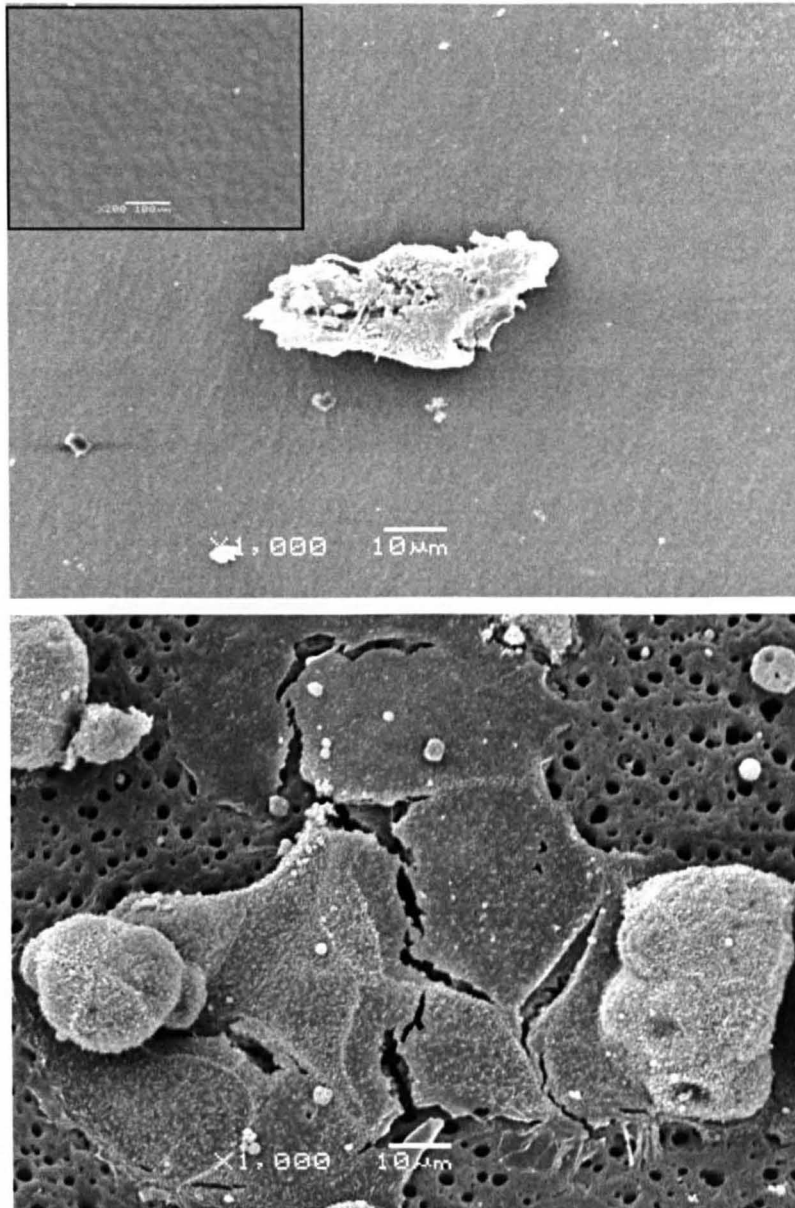
Figure 4.8: Representative SEM imaging shows caco-2 cells on the shiny side of the uPLGA (top) films were few (see inset image) and had a distorted appearance. The cells on the shiny ePLGA (bottom) film had some rounded cells but many appeared spread out.

Detailed analysis of the SEM images revealed that the uPLGA surface occasionally had cell clusters comprised of rounded cells with some having a hollow appearance (figure 4.9 top). The microvilli present on Caco-2 cells were especially distinct on the cells cultured on ePLGA surfaces (figure 4.9 bottom).
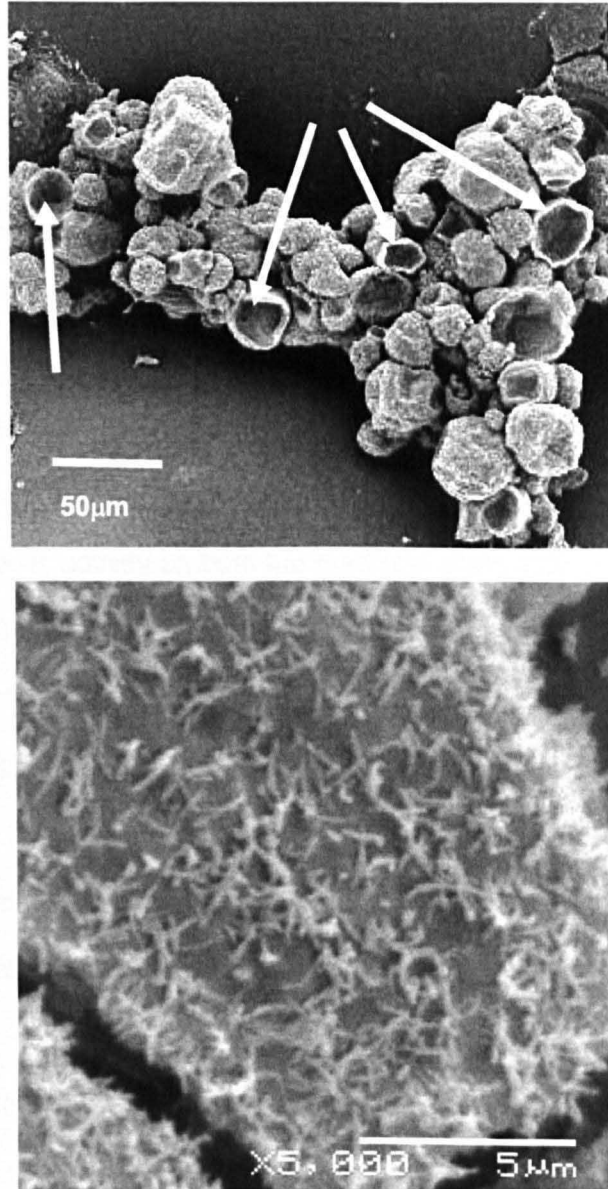
Figure 4.9: The top image shows cell clusters with hollow cells (white arrow) on the representative uPLGA surface while the bottom image shows microvilli present on the surface of the Caco-2 cells on an ePLGA surface.

4.4.4 Cell Metabolic Activity and Proliferation

Live cells will often exhibit metabolic activity in response to intracellular activity such as protein manufacture and related processes such as cell growth and division (O'Brien et al., 2000). While it was determined already that the Caco-2 cells cultured on the ePLGA scaffold were alive, a further measure of success of the scaffold was to determine if the cells were metabolically active. The intestinal cells were therefore cultured onto uPLGA, ePLGA and as a positive control, tissue culture plastic (TCP) for periods upto 7 days.

To quantify the metabolic activity of the cell, an Alamar Blue assay was used (see Chapter 2). Cells cultured on the oxygen plasma treated ePLGA surfaces showed comparable metabolic activity on both the matt and shiny side through 7 days in culture (figure 4.10). The uPLGA matt and shiny surfaces had consistently lower values than their etched counterparts and this was more pronounced on day 5 and 7. On both these days the metabolic activity of the cells on the ePLGA surfaces was statistically higher than the uPLGA surfaces. The metabolic activity on the control TCP was statistically higher than all the surfaces on day 7 whether unmodified or oxygen treated (see figure 4.10).

Proliferation of cells would lead to an increase in DNA. For this reason a Hoechst 33258 assay (see Chapter 2) was undertaken (figure 4.11). This was performed in order to assess if the increase in cell activity could be attributed to proliferation. The assay revealed that there were similar quantities of DNA on the ePLGA surface and uPLGA surface initially. The amount of DNA increased slightly on the etched surfaces and on tissue culture plastic on day 5. By day 7, the cell number on the etched surfaces increased significantly while that on the uPLGA surfaces remained similar to day 1.
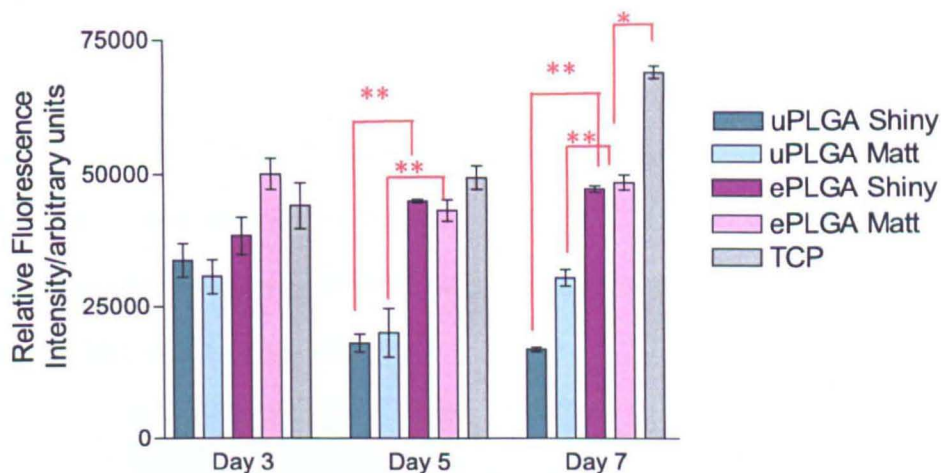
Figure 4.10: Caco-2 cell metabolic activity was measured during 7 days in culture using Alamar Blue. Over this time period cells on the oxygen etched surfaces showed increased metabolic activity compared to un-etched surfaces. Error bars represent mean ± SEM for n=6 (* = p≤0.01, ** = p≤0.001, ***= p≤0.0001. Not shown on the graph day 7 TCP v ePLGA Shiny = *)
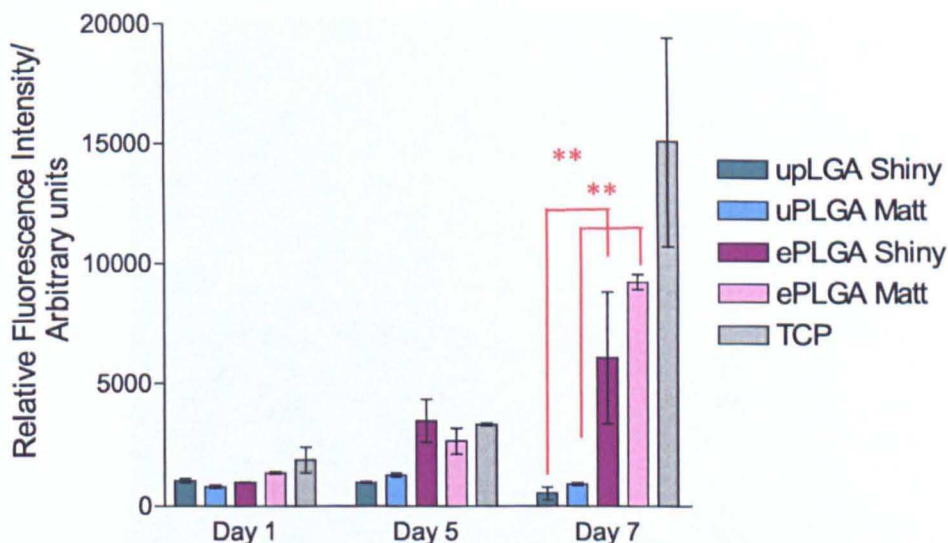
Figure 4.11: A Hoechst 33258 DNA assay was undertaken to estimate DNA content of the samples over 7 days. Error bars represent mean ± SEM for n=3. (* = p≤0.01, **=p≤0.001. Not shown on the graph TCP v all surfaces on day 7 ***= p≤0.0001).

4.4.5 Cells for the Two Dimensional Coculture Model

Caco-2 and CCD-18Co cells were grown in coculture. To begin the experiment CCD-18Co cells were grown on one side of PET filters as well as ePLGA scaffolds. This was confirmed by light microscopy for the filters and via a CellTracker assay for the PLGA surfaces (fig 4.12).
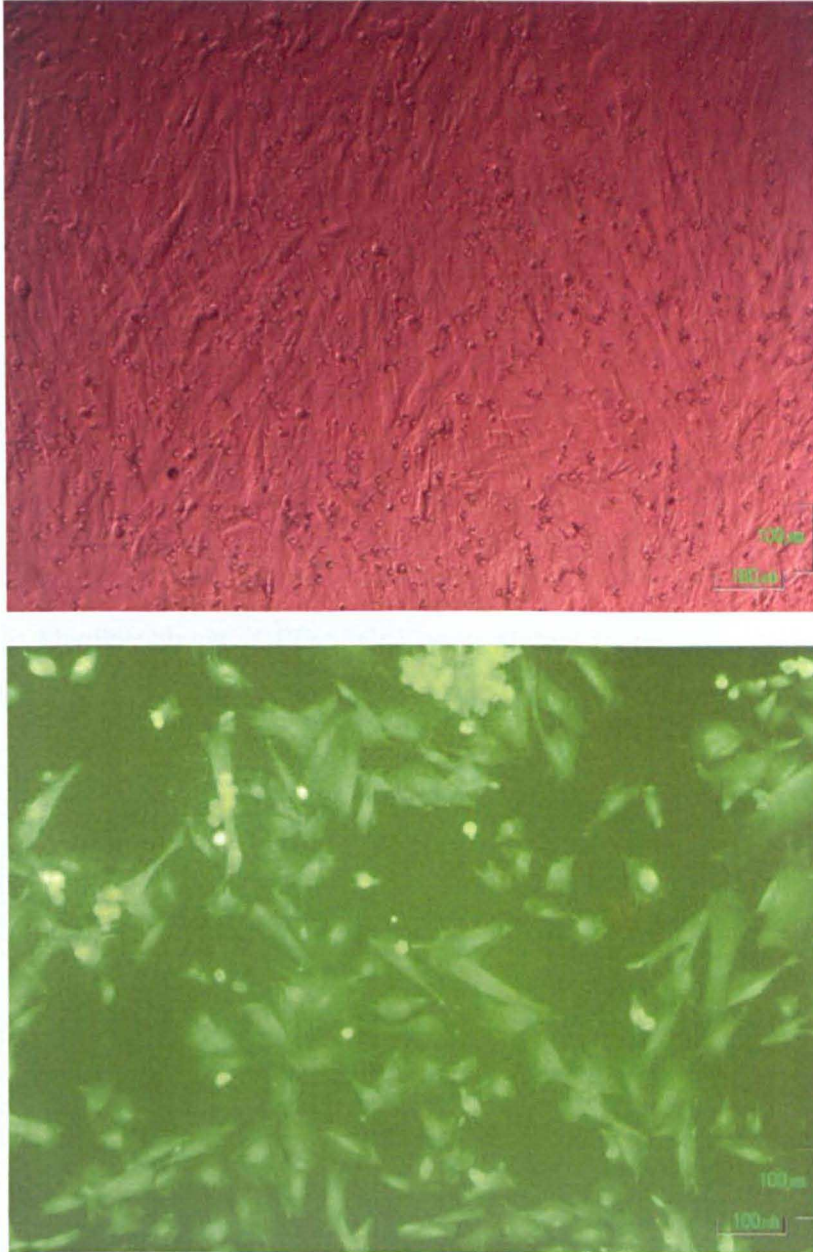
Figure 4.12: A light transmission microscopic view of confluent CCD-18Co cells on a PET filter (top) and a CellTracker stained CCD-18Co cells on an ePLGA membrane (bottom).

To confirm key phenotypic properties, the CCD-18Co cells were tested and shown to be positive for α smooth muscle actin typical for myofibroblasts (figure 4.13). Caco-2 cells were cultured on the reverse side of the filter or ePLGA membrane. These cells were tested and found to be positive for E-cadherin which is a protein present at tight junctions (figure 4.14).
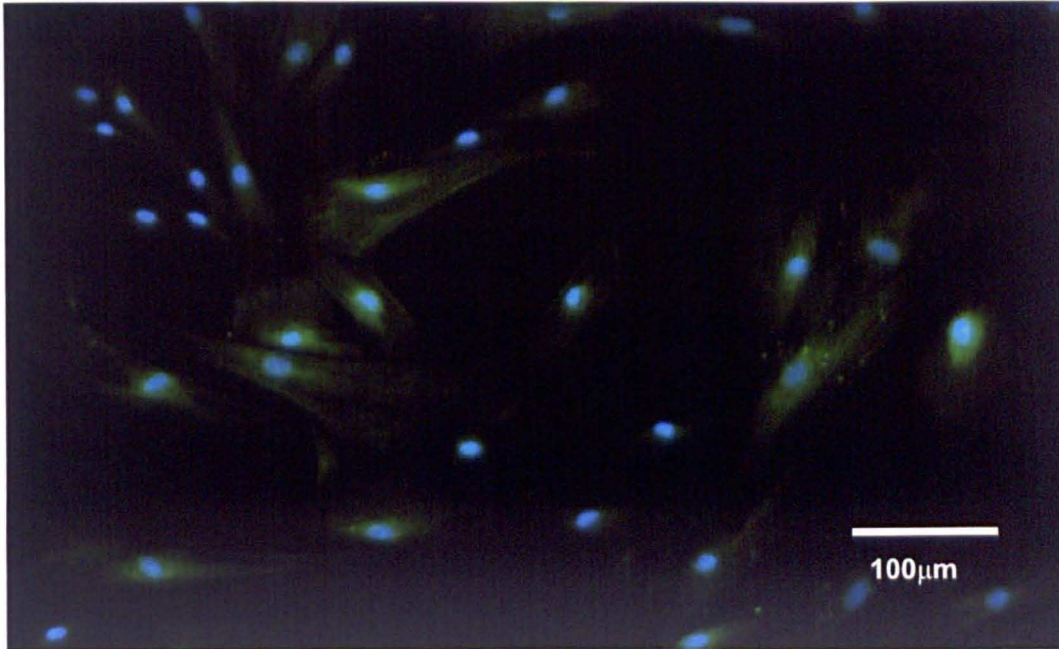
Figure 4.13: Myofibroblasts (CCD-18Co) were shown to be positive for α smooth muscle actin. The nuclei are counterstained with DAPI (blue fluorescence).
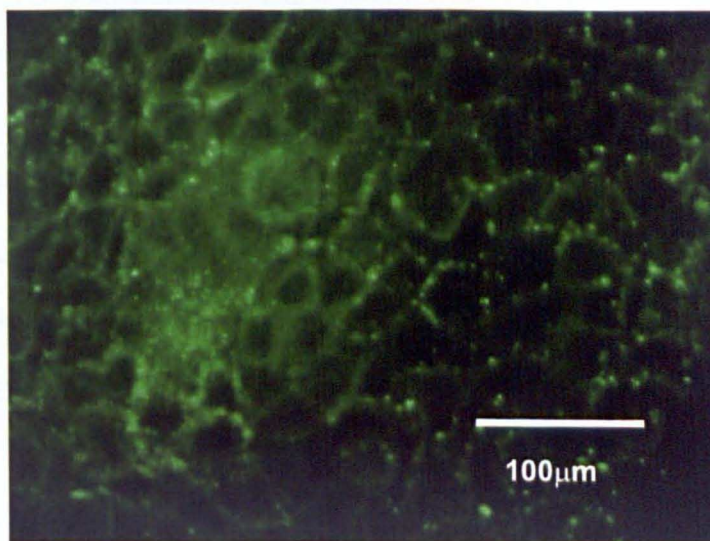
Figure 4.14: Extensive E-cadherin staining around the periphery of Caco-2 cells was observed as indicated by the green fluorescence in the representative image.

4.4.6 Transepithelial Electrical Resistance (TEER) of Cells in Monoculture and Coculture

The barrier function that characterizes the epithelial cell layer is formed by tight junctions between the cells. The transepithelial electrical resistance (TEER) has previously been shown to rise with increasing formation of tight junctions in Caco-2 cells (Hidalgo *et al.*, 1989). It was therefore monitored in order to observe any changes or fluctuations. Caco-2 cells cultured in monoculture on PET filters showed a gradual rise in TEER over the course of 14 days (figure 4.15). The average TEER of the cells in coculture with CCD-18Co cells was consistently higher compared to cells in monoculture. In some cases this was statistically significant as denoted on the graph in figure 4.13. The only exception to this was on day 6 but the TEER values were similar on that day.

On the ePLGA membrane the TEER of the Caco-2 cells in monoculture exhibited an almost similar trend to the PET filters. Initially the TEER rose over the first 6 days before falling on day 8, it then increased once more and remained relatively steady until day 14 (figure 4.15). The TEER trend of the cells in coculture on the ePLGA membrane was similar in some aspects to cells in coculture on the PET filters. For example there was a pattern of increasing TEER as on the PET coculture experiment. The exception to this was between day 10 and 14 when the TEER was relatively steady. Also the TEER value was higher on cells in coculture compared to monoculture similar to the trend observed on the PET filters and was statistically significant on day 1, 8, 10,12 and 14 (figure 4.15).

A notable difference between the PET filters and the ePLGA membrane was the difference in magnitude of the TEER. On the ePLGA membrane, the highest TEER achieved was 147Ω cm^2 by the cells in coculture on day 10. This value was

surpassed on day 4 by cells in both monoculture and coculture on the PET filters.

The cells on the PET filters peaked at 387 Ω cm^2 on day 12.
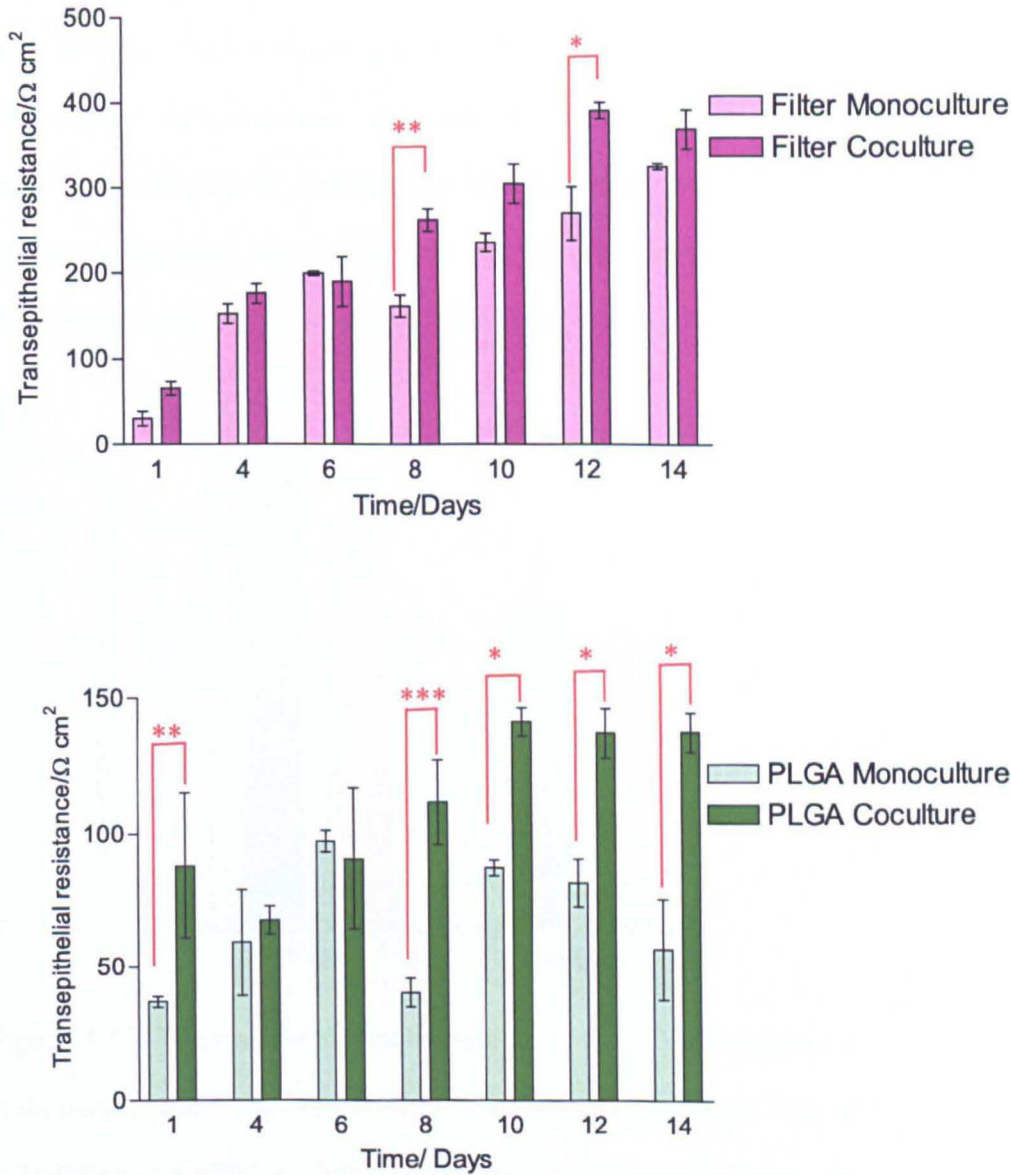
Figure 4.15: The transepithelial resistance of the Caco-2 cells grown in coculture was generally higher than that of cells grown in monoculture. Top graph shows TEER for cells cultured on PET filters and the bottom graph shows the values obtained for cells cultured on the ePLGA membrane. Error bars represent mean $\pm$ SEM for n =9. (* = p$\leq$0.01, ** = p$\leq$0.001, ***= p$\leq$0.0001).

4.4.7 Myofibroblasts do not contribute to TEER

Primary isolated myofibroblasts are known to enhance barrier function in certain epithelial cells but are not known to directly to form tight junctions that contribute to the TEER rise. To attribute the rise in TEER in the coculture study to the epithelial cells alone, it was therefore, necessary to validate that the myofibroblasts cell line CCD-18Co behaved in a similar way and did not contribute to transepithelial resistance (figure 4.16). On both the ePLGA and filters a confluent monolayer of the CCD-18Co cells slightly raised the TEER but not significantly.
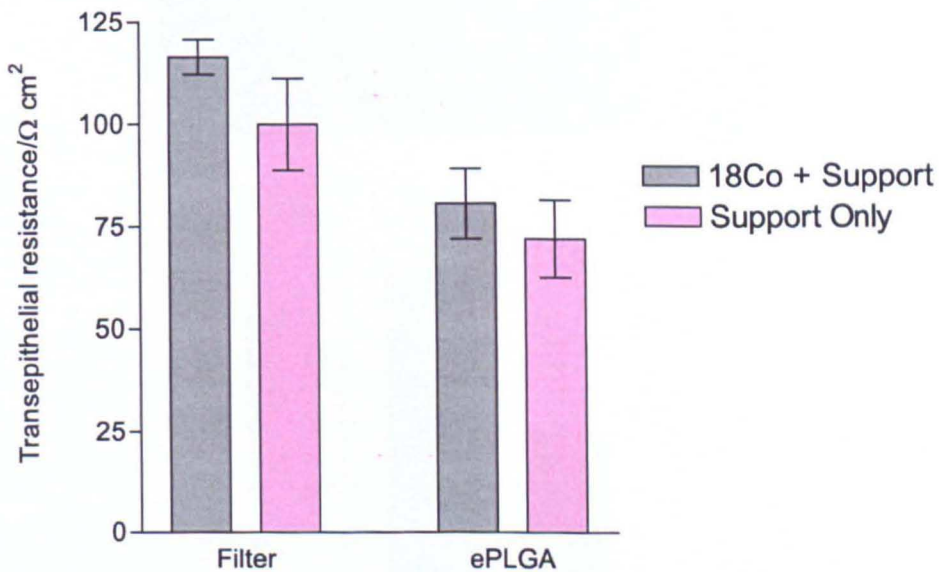
Figure 4.16: The transepithelial resistance of a confluent monolayer of CCD-18Co cells was similar to the TEER of cell supports without cells. This was observed for both filters and ePLGA. Error bars represent mean ± SEM for n=9.

4.4.8 Epithelial Cell coverage after 14 days

To explain the difference in the numerical value of TEER in cocultures on PET filters and ePLGA scaffolds, DAPI staining was used to assess the coverage of the cell supports by Caco-2 cells. It was revealed that the filters were extensively covered by the epithelial cells and were close to confluent while the ePLGA cell coverage ranged from just under 50% to 75% (figure 4.17).
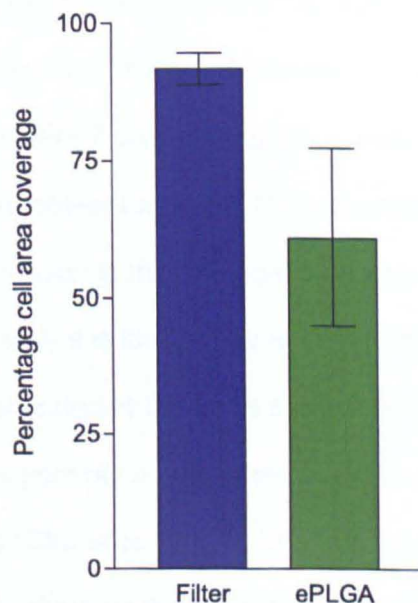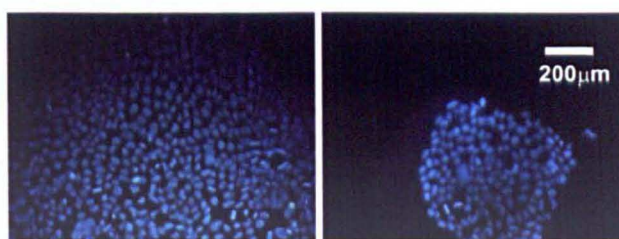
Figure 4.17: Caco-2 cell coverage after 14 days in coculture. Images above show cells stained with DAPI on PET filters (left) and on ePLGA films (right). For the graph, error bars represent mean ± SEM for n=3.

4.5 DISCUSSION

4.5.1 Modification of Scaffold for Tissue Engineering

The uPLGA membrane as produced by phase inversion had conduits present within it (see Chapter 3) but lacked the surface porosity necessary to mimic the *in vivo* intestinal basement membrane. Oxygen plasma treatment created the necessary porosity and it was possible to control and determine the ideal plasma conditions to obtain a suitable *in vitro* scaffold. Increasing the etching time resulted in an increase in the pore diameter on the matt side of the ePLGA scaffold, while surface porosity on the shiny side of the ePLGA scaffold did not vary greatly both in size and extent of coverage. The first likely reason for this observation is that the matt side is more susceptible to plasma effects. This conclusion is supported by the degradation experiment observation in chapter 3 which showed that the untreated films developed surface pores after 7 days in degrading media on the matt side only. This may perhaps indicate an inherent ability of the material to form pores easily on this side. The second likely reason is that the matt side was the most upper facing part to the plasma, consequently it is likely to have experienced greater effects compared to the shiny side due to the large surface to volume ratio. However, both sides developed surface porosity as the plasma and its etching effect is not restricted to line of sight (Chu *et al.*, 2002). The 90s time point used previously in chapter 3 was seen to best mimic the porosity of the *in vivo* basement membrane (Mahida *et al.*, 1997a).

4.5.2 Cell Attachment to Modified Scaffold

In chapter 3, it is reported that the etching of the scaffold did not change the surface chemistry functional groups. However the morphology of the surface was greatly

106

changed. Having modified these films through etching, it was essential to explore

any changes to cell behaviour. Cells attached to both the untreated and etched films

but there were significant qualitative differences. First a live/dead assay showed that

there were more dead cells on the uPLGA surface compared to the oxygen plasma

treated ePLGA surface. The presence of a greater proportion of dead cells could

signify that either the cells were not attaching or that the attachments were weak,

and therefore the cells could easily detach and apoptose perhaps through an FAK

mediated pathway (Gomperts B and Kramer I, 2003).

Lending support to this conclusion was seen in the second qualitative observation.

The morphology of the cells on the surface of the two scaffolds was strikingly

different. The Caco-2 cells were much more rounded on the untreated surface

compared to flat spread out cells on the surface of the etched PLGA films. Epithelial

cells such as the Caco-2 cell type are attachment dependent cells. They obtain a flat

morphology when attached to a suitable surface (Beckerle, 2002). In addition the

ePLGA surfaces had cells with distinct and characteristic microvilli while the uPLGA

samples exhibited cell clusters and hollow cells. The microvilli are important for the

absorptive function of the Caco-2 cells (Solmi et al., 2008, Fath and Burgess, 1995).

The hollow cells are unusual and their presence within the cluster of rounded cells

may indicate that the cells were currently undergoing or have undergone

programmed cell death.

The surface chemistry of the membranes is very similar before and after

modification. For this reason, the most plausible explanation for the difference in cell

attachment is the difference in surface topography. Inducing porosity appears to

create favourable conditions for the attachment of the cells while the unmodified

scaffold with its non-porous surface is not as supportive for the same purpose.

4.5.3 Cell Metabolic Activity and Proliferation on the Scaffolds

Having noted differences in the cell attachment, it was crucial to analyse linked changes to cell behaviour such as proliferation (Basson *et al.*, 1996). As such, the cell metabolic activity and proliferation were studied. The oxygen plasma treated ePLGA scaffold again showed statistically higher cell metabolic activity and proliferation compared to the uPLGA membrane and showed comparable values to tissue culture plastic. It is worth noting that the cells on the tissue culture plastic displayed the greatest metabolic activity and DNA content. The reason for the differences seen between the uPLGA and ePLGA surfaces probably stem from the initial cell attachment which was more pronounced on the etched membrane. Although not directly investigated in this work, there are a number of published works which elaborate further on the link between cytoskeletal remodelling which controls the cell shape and control of this by signalling differences caused by type or strength of attachment changes point to differences in signalling in rounded and spread out cells (Giancotti and Ruoslahti, 1999, Diener *et al.*, 2005, Wilson *et al.*, 1994). One study using attachment dependent rat fibroblasts has also shown that proliferation is enhanced in cells exhibiting a spread morphology over unspread or rounded cells (Hunter *et al.*, 1995). The increase in proliferation with the spread cells on the ePLGA suggests that the topography change creates changes to the cell attachment and that there signalling transduction differences between the uPLGA and ePLGA surfaces.

4.5.4 A Two Dimensional Intestinal Model

Having ascertained suitable cell attachment and proliferation, the ePLGA film was employed as an artificial basement membrane in a two dimensional *in vitro* intestinal model. Caco-2 cells were grown in monoculture and coculture with myofibroblast

cells (CCD-18Co). Immunostaining confirmed that the Caco-2 cells were positive for

E-cadherin which is present at and a marker for tight junctions while the

myofibroblast cells demonstrated phenotypic α smooth muscle actin staining

(Valentich et al., 1997, Eaton and Simons, 1995).

The performance of the biodegradable ePLGA scaffold was measured against PET

filters which are routinely used in monolayer and coculture studies of the intestine.

The ePLGA membrane was able to support both the epithelial cells (Caco-2) as

extensively studied and the myofibroblasts (CCD-18Co) as shown by a CellTracker

assay. In both monoculture and coculture, the Caco-2 cells showed increasing

TEER values which are typical of increasing formation of tight junctions (Hidalgo et

al., 1989). Myofibroblasts on their own do not generally display an increase in TEER

over time, however in coculture with certain colonic cell types, they are known to

enhance TEER of the epithelial cells (Beltinger et al., 1999). It was notable that the

myofibroblasts had a more dominant effect with the ePLGA films enhancing the

transepithelial resistance of the Caco-2 cells significantly when grown in coculture

compared to monoculture. The cells on the PET filters experienced enhancement of

TEER when grown in coculture with the CCD-18Co cells but this was not as

consistent compared to the ePLGA surface.

The final observation was that the Caco-2 cells cultured on the PET filters reached a

much higher TEER than those on the PLGA films. This difference was attributed to

the significantly higher level of confluency attained by the PET filters compared to

the ePLGA films. This may be attributable to the porosity of the ePLGA films which

may prevent formation of a confluent monolayer. This has previously been observed

with oesophageal cells on a variety of synthetic scaffolds including PLGA

(Beckstead et al., 2005). Confluency is an important factor especially as contact

inhibition is crucial for the differentiation of the Caco-2 cells (Hubatsch et al., 2007,

Jenkins and Milla, 1993). This experiment was a direct comparison between the PET filters and the ePLGA scaffolds. One modification that could be made to improve the TEER would be to seed cells at higher numbers to encourage greater confluency.

4.6 SUMMARY

The aim of the work in this chapter was to create and characterise a suitable material and design an artificial *in vitro* epithelial intestinal model. The PLGA membrane when modified by oxygen etching (ePLGA) was proven to enhance cell attachment by allowing a more spread out morphology compared to unmodified uPLGA. Consequently, statistically significant improvements were observed in the metabolic activity and proliferation of Caco-2 intestinal cells cultured onto its surface, again in comparison to uPLGA. These effects were theorised to be mediated through the change of surface topography.

The ePLGA film was used as a synthetic basement membrane in a two dimensional *in vitro* intestinal model and compared to a PET filter model. It was able to support the coculture of epithelial and myofibroblast cell lines over a period of 2 weeks with increasing transepithelial electrical resistance of the epithelial cells noted between day 0 and day 14. The epithelial cells grown in coculture on the ePLGA surface experienced enhancement to their transepithelial electrical resistance compared to cells that were grown in monoculture. The TEER of the ePLGA surface was not as high as that obtained by PET filters which are widely used in the pharmaceutical industry. This was attributed to the lower confluency of the epithelial layer on the ePLGA surface compared to the PET surface.

The ePLGA surface is a suitable degradable *in vitro* basement membrane substitute

for intestinal cells. It is proposed that higher cell seeding could improve the

confluency of the Caco-2 cells.

CHAPTER 5: A Three Dimensional Micron Scale Scaffold and Cell Sheets for Intestinal Tissue Engineering

This Chapter describes the design and manufacture of a three dimensional scaffold for colon tissue engineering. The current penchant for two dimensional and larger scale three dimensional models is discussed initially highlighting the achievements thus far and needs for progress. The design of the scaffold and unique seeding with cell sheets is then presented.

5.1 INTRODUCTION

The three dimensional architecture of the intestine is an important consideration in tissue engineering. This is because *in vivo* the crypts have key absorptive and secretory functions, controlling the uptake of water to the body (Geibel, 2005). Additionally the organisation of the cells in the crypt helps the homeostatic maintenance of the colon epithelium by creating restricted regions of proliferation, differentiation and apoptosis (Peifer, 2002). This was discussed more extensively in chapter 1.

Studies in the tissue engineering field account for the three dimensional perspective of the intestine in different ways. For example, on a macro-scale, tubular scaffolds have been designed to mimic the shape of the intestine as a whole (Mooney *et al.*, 1994, Wake *et al.*, 1996). These were created using PLGA or a blend of PLGA and PEG in the latter case to enhance pliability of the tube. The microscale features of the intestine were however not considered. As mentioned in chapter 1, for *in vivo* work, it is common to use organoid units sectioned from the intestine directly, therefore already bearing the desired 3-D structure. However with *in vitro* work, organoids have limited potential due to the tendency of the crypt structure to disintegrate. This was more extensively discussed in chapter 1.

In a separate study, to demonstrate the applicability of three dimensional printing, a scaffold with villi like features was created (Lee *et al.*, 2005). However, this model was not based on measurements from the intestine and the dimensions of the features were in the millimetre range. Hence, although the scaffold bore villi-like features, it was truly not reflective of the *in vivo* intestine.

The aim of the present work is to design a three dimensional scaffold which would

be reflective of the *in vivo* colon. An important consideration for this is that the

features of the intestine specifically the crypt dimensions would be in the micron

range. One perceived potential difficulty of this approach would be seeding cells

onto this scaffold. Conventionally, cells are seeded individually (single cells

suspended in media) onto scaffolds after trypsin treatment from a cell culture flask.

Trypsin is a proteolytic enzyme which is known to cleave peptide bonds and is

successful at detaching cells but is also thought to affect critical cell surface proteins

(Okano *et al.*, 1993). This method is widely used in research but there are

alternatives for instances when individual cell seeding may not be as successful.

One of these alternatives is the use of cell sheets. In 1993, Okano *et al*, published a

novel system for culturing cells on a temperature responsive polymer poly (N-

isopropyl acrylamide). The polymer is hydrophilic at temperatures above 32°C

allowing cell attachment but becomes hydrophobic below that temperature (Okano

et al., 1995). The change in surface energy causes the cells to lift off the polymer

and detach as a cell sheet with limited damage to cell receptors (Canavan *et al.*,

2005). This technique has grown in popularity finding applications in varying areas

including corneal regeneration, cardiac and liver regeneration (Yang *et al.*, 2005,

Miyahara *et al.*, 2006, Matsuda *et al.*, 2007). The main draw back of this technique

is that for the proposed cell type for the intestinal model, Caco-2 cells, the surface

has been seen as potentially cytotoxic if cells are cultured for 12 hours at

physiological temperature (37°C) (Vihola *et al.*, 2005).

An alternative technique to produce cell sheets was described by L'Heureux and

colleagues. They observed spontaneous cell sheet formation when human smooth

muscle cells were cultured to confluence (L'Heureux *et al.*, 1998). Separately,

though not describing cell sheets, the MacNeil group reported work on the use of

plasma polymerised surfaces to culture and transfer keratinocyte cells to a wound bed (Haddow *et al.*, 2003). This work is of interest as the cells were separated from the plasma polymerised surface without additional aids and the authors reported subsequent extensive coverage of the wound bed.

The final consideration in the scaffold design is that the cells of the colon have intricate signalling pathways that control the cell movement and behaviour in the crypt. This was described in more depth in Chapter 1. As the proposed 3D scaffold is based on microparticles, it is possible to mimic the isolating effect of the Wnt proteins of the colon. This would entail incorporating protein containing particles isolated to the lower crypt region and plain polymer samples in the upper section, creating a bilayer scaffold as seen in figure 5.1.

Cell seeding Scaffold   **Bilayer Scaffold**

O   Plain polymer particle   O Plain polymer particle
⬭   Intestinal Cell   O Protein containing particle
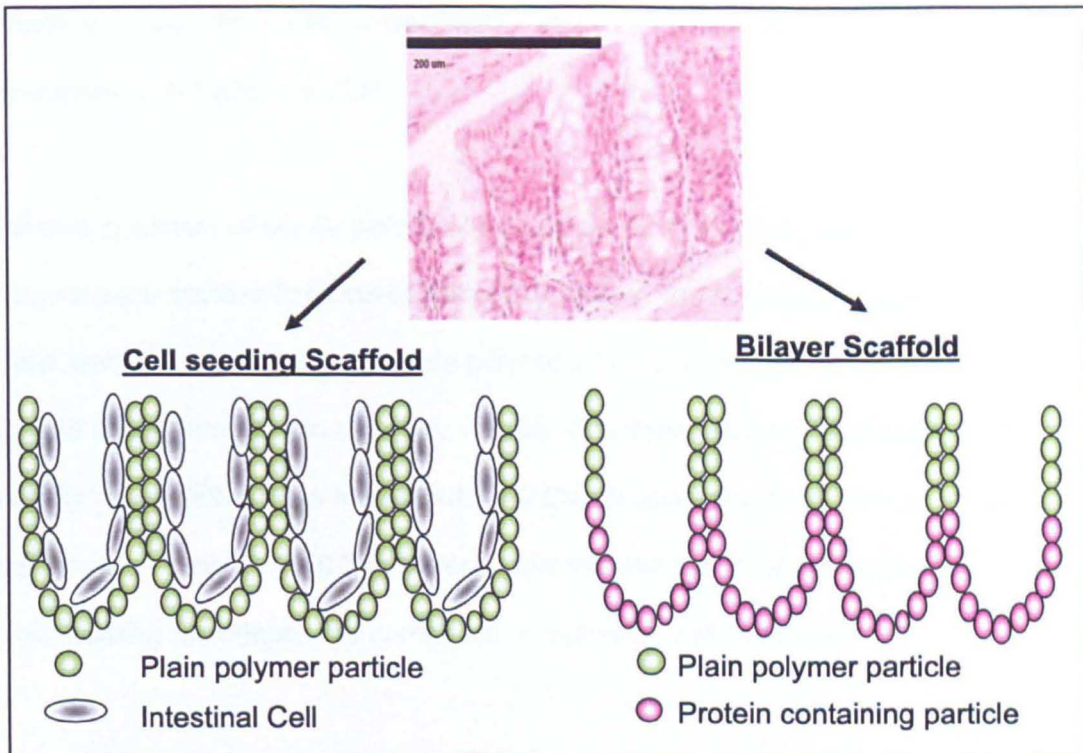
Figure 5.1: The two proposed three dimensional scaffolds for colon tissue engineering. At the top a histological staining of a mouse colon is shown to demonstrate the position and shape of the crypts.

This present work reports on the development of a novel method to culture intestinal cells for use in tissue engineering. Using plasma polymerised surfaces, intestinal cells were grown to confluence and lifted off the surfaces for transfer to scaffolds. The scaffold itself is also novel and three dimensional with invaginations similar to those found in mouse colon. As proof of concept, a model protein was incorporated into the scaffold to demonstrate that in future more relevant signalling proteins could be utilised.

5.2 EXPERIMENTAL

Following is a summary of the experimental methods, full details can be found in chapter 2. A three dimensional scaffold was formed using measurements from histological sections of mouse intestine. Electron beam lithography was used to create a mould which was subsequently filled by PLGA particles of a suitable size as measured with SEM and DLS.

Plasma polymers of acrylic acid (ppAAc) produced at varying plasma discharge powers were studied in terms of wettability (WCA) and surface chemistry (XPS). Cells were then cultured onto these polymers and cell response in terms of cell spread area (microscopic images), viability (live/dead staining) and cell metabolic activity (alamarBlue) was measured. Cell sheets produced by growing the cells to confluence on ppAAc and these were used to seed the three dimensional scaffold. This seeding technique was compared to individual cell seeding.

Finally a model protein, horse radish peroxidase (HRP) was incorporated into PLGA particles to form PLGA-HRP particles. Post incorporation, the PLGA-HRP particles were tested for peroxidase activity using an enzyme/substrate reaction. PLGA-HRP particles were isolated to the bottom of the scaffold by applying a small volume of

suspended PLGA particles to the mould first before adding the PLGA-HRP particles and sintering. The feasibility of this approach was examined using ToF SIMS to detect the peptide backbone.

5.3 RESULTS

5.3.1 Mould Dimensions and Design

The scaffold was fabricated on the basis of measurements from several histological sections of mouse colon (figure 5.2). The dimensions considered were the average dimensions of crypt depth, width and spacing and the results of these measurements are shown in table 5.1.

Crypt depth

Crypt width

Crypt spacing
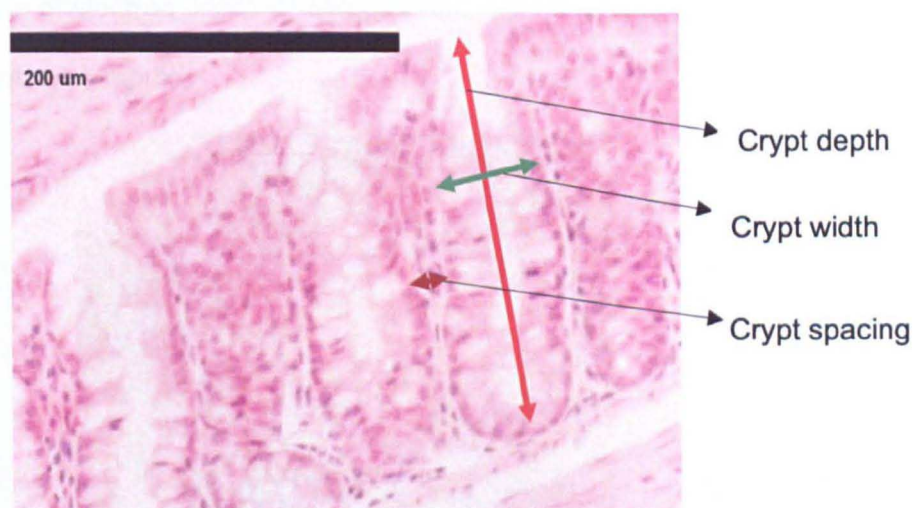
Figure 5.2: Representative haematoxylin and eosin stained mouse colon showing intestinal crypts and the dimensions taken into consideration for the mould formation as described in section 5.3.2.

Table 5.1: Statistical analysis of crypt dimensions based on mouse colon. Error

shows mean ± SD for n =20

Section of Colon	Dimension / μm
Crypt depth	179.44 ± 12.17
Crypt width	61.82 ± 3.06
Spacing between crypts	12.55 ± 1.37

5.3.2 Mould Fabrication

The mould for the scaffold was formed by electron beam lithography. AFM was used

to verify the pattern of pillars of the resulting POP mould. There was some evidence

of slight beam damage to the pillars (figure 5.3) but overall the pattern was

produced accurately over 1cm by 1cm area (not shown).

Due to constraints of electron beam lithography, the pillar height was limited to

50μm for this prototype mould.
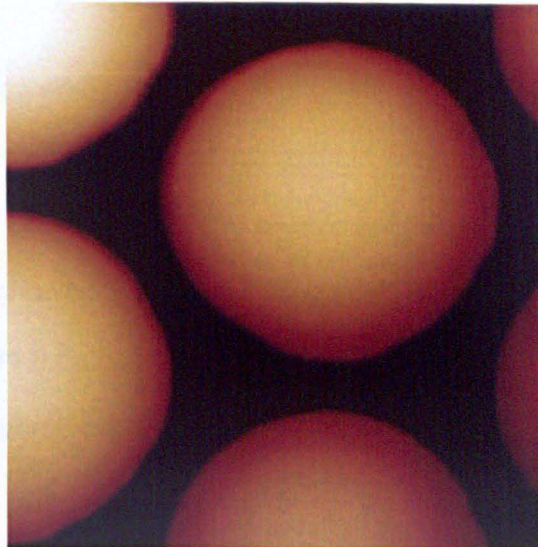
Figure 5.3: AFM image of mould produced by electron beam lithography. Image

shows pillars of specified width and separation. Area shown measures 110μm

x110μm.

5.3.3 Particle Size

PLGA particles were prepared using an emulsion method and in order to ascertain particle size, SEM and DLS were used. SEM images showed that the particles as prepared were spherical and appeared to be relatively small in diameter (figure 5.4). To confirm that the particles were of a suitable size for mould filling, the particle diameter was measured using DLS. The particles as prepared were shown to be non-homogenous in diameter, ranging in size from 137nm to 3.4μm (figure 5.5). The particles measuring on average 533nm in diameter were the largest fraction (63.4% of total volume).

Taking into consideration a mould spacing of 12 microns, the particles as prepared were deemed to be of a suitable size for the purpose of filling mould to prepare the scaffold.

5.3.4 Formation of the Three Dimensional Scaffold

The scaffold was prepared by filling the mould with a suspension of PLGA particles. The three dimensional appearance of the scaffold was an important result as the aim was to mimic the architecture of the colonic epithelium. Scanning electron microscopy imaging showed that the resulting scaffold had accurate features with a crypt like shape (figure 5.6a) with space to seed cells (figure 5.6 b and c). This prototype scaffold covered an area of 1cm^2.
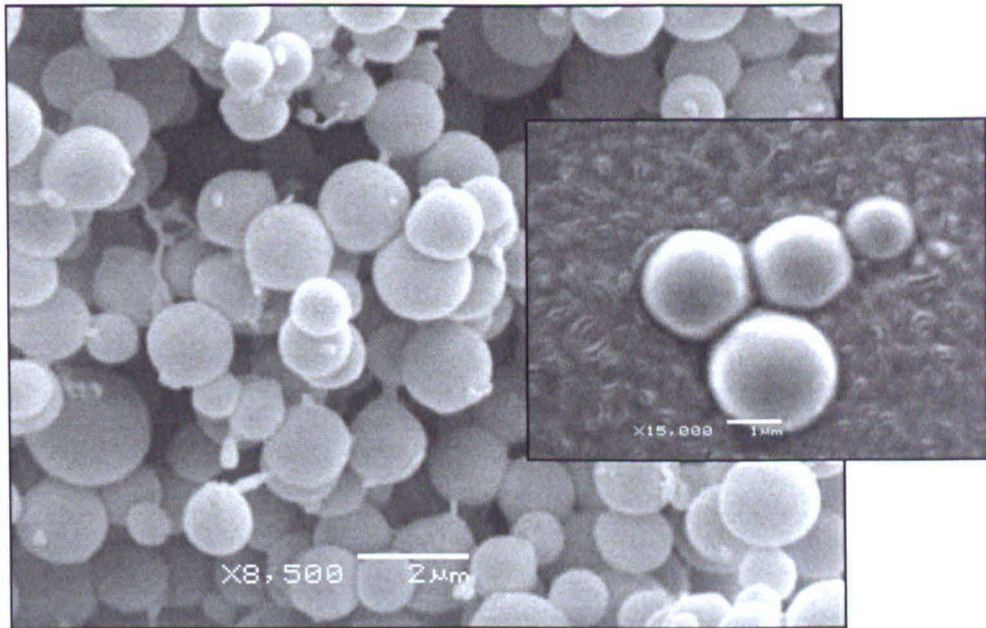
Figure 5.4: Representative SEM images show the spherical shape and varying sizes of the particles formed. Inset is a higher magnification view showing the particle diameter.
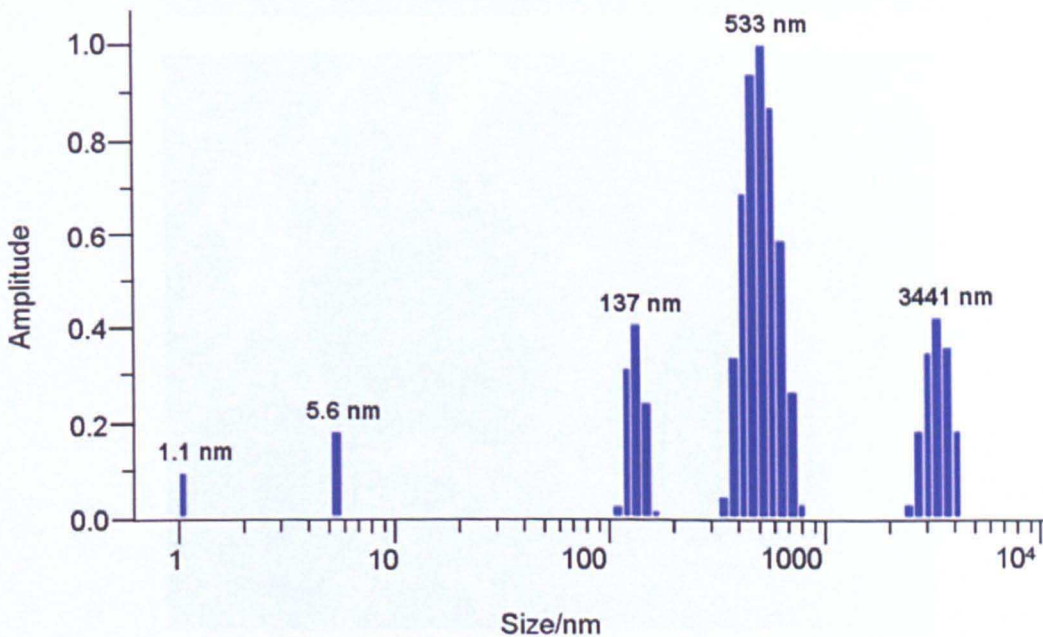
Figure 5.5: Particle size ranged from 1nm to 3.4 microns. Shown above is a representative graph from 1 of 3 samples.
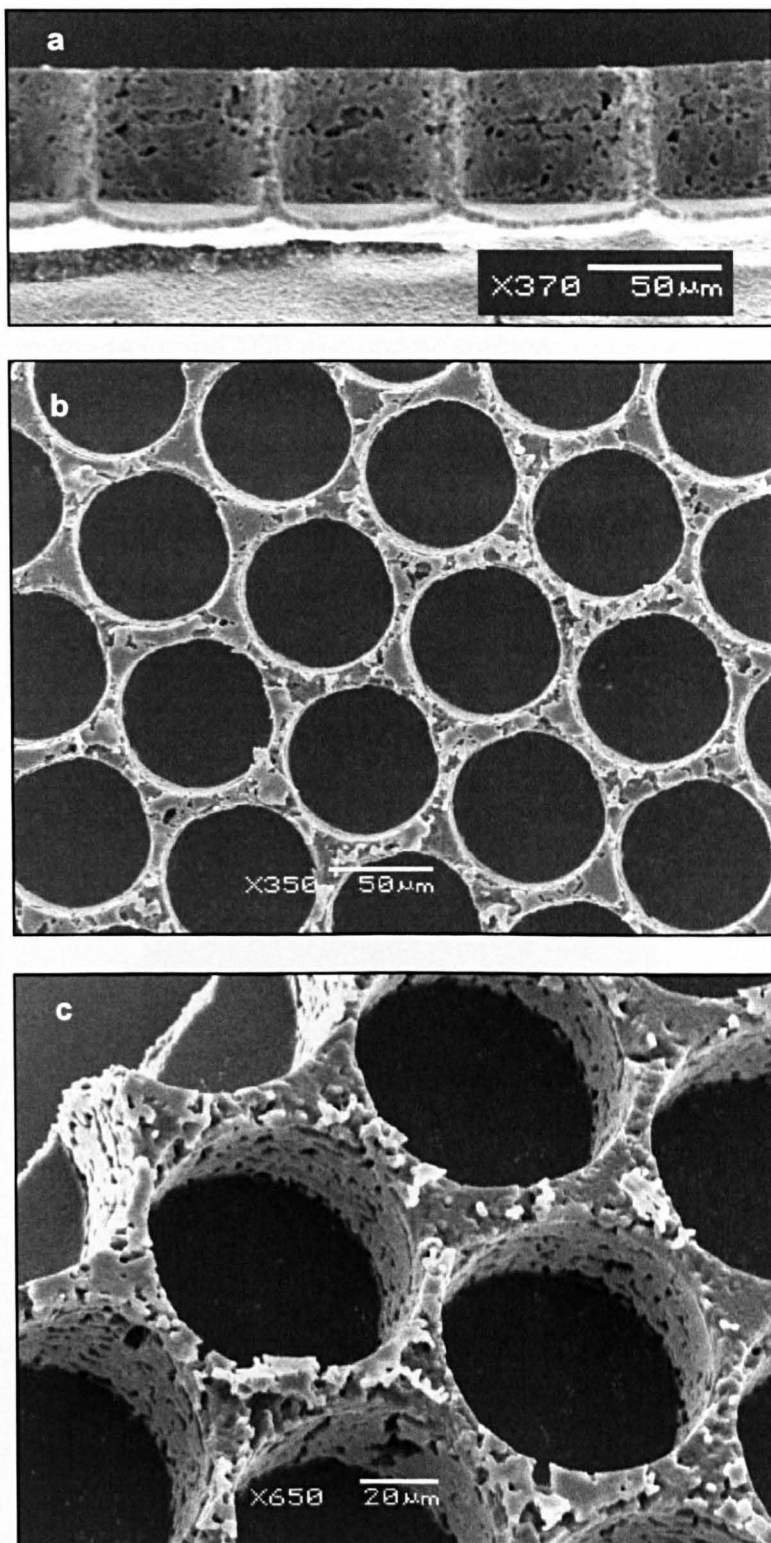
Figure 5.6: Representative images show the architecture of the three dimensional scaffold. Views are shown the side/transverse section (a), the top (b) and at an angled view (c).

5.3.5 Cell Response to Surfaces

Caco-2 cells were grown on three surfaces, TCP, ppAAc coated glass coverslips (discharge power of 20W) and uncoated glass coverslips (figure 5.7). Although the cells were initially seeded at the same levels and cultured in the same conditions, the cell area coverage for the TCP and ppAAc surfaces appeared comparable while that on the glass surface appeared significantly less. The cells were able to grow to confluence on ppAAc and TCP surfaces only.
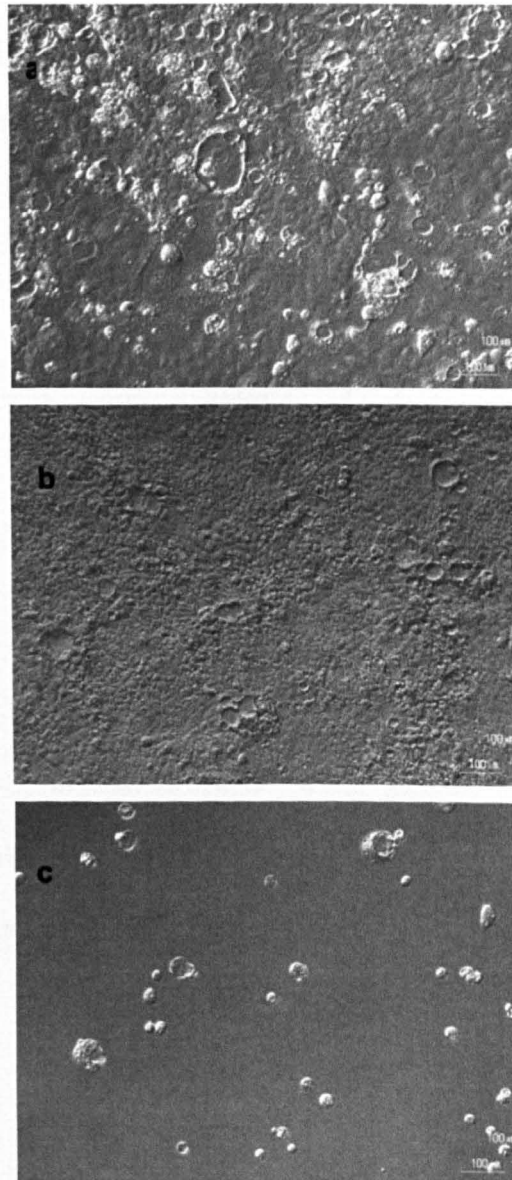
Figure 5.7: Representative light microscope images showing Caco-2 cells as grown on tissue culture plastic (a), ppAAc (depositing power =20W) coated glass (b) and uncoated glass (c). Cells were cultured for 5 days prior to imaging.

To further investigate these differences, the cell area occupied on each surface was determined using image analysis software. The qualitative differences observed were confirmed quantitatively. Cell area was slightly higher on average on the ppAAc surface compared to the TCP surface (figure 5.8), however this difference was not significant. This was unlike the difference between the ppAAc surface and glass surface as well as the TCP surface and the glass surface too. In both these cases, the statistical difference was high ($p<0.01$) with the ppAAc and TCP surfaces reaching over 75% cell area coverage while the glass surface was just under 3% (figure 5.8). Cells therefore preferentially adhered and reached near confluence on ppAAc and TCP surfaces.
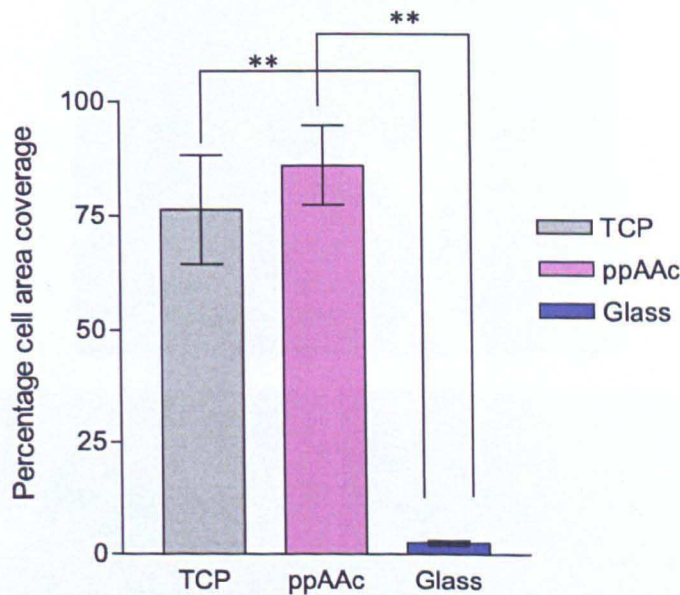
Figure 5.8: The cell area coverage for TCP and ppAAc was significantly higher compared to plain glass coverslips. Error bars represent mean ± SEM for n=4 (** = $p<0.01$).

5.3.6 Production of Cell Sheets

Cell sheets were formed only on the ppAAc surfaces. They were produced after culturing Caco-2 cells to confluence for approximately 5 days. The cell sheets (figure 5.9 a and b) were lifted off the ppAAc coated glass by gentle agitation of the cell culture dish. The cell sheet contracted in size as seen in figure 5.9 a. A CellTracker assay was used to confirm that the cells of the cell sheet were live cells. Extensive green fluorescence was observed indicating the presence of live cells on the cell sheet (figure 5.9 c)
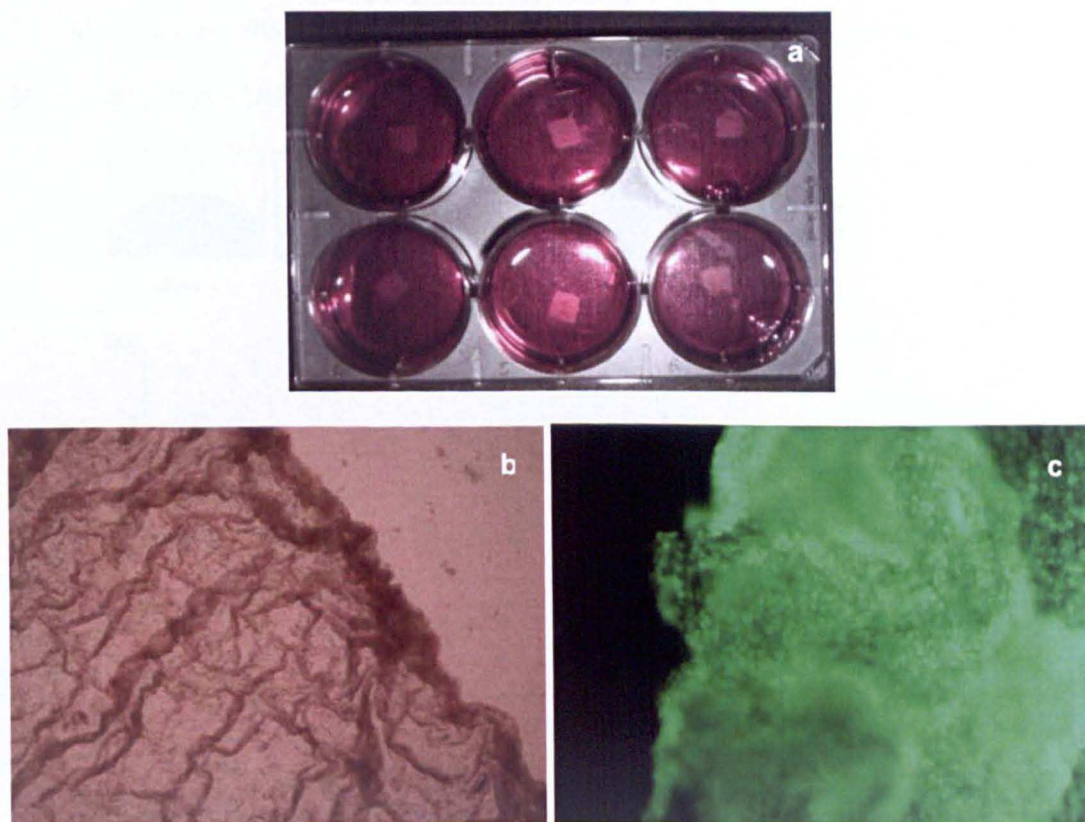
Figure 5.9: Cell sheets are shown in a cell culture well plate (a). Representative images show the edge of cell sheet (b) and green fluorescence from a CellTracker assay indicates live cells (c).

5.3.7 Changes to ppAAc Water Contact Angle with Variable Plasma Deposition Power

Changes to plasma conditions when producing plasma polymers can alter the surface wettability. To monitor any changes, water contact angle measurements were undertaken. The results of these measurements show that prior to plasma coating, the glass surface (oxygen etched for 5 minutes) was quite hydrophilic with a contact angle of 44° (see figure 5.10). As the depositing power of the plasma increased, the surface became less hydrophilic demonstrated by the water contact angle increasing to 53° when the plasma was struck at 20W and gradually rising to 70° when ppAAc was deposited at 60W. Further increasing the discharge power to 80W resulted in a decrease to the water contact angle to 63°.
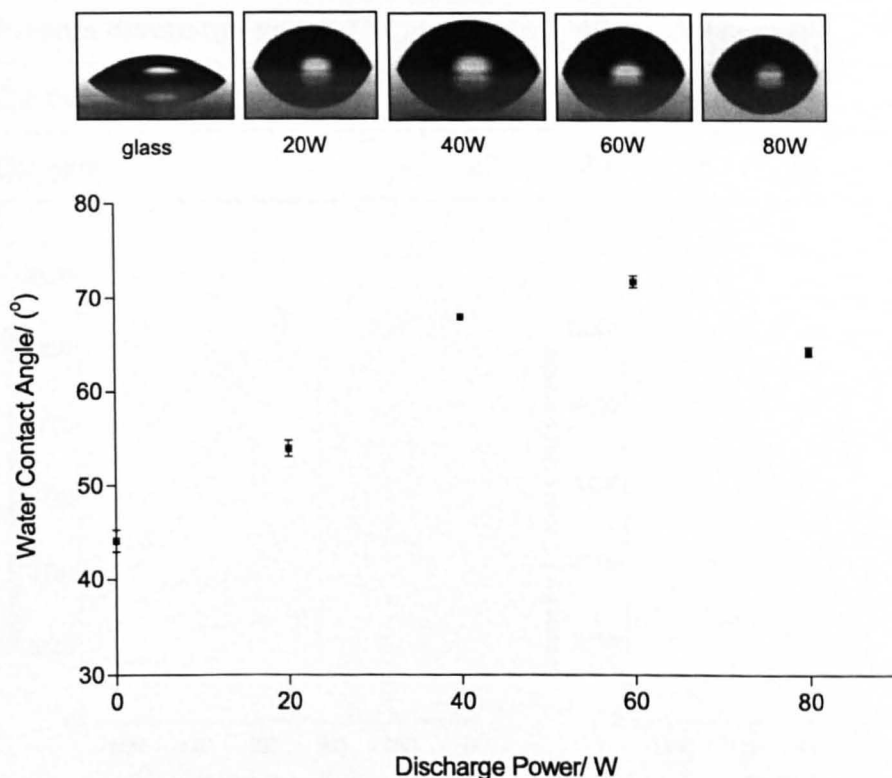
Figure 5.10: Water droplets on the surface of glass and ppAAc coverslips are shown above. The graph traces the changes to the ppAAc water contact angle as plasma discharge power increased. Error bars represent mean ± SEM for n=4.

5.3.8 Surface Chemical Analysis with XPS

To further investigate the changes in water contact angle, the surface chemistry of the ppAAc surfaces was investigated. A survey scan (figure 5.11) revealed the presence of carbon (corrected to C1s 285 eV) and oxygen (O1s 533 eV) on the surface of the ppAAc coated samples (20W to 100W depositing power). The 20W and 40W samples had trace amounts of sodium (Na 1s 1072eV -0.31% for 20W and 0.08% for 40W) likely from the glass coverslip. Table 5.2 shows the elemental composition for all the ppAAc coatings.

Table 5.2: Elemental composition table showing carbon and oxygen atomic percentage on the surface of ppAAc coated glass coverslips. Figures shown represent mean of 4 samples. The SEM for all values was below ± 1%.

Plasma discharge power / W	20	40	60	80	100
Carbon	77	80	82	85	89
Oxygen	23	20	18	15	11
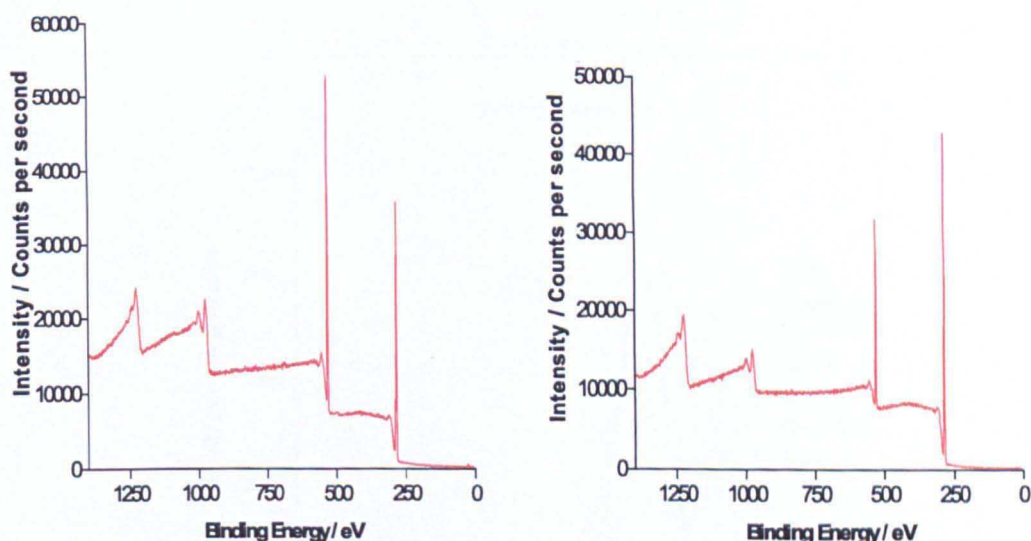
Figure 5.11: Representative XPS wide spectra of ppAAc coated glass samples showing oxygen (O1s 533 eV) and carbon (C1s 285 eV) peaks. The spectrum to the left is a ppAAc coating deposited at a discharge power of 20W and to the right is a spectrum of the same coating deposited at a discharge power of 100W.

5.3.9 Detailed Analysis of C1s Region

Peak fits were performed on the high resolution C1s signal to determine the relative amount of functional groups on the surface. According to literature (O'Toole *et al.*, 1996), the components were identified as C-C/C-H (284.90 eV), C-COOX (285.64eV), C-OX (286.62eV), C=O (287.92eV) and COOX (289.23eV) groups (figure 5.12). For the peak fits, the full widths at half maximum (FWHM) were constrained such that FWHM(C-OX) = FWHM(C=O) = FWHM(C-C/CH) and FWHM(C-COOX) = FWHM(COOX). The area of C-COOX was set to equal that of COOX.
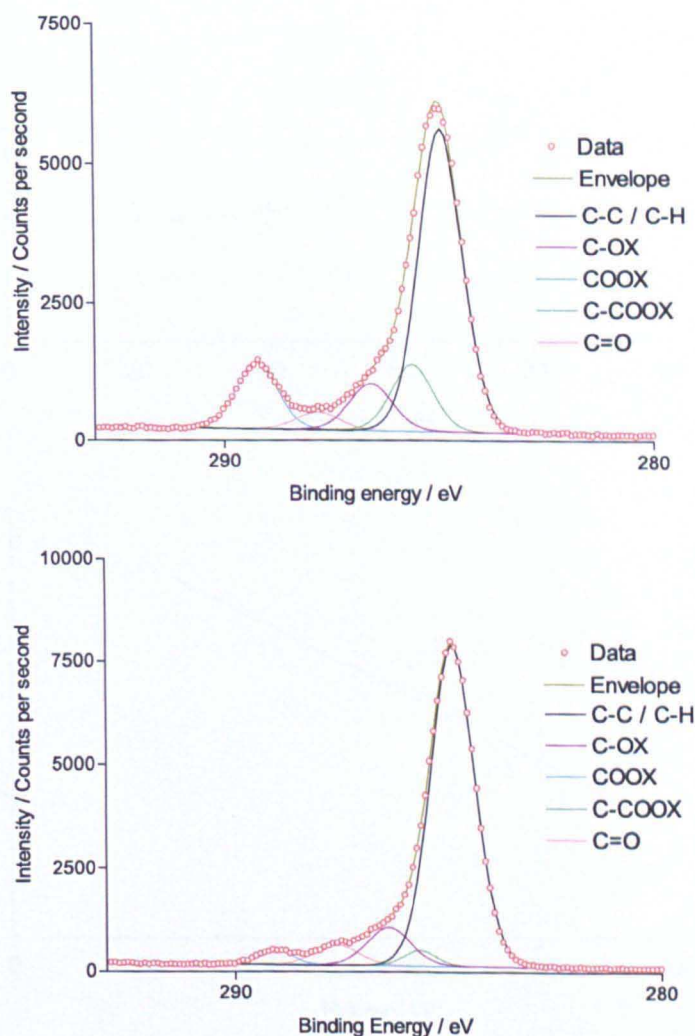
Figure 5.12: Representative C1s high resolution spectra are shown above with a visible decrease in the COOX functionality on 20W (top) compared to 100W (bottom).

The high resolution spectra revealed that as the discharge power increased, the hydrocarbon functionality (C-C/C-H) increased in content while the carboxyl (COOX) content of the ppAAc films decreased. The relationship of these groups to the discharge power was analysed further. As the plasma discharge power increased from 20W to 100W, the hydrocarbon functionality was relatively constant between 20W and 60 W before increasing rapidly between discharge powers of 80 and 100W (figure 5.13). At the same time the carboxyl content (COOX) of the ppAAc films decreased steadily with increasing discharge power (figure 5.13).
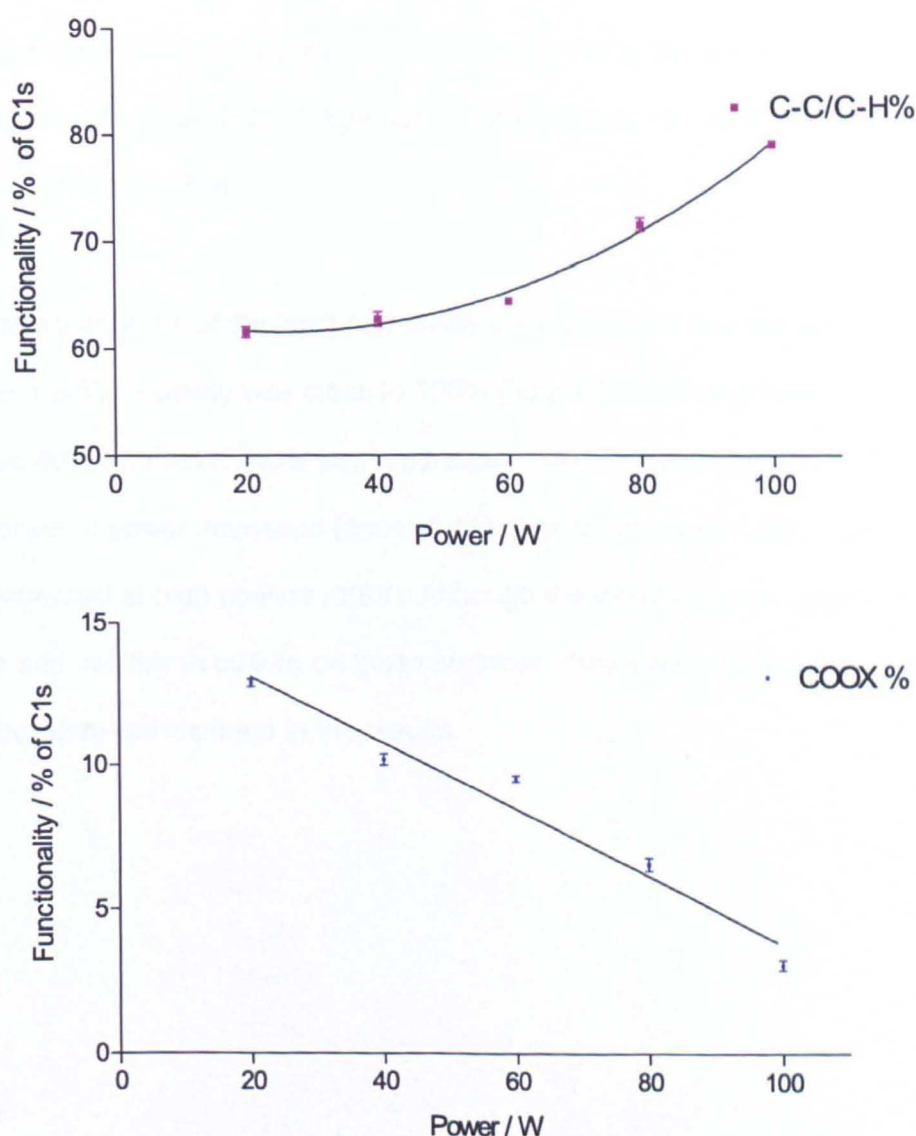
Figure 5.13: The hydrocarbon functionality increased with applied power (top) while the carboxyl content of the ppAAc films decreased. Error bars represent mean ± SEM for n=4.

5.3.10 Cell Response to Plasma Polymer Film

With expected changes to the surface chemistry and wettability of the plasma polymerised acrylic acid film, it was important to study changes to cell activity. A live/dead assay was therefore undertaken to determine the cell viability defined in this case as the relative number of live cells. The assay indicated that cell viability was affected by deposition power. At low discharge powers, there was extensive green fluorescence indicative of live cells but as the discharge power used to create the ppAAc films increased, red fluorescence began to dominate showing that the number of dead cells was increasing. This is depicted in figure 5.14 with comparison staining for a low plasma discharge power - 20W ppAAc film and a high discharge power - 60W ppAAc film.

Quantitative analysis of the live/dead assay showed that at low deposition powers (20W and 30W), viability was close to 100% (figure 5.15). It also revealed that between 40W and 60W, there was a consistent and steep decrease in viability as the deposition power increased (figure 5.15). Cell sheets were not formed on ppAAc films deposited at high powers (80W). Although the intestinal cells appeared to adhere and multiply in culture on these surfaces, they were not able to detach and were therefore not included in the results.
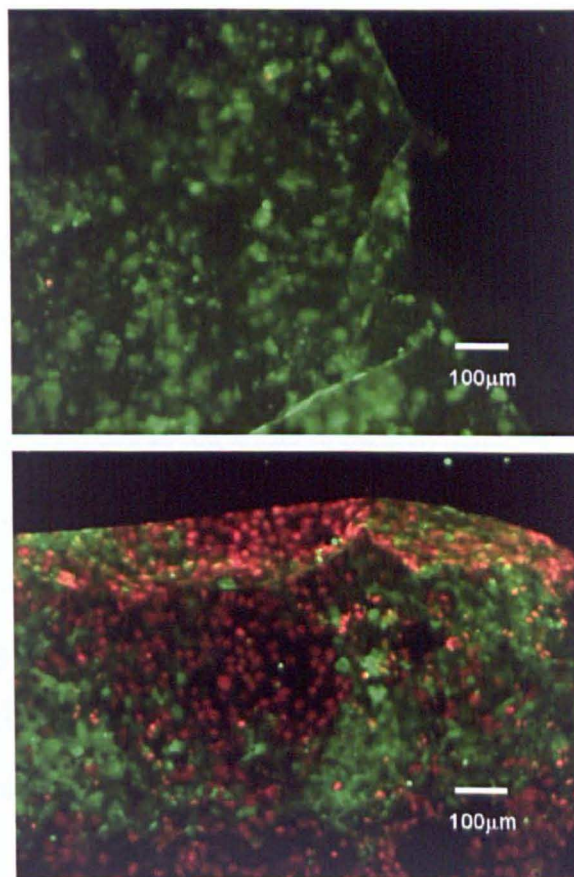
Figure 5.14: Distinct differences in live/dead staining were noted. Cell sheets from ppAAc coverslips formed at a discharge power of 20W (top) show extensive green fluorescence indicating the dominance of live cells. At 60W (bottom) both red and green fluorescence are present indicating both live and dead cells. The images shown are representative of several observations.
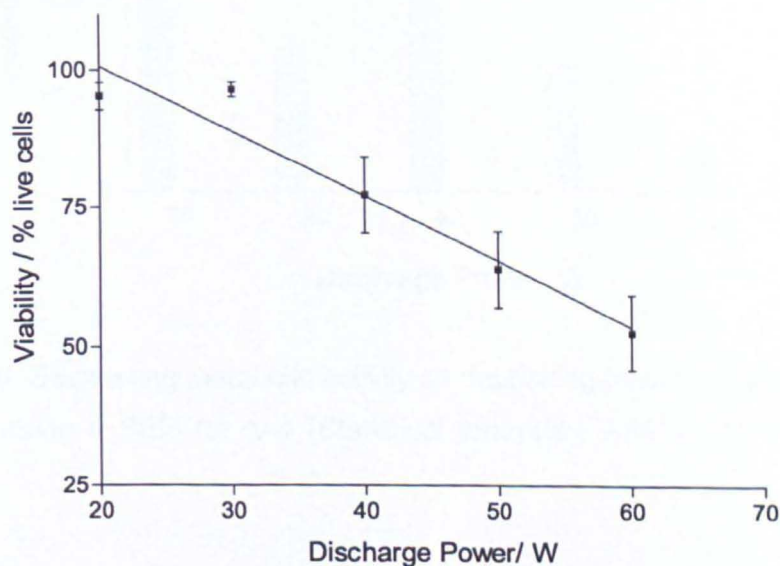
Figure 5.15: Quantitative live/dead staining shows that the viability of the cells decreased as the deposition power increased. Error bars are mean ± SEM for n=4.

5.3.11 Metabolic Activity of Cell Sheets

As a complimentary test to the live/dead assay, the metabolic activity of the cells was tested using an alamarBlue assay. There was a large decrease in metabolic activity between 20W and 30W, despite the live/dead assay showing comparable live cell numbers (figure 5.15 and 5.16). Between 40W and 60W the metabolic activity showed a similar trend to the live/dead assay with consistent and gradual decreases as the discharge power increased (figure 5.16).

The cells had a statistical significantly higher metabolic activity at 20W than at any other power (figure 5.16). The metabolic activity between 40W and 60W was also statistically significant.
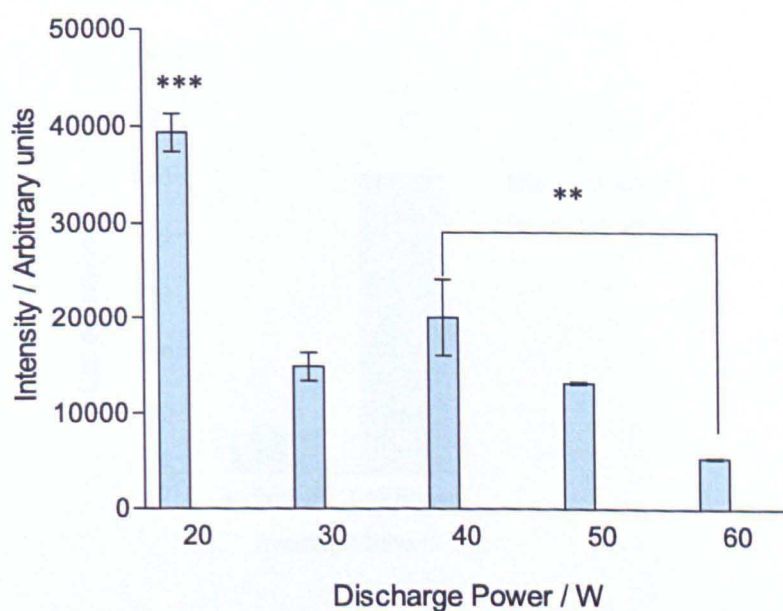
Figure 5.16: Decreasing metabolic activity as depositing power increases. Error bars represent mean ± SEM for n=4 (Statistical analysis - ANOVA ***= $p<0.001$, ** = $p<0.01$).

5.3.12 Cell Seeding on 3D Scaffold

Cell sheets were used to seed the 3D scaffolds and this was compared to individual cell seeding. A CellTracker assay was undertaken after 5 days in culture and revealed that the scaffolds seeded with cell sheets had a significantly greater number of live cells compared to individually seeded cells (fig 5.17).
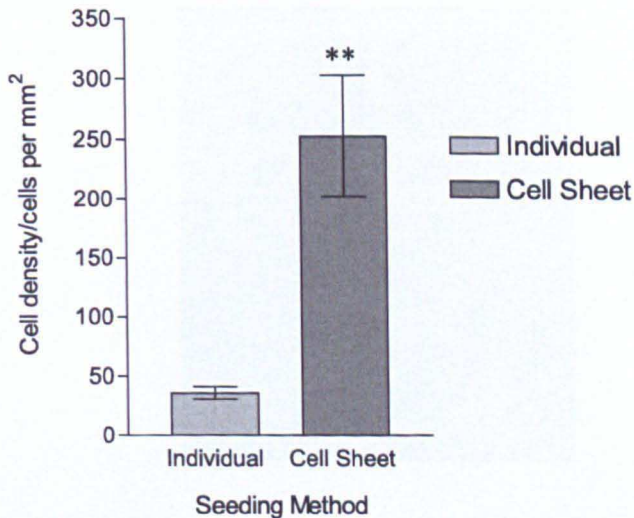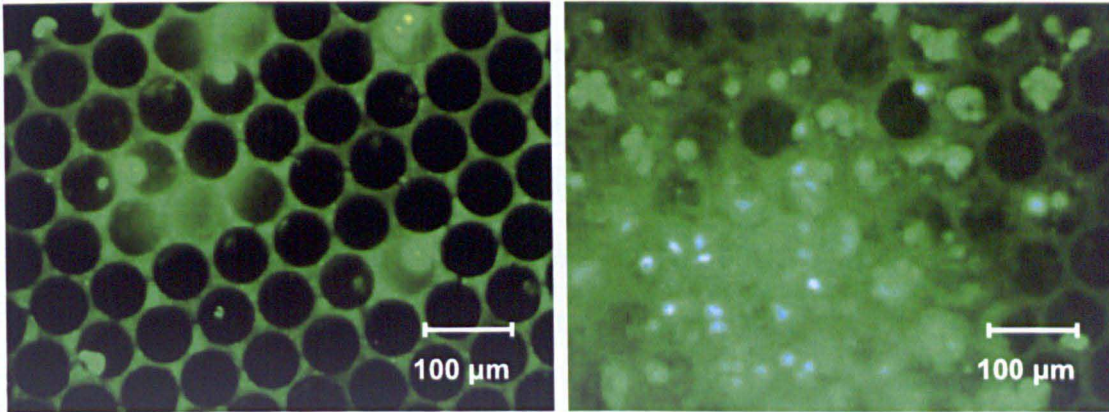
Figure 5.17: Cell seeding was quantified using green fluorescence emitted by live cells stained with CellTracker on the micron scale scaffold. Individual cells were used to seed the scaffold (top left) while a cell sheet was used in the image shown at the top right. Cell numbers are shown for an area measuring 564μm x 740μm. In the graph, error bars represent mean ± SEM for n=5 (Statistical analysis - t test, p=0.0072).

5.3.13 PLGA-HRP Particles for Bilayer Scaffold

To indicate the feasibility of forming a bilayer scaffold (see figure 5.1), a model protein, HRP was incorporated into the particles. This enzyme was selected as in the presence of its substrate, TMB, a colour change from colourless to blue/blue green occurs allowing for quick determination of protein activity or presence.

The prepared plain PLGA and PLGA-HRP particles were sintered in separate glass vials for 1.5 hours at 60°C to mimic the conditions that the bilayer scaffold would undergo. After cooling down, a few drops of the TMB substrate were added to each vial. There was no colour change to the TMB with the PLGA particles (figure 5.18). The PLGA-HRP particles did change the TMB from colourless to a deep blue-green colour.

Figure 5.18: Enzyme activity was not detected with PLGA particles (left in the image) but was marked by a colour change of the TMB substrate to dark blue/green in the presence of PLGA-HRP particles.

5.3.14 Protein Detection through ToF SIMS of Bilayer Scaffold

To create the bilayer scaffold, PLGA-HRP particles were isolated to the bottom of the scaffold while the top was filled with plain PLGA particles (see chapter 2 and figure 5.19). As the scaffold is a micron scale model, ToF SIMS was used to detect if there had been successful isolation of the protein in the final scaffold. Ion fragment maps were taken from two separate sections of the scaffold. First, the top of the scaffold where PLGA particles were expected to dominate and separately the scaffold was sectioned with a microtome (Leica RM2165), removing the top 30μm to expose the region where PLGA-HRP particles were in turn expected to be present and this section was imaged (figure 5.19).

Section Line

○ PLGA particle
◉ PLGA-HRP particle
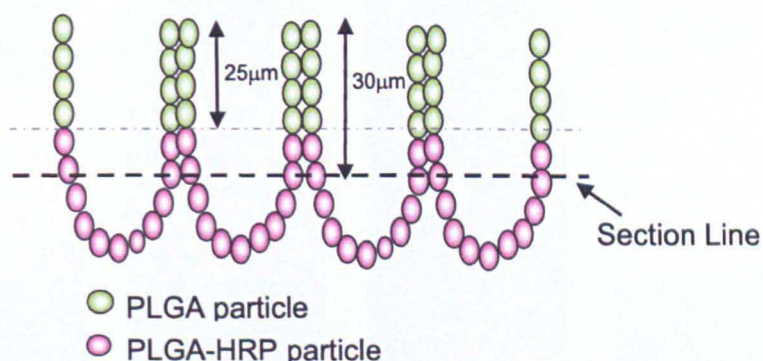
Figure 5.19: Illustration of bilayer scaffold showing the expected locations of PLGA and PLGA-HRP particles.

Signals that can be attributed to the peptide backbone of the HRP enzyme were identified as potential key differences between the PLGA-HRP particles and the plain PLGA particles. These were specifically the two ion fragments CN^- and CNO^- (m/z 26 and 42 respectively). The ion fragment map showed evidence of these fragments more distinctly on the PLGA-HRP particles and scaffold compared to the plain PLGA particles and scaffold (figure 5.20). Detailed analysis of the ToF SIMS negative ion spectra for all surfaces showed evidence of peaks attributed to the peptide backbone (figure 5.21).
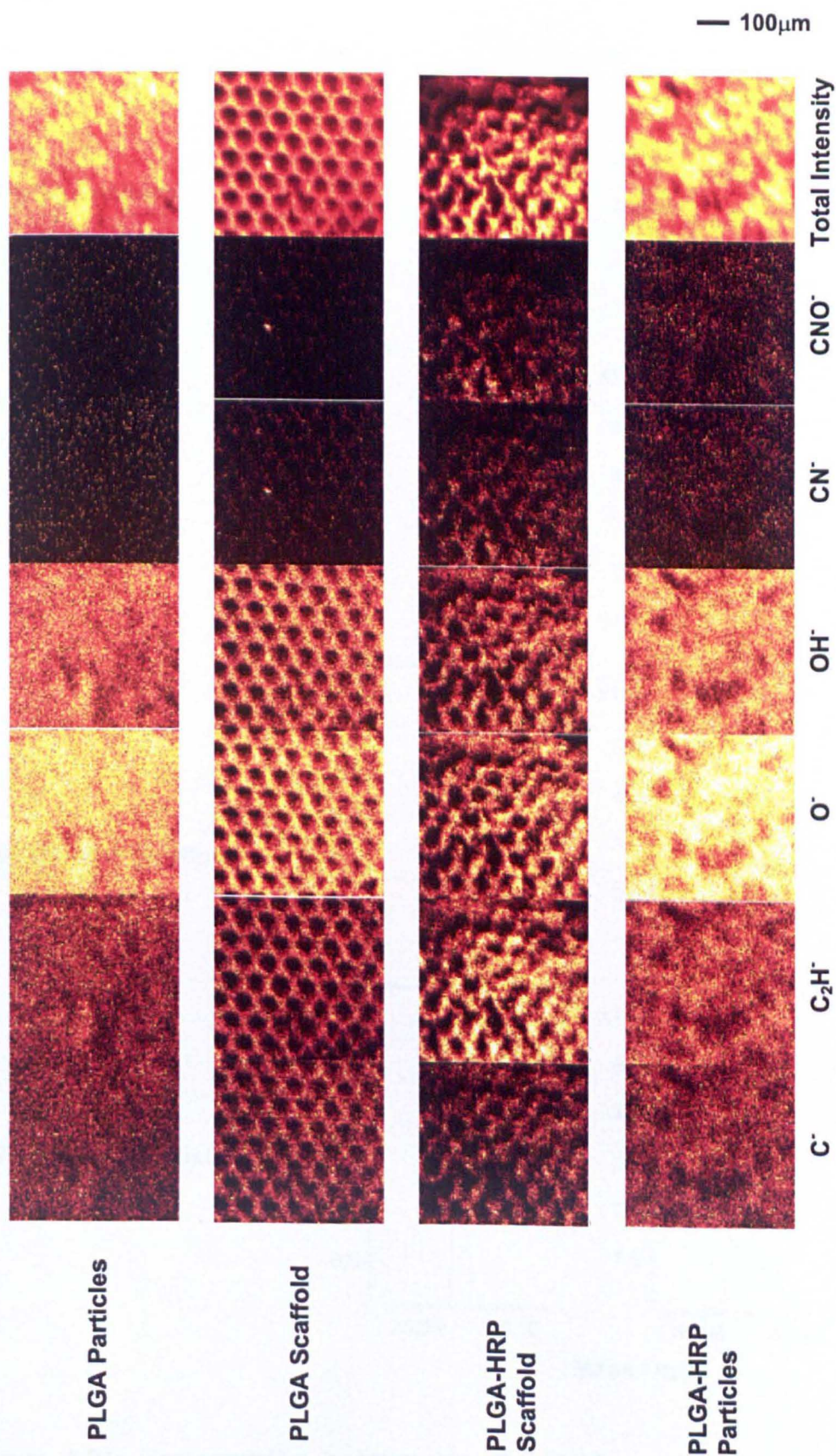
Figure 5.20: Negative ion fragment map for PLGA particles, PLGA scaffold, PLGA-HRP scaffold and PLGA-HRP particles respectively.
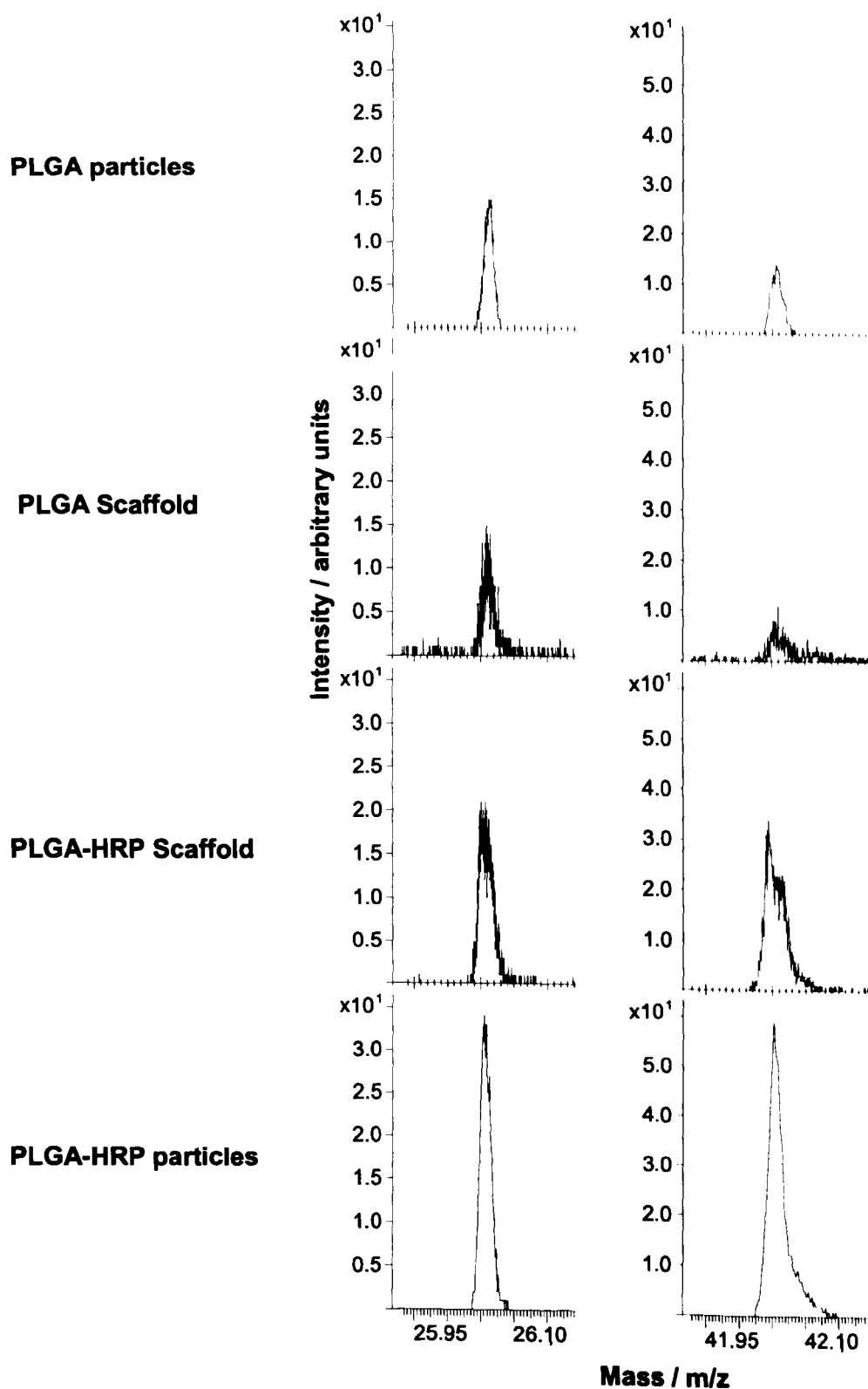
Figure 5.21: Representative negative ion ToF-SIMS spectra showing peptide backbone peaks for CN⁻ and CNO⁻ (m/z 26 and 42 respectively).

It was evident that the peaks for the plain PLGA particles and the PLGA surface of the scaffold were smaller than those of the PLGA-HRP particles and the PLGA-HRP surface of the scaffold (figure 5.21). Further analysis of the ion intensities showed that the relative content of CN^- and CNO^- on the PLGA-HRP scaffold was higher (table 5.3). Relative intensity was calculated by dividing the total count for each ion by the total negative ion count. All four samples were then scaled against the lowest value. This was repeated separately for CN^- and CNO^-.

Table 5.3: Summary of the total ion count from the negative spectra with relation to CN^- and CNO^-

	Ion Count For CN⁻	Ion Count for CNO⁻	Total Negative Ion Count	Relative CN⁻	Relative CNO⁻
PLGA particles	5124	2686	3940258	1.0	1.0
PLGA Scaffold	7400	2667	3430099	1.7	1.1
PLGA-HRP Scaffold	28965	24583	5916884	3.8	6.1
PLGA-HRP Particles	18782	19467	5751844	2.5	5.0

5.4 DISCUSSION

5.4.1 Design of 3D Scaffold

A three dimensional scaffold mimicking the crypt structure of the colon was successfully designed and achieved. Using histological images of the mouse crypt, accurate dimensions of the crypt width and spacing were attained but constraints of electron beam lithography limited the depth of the mould to 50 microns. Micron and submicron sized particles were used to fill the mould. The low molecular weight of the PLGA polymer and the relatively high content of the surfactant PVA allowed the desired particle size to be achieved. A 10% PVA concentration with a 3% PLGA solution has previously been shown to decrease particle size into the submicron range and improve the heterogeneity commonly associated with the emulsion technique (Rafati *et al.*, 1997). The particle size range produced was within mould filling range (under 5μm). The resulting scaffold was reminiscent of the colon architecture with crypt like features and space to seed cells.

5.4.2 Plasma Polymer for production of Cell Sheets

The new scaffold required unique cell seeding. A new approach applying a plasma polymer film of acrylic acid to culture cells and then allow them to lift off as a cell sheet was used. Previous reports by the MacNeil group have shown the ability of skin epithelial cells, keratinocytes, to grow on plasma polymers which include acrylic acid as a monomer. The cells can be subsequently transferred to a wound bed (Haddow *et al.*, 2003, Haddow *et al.*, 2006). The novel approach in this work was to use ppAAc to culture intestinal epithelial cells and lift them off as a cell sheet for easy transfer to the three dimensional scaffold. The mechanism by which this happens is not known. Based on the observations made during this work and on

known literature a mechanism is proposed (figure 5.22). This mechanism takes into account literature such as plasma polymer swelling and deformation in the presence of water. This has been reported for amine and hexane plasma polymer surfaces ((Vasilev et al., 2008, Zelzer, 2009). The mechanism also incorporates known cell behaviour such as Caco-2 cells producing extracellular matrix proteins (Vachon et al., 1993). Additionally observations such as contraction of the cell sheet were accounted for. There is insufficient data at the present time to support a definitive theory.

Initial cell culture studies revealed that the cell area coverage of the Caco-2 intestinal cells on the ppAAc glass compared well to tissue culture plastic which is a standard cell culture surface. Plain glass coverslips without the plasma polymer coating did not allow the cells to attach showing the presence of the plasma polymer was essential for cell proliferation. Further studies on the ppAAc glass coverslips demonstrated that increasing the discharge power of the plasma led to an increase in water contact angle between 20W and 60W before decreasing slightly at 80W. The change in water contact angle of the plasma polymer film is likely to be related to changes in the surface properties. Thin plasma polymer films tend to be topographically smooth and therefore the differences are likely to be attributed to changes in surface chemistry (Siow et al., 2006, Chatelier et al., 1995). The XPS data showed that as the discharge power increased, the proportional surface hydrocarbon content increased with a mutual decrease in carboxyl content. This has been shown previously at lower plasma discharge powers (1W and10W) (O'Toole et al., 1996).This present work therefore expands this observation with a greater span of plasma discharge powers. As plasma discharge power increases, the likelihood of fragmenting the particles within the plasma increases and it is therefore not unexpected that the carboxyl content would decrease in favour of the smaller hydrocarbon. Functional group retention if desired is possible with control of plasma

1998).

polymer conditions such as plasma power and monomer flow rate (Daw *et al.*,

Biological Theory

Force Theory

Cells attach initially to the surface through integrins and adsorbed protein on the plasma polymer

Initial force is a binding force to the glass surface by the plasma polymer

Cells proliferate and produce their own extracellular matrix to maintain attachments to the plasma polymer

Cells proliferate and are bound to the plasma polymer through contributing to the downward force

Cells adhere strongly to each other while fluid is taken up by the plasma polymer causing it to swell and degrade

Contractile forces are produced in the cell layer due to strong cell-cell adhesions

Cells detach as a sheet due to the strong cell to cell adhesions and weakening plasma polymer

Contractile forces greatly exceed the downward binding force causing the cells to lift off as a cell sheet

Legend

Plasma polymer	Cell
Glass surface	Integrin
	Serum protein
	Cell –made protein
	Cell to cell adhesions
	Force

Figure 5.22: Schematic illustrating possible mechanisms by which cell sheets are

formed and lifted off the ppAAc.

5.4.3 Cell Behaviour on ppAAc

As discussed in Chapter 1, changes to the surface chemistry and wettability can affect cell behaviour. For this reason, a live/dead assay was employed to check cell viability. There was not much difference between discharge powers of 20 and 30W, but between 40W and 60W the viability decreased steadily to just over 50% of cells being viable at 60W. However, the metabolic activity of the cells showed that only at 20W was the activity sufficiently high while ppAAc surfaces created at higher discharge powers had cells with significantly lower activity. Previous work on osteoblasts cultured on octadiene and acrylic acid polymers showed no correlation between surface wettability and cell attachment (Daw et al., 1998). It is, however, likely that the Caco-2 cells may show increased viability and metabolic activity due to the high content of the carboxyl function group. This conclusion is supported by previous observations with keratinocytes which showed that those epithelial cells responded to the carboxylic acid functional group in plasma polymers of acrylic acid (Haddow et al., 1999).

On the basis of these observations, it was determined that a cell sheet produced at 20W was ideal for cell seeding of the colon scaffold. The cell sheet was successfully transferred to the scaffold and as predicted, this method of seeding led to a significantly higher number of cells present on the scaffold surface compared to individual cell seeding. A likely reason for this is that more cells were able to attach to the confined spaces of the 3D scaffold when a cell sheet was used compared to individual cells.

5.4.4 Bilayer Model Scaffold

Finally a prototype design for incorporation of proteins was proposed. As discussed in chapter 1, Wnt proteins play an important role in the maintenance of the colonic epithelium. The intestinal epithelium maintains itself through intricate signalling generated from the mesenchyme and this process is vital in ensuring that the cells function correctly at each position in the crypt. The design of the first prototype PLGA particle scaffold allows mimicry of the three dimensional architecture but as only one cell type can be used, to be a useful model, incorporation of signalling molecules would be essential. To address this issue, the second prototype scaffold is an illustrative model which isolates a model protein (HRP) to the lower half of the colon model to demonstrate the ability of the scaffold to segregate signalling molecules.

Incorporation of the HRP into PLGA-HRP particles was successful and after sintering, the PLGA-HRP particles were positive for peroxidase activity while the PLGA particles predictably did not show any signs of enzyme activity. Owing to the small dimensions of the scaffold, it was not possible to observe a localized enzyme/substrate reaction due to the presence of PLGA-HRP particles in the bottom half of the scaffold. ToF SIMS was therefore used to check the isolating effect of the bilayer scaffold with the expected detection of the peptide backbone within the PLGA-HRP layer and its absence in the PLGA layer. Signals likely from a peptide backbone appeared in all the negative ToF SIMS spectra. However, the total ion content of CN⁻ and CNO⁻ were substantially higher on the PLGA-HRP scaffold compared to the PLGA scaffold. This was therefore evidence of a higher protein content in the lower half of the scaffold compared to the upper half of the scaffold and most likely due to the presence of the PLGA-HRP particles.

5.5 SUMMARY

The work in this chapter described the production of a novel three dimensional scaffold mimicking the architectural features of the colon. This model scaffold was formed from a mould designed using electron beam lithography. The mould served as template for the PLGA spheres which made up the scaffold. Careful consideration was given to particle size as mould filling required mainly submicron particles.

Cell seeding by conventional single cells after trypsin treatment was not sufficient to populate the scaffold and therefore a cell sheet approach was utilized. The intestinal cell sheets were produced using a new approach. They were cultured on a plasma polymer of acrylic acid and lifted off spontaneously at confluence. Comparable cell spread area was noted on the plasma polymer surface and tissue culture plastic. Further investigation of the ppAAc surface revealed changes to wettability as discharge power increased. Changes to the surface chemistry were noted and were particularly pronounced for the carboxyl functional group which showed an appreciable decrease in surface content as the discharge power increased. Cell culture studies revealed cell viability and metabolic activity decreased with increasing plasma discharge power. The ppAAc cell sheet did allow significantly more cells to be seeded onto the scaffold.

Finally a second 3D model scaffold was created by layering PLGA particles and protein containing PLGA-HRP particles. The purpose of this bilayer scaffold was to demonstrate isolation of a model protein in the lower half of the scaffold in part mimicking the native colon which has Wnt proteins located at the bottom of the crypt. There was a higher peptide backbone content on the PLGA-HRP section of the scaffold compared to the PLGA section.

Conclusively, two model three dimensional scaffolds were designed and produced. The present work shows that successful seeding on these scaffolds can occur with cell sheets and as the scaffold is particle based, protein incorporation for cell signalling purposes can be considered in future.

CHAPTER 6: THESIS SUMMARY

This chapter highlights the conclusions drawn from the work

presented and outlines prospective future work.

6.1 SUMMARY OF OBJECTIVES

The work described in this thesis was aimed at advancing *in vitro* intestinal tissue

engineering by describing and designing two scaffold based models. The

introductory chapter highlighted the current state of intestinal tissue engineering and

it is apparent that while great progress has happened *in vivo*, there are key

obstacles to adapting similar techniques to an *in vitro* approach. One of these

obstacles highlighted in Chapter 1 was the use of organoids to seed scaffolds. As

the organoids are sourced from healthy tissue, perceived difficulties may arise for

autologous sources in the case of colorectal where sections of the remaining healthy

intestine may need to be resected.

An indirect translation of the *in vivo* work was therefore necessary. Consideration

was given to the cell source and existing cell lines were proposed for use as they

are proliferative and easily sourced providing a viable alternative to primary cells.

The next consideration was to the structure of the intestinal epithelium with

emphasis on the presence of two cell types and architecture. Two models were

therefore proposed with one incorporating the two cell types and the second with

appropriate colon architecture. These models required individual scaffolds and

unique cell seeding as described next.

6.2 A TWO DIMENSIONAL INTESTINAL EPITHELIAL MODEL

The first scaffold described in this thesis in Chapter 3 and 4 was based on PLGA

which is a degradable polymer. Thin films or membranes of PLGA were

manufactured using a phase inversion technique with the films bearing matt and

shiny sides due to topographical differences as an artefact of production. Plasma

polymerisation was used to etch the surface of the thin films creating pores of a

suitable size to mimic those normally found in the basement membrane of the intestine. This led to changes to the surface topography but interestingly little change to the surface chemistry functional groups occurred in spite of the use of an oxygen plasma.

A degradation experiment was conducted on the etched and native films. Surface changes were noted with the pores on the etched membrane appearing to become smaller over time. The native films however showed the development of pores on the matt surface after 1 week of degradation and these pores did eventually appear distorted possibly due to internal collapse.

The degradation experiment also revealed that the etched films decreased substantially in molecular weight and already showed signs of heterogeneous degradation prior to being placed in degradation media. This was attributed to the oxygen plasma being sufficiently energetic to bombard and degrade the polymer film. However as the experiment progressed, the initial heterogeneous degradation was replaced by a homogeneous mode similar to that seen with the native non-plasma etched films. Both films also showed similar degradation profiles with the exception that the lower molecular weight etched PLGA reached a substantially lower final weight after 42 days compared to the untreated PLGA films after 60 days of degradation.

The surface chemistry as studied by XPS showed very little variance in both the etched and untreated films over the degradation period. This lack of variance was deemed ideal for tissue engineering as cells attaching to the surface of the material will have a chemically constant surface.

After the degradation study, the etched film was then tested for use as a two dimensional surface. The pores present on the surface due to plasma etching were shown to vary over time with longer times in plasma giving rise to larger pores. Ultimately the 90s plasma used in the degradation study produced porosity in the etched PLGA films similar to that of the *in vivo* basement membrane and was therefore used for further studies.

Cell attachment studies with a live/dead assay showed that intestinal cells on the etched films appeared to have a more extensive presence of live cells compared to the untreated films. Further studies on the morphology of the cells indicated that these cells were more extensively spread out on the etched films compared to the untreated films. Additionally there were signs of possible apoptotic cells on the uPLGA films while the cells on the ePLGA films showed normal intestinal morphology with the presence of microvilli.

To further assess cell behaviour, the metabolic activity and proliferation of the cells were tested. Again, the ePLGA scaffolds performed significantly better than the uPLGA scaffolds in both assays. It is predictable that an increase in cell number is likely to lead to an increase in metabolic activity and therefore this result was not unexpected. It was confirmation that the ePLGA films were more ideal for further work on the two dimensional epithelial model.

The 2D model was constructed by coculturing epithelial cells on one side of the membrane with intestinal myofibroblasts on the opposite side. The degradable model based on the etched scaffold was compared to a conventional PET surface. The transepithelial electrical resistance was measured and was expected to rise with time in culture as well as with cells in coculture compared to monoculture. The ePLGA film and PET surface both showed these trends however the ePLGA

scaffold did not achieve a TEER as high as the PET surface. This was attributed to the slower cell area coverage and would likely be redeemed by a higher starting cell seeding density.

Conclusively, the design and modification a degradable PLGA scaffold was described. Its degradation properties were investigated in depth showing changes to surface topography but not surface chemistry. The modification process with plasma did cause degradation to the PLGA scaffold. Finally the scaffold was utilised in a two dimensional epithelial model and was shown to support the intestinal cell growth and function.

6.3 A THREE DIMENSIONAL INTESTINAL EPITHELIAL MODEL

The 2D model took into account the presence of epithelial and myofibroblasts cells at the epithelial surface of the intestine but not the three dimensional architecture of the colon. Towards this goal, a three dimensional model was proposed utilising a 3D scaffold and one cell type (epithelial cells only). As this scaffold could not incorporate the myofibroblasts, it was proposed that the particles of the scaffold could in future be used to release protein based signalling molecules. For this scaffold a model protein would be incorporated as an illustrative effect of the possibility of isolating protein in a bilayer scaffold.

The scaffold was successfully designed using electron beam lithography to create a mould upon which PLGA particles could be seeded onto. The scaffold was constructed on the basis of histological sections of mouse intestine and was produced with accurate replications of the selected measurements. The particle size was carefully controlled to ensure good mould filling.

Seeding the scaffold with individual cells proved to be a difficulty due to the size constraints of the scaffold. Therefore the use of cell sheets was therefore proposed. For the proposed Caco-2 cells, a plasma polymer surface was used to culture the cells to confluence prior to lifting them off as a cell sheet. Changes to the plasma discharge power to create the ppAAc film led to changes in wettability and surface chemistry. Higher functional group retention in the film was noted at lower plasma powers.

Furthermore, changes to cell behaviour were noted with cells showing higher viability and metabolic activity at lower discharge powers (20-30W) compared to higher discharge powers (40W and over). These studies enabled selection of the 20W ppAAc plasma being used for further cell studies. The seeding of the scaffold with a cell sheet proved to facilitate a greater cell number on the surface of the 3D scaffold compared to individual cell seeding.

Finally a bilayer scaffold was formed with a model protein (horse radish peroxidase - HRP) incorporated into the lower section of the scaffold and plain PLGA particles in the upper section. This was done to mimic the presence of Wnt proteins in the lower crypt region of the in vivo intestine. The PLGA-HRP particles were positive for protein activity with an enzyme/substrate interaction test.

The localization of this protein was then studied with TOF-SIMS with the protein backbone serving as a potential key difference between the two sections. The ion fragment map showed presence of the protein backbone more distinctly in the PLGA-HRP section compared to the PLGA section. Further analysis of this showed that the PLGA-HRP section had a higher content of the peptide backbone compared to the plain PLGA scaffold. This was sufficient indication of the bilayer effect of the scaffold.

Conclusively, a three dimensional scaffold mimicking colon architecture was designed and seeded with cell sheets formed on ppAAc surfaces. Further to this a bilayer scaffold was formed which could localize protein to the lower half of the scaffold.

6.4 FUTURE WORK

The work done within this thesis extensively defines a scaffold that can be used as a degradable surface for a two dimensional epithelial model. The degradation properties and changes to the surface due to plasma modification have been described. Potential future work with the two dimensional model could further expand on the application of the scaffold. Seeding the scaffold with cells at a higher seeding density and maintaining cell culture for a prolonged period may aid in improving the cell coverage area and hence the TEER . The work done within this thesis defines the scaffold surface and allows selection of alternate pore sizes should this be desired.

The three dimensional model can also be expanded upon further with more work into protein incorporation and release levels. When appropriate, incorporation of intestinal stimulating growth factors can be applied with subsequent cell behaviour studied. Additionally further experiments can be performed to deduce the exact mechanism by which the cell sheets are produced.

REFERENCES

AGRAWAL, C. M., MCKINNEY, J. S., LANCTOT, D. & ATHANASIOU, K. A. (2000) Effects of fluid flow on the in vitro degradation kinetics of biodegradable scaffolds for tissue engineering. *Biomaterials*, 21, 2443-2452.

ALEXIS, F. (2005) Factors affecting the degradation and drug-release mechanism of poly(lactic acid) and poly[(lactic acid)-co-(glycolic acid)]. *Polymer International*, 54, 36-46.

ALTANKOV, G., GRINNELL, F. & GROTH, T. (1996) Studies on the biocompatibility of materials: Fibroblast reorganization of substratum-bound fibronectin on surfaces varying in wettability. *Journal of Biomedical Materials Research*, 30, 385-391.

ANDERSON, J. M. & VANITALLIE, C. M. (1995) Tight Junctions and the Molecular-Basis for Regulation of Paracellular Permeability. *American Journal of Physiology-Gastrointestinal and Liver Physiology*, 32, G467-G475.

ANSELME, K. (2000) Osteoblast adhesion on biomaterials. *Biomaterials*, 21, 667-681.

ARTURSSON, P. (1991) Cell-Cultures as Models for Drug Absorption across the Intestinal-Mucosa. *Critical Reviews in Therapeutic Drug Carrier Systems*, 8, 305-330

ATALA, A., BAUER, S. B., SOKER, S., YOO, J. J. & RETIK, A. B. (2006) Tissue-engineered autologous bladders for patients needing cystoplasty. *Lancet*, 367, 1241-1246.

BABENSEE, J. E., ANDERSON, J. M., MCINTIRE, L. V. & MIKOS, A. G. (1998) Host response to tissue engineered devices. *Advanced Drug Delivery Reviews*, 33, 111-139.

BALDA, M. S. & MATTER, K. (2003) Epithelial cell adhesion and the regulation of gene expression. *Trends in Cell Biology*, 13, 310-318.

BARKER, N., VAN ES, J. H., KUIPERS, J., KUJALA, P., VAN DEN BORN, M., COZIJNSEN, M., HAEGEBARTH, A., KORVING, J., BEGTHEL, H., PETERS, P. J. & CLEVERS, H. (2007) Identification of stem cells in small intestine and colon by marker gene Lgr5. *Nature*, 449, 1003-U1.

BARRY, J. J. A., HOWARD, D., SHAKESHEFF, K. M., HOWDLE, S. M. & ALEXANDER, M. R. (2006) Using a core-sheath distribution of surface chemistry through 3D tissue engineering scaffolds to control cell ingress. *Advanced Materials,* 18, 1406-+.

BASSON, M. D., TUROWSKI, G. & EMENAKER, *N. J. (1996)* Regulation of human (Caco-2) intestinal epithelial cell differentiation by extracellular matrix proteins. *Experimental Cell Research,* 225, 301-305.

BATLLE, E., HENDERSON, J. T., BEGHTEL, H., VAN DEN BORN, M. M. W., SANCHO, E., HUIS, G., MEELDIJK, J., ROBERTSON, J., VAN DE WETERING, M., PAWSON, T. & CLEVERS, H. (2002) beta-catenin and TCF mediate cell positioning in the intestinal epithelium by controlling the expression of EphB/EphrinB. *Cell,* 111, 251-263.

BECKERLE, M. (2002) *Cell Adhesion,* Oxford, Oxford University Press, pp436

BECKSTEAD, B. L., PAN, S., BHRANY, A. D., BRATT-LEAL, A. M., RATNER, B. D. & GIACHELLI, C. M. (2005) Esophageal epithelial cell interaction with synthetic and natural scaffolds for tissue engineering. *Biomaterials,* 26, 6217-6228.

BELTINGER, J., MCKAIG, B. C., MAKH, S., STACK, W. A., HAWKEY, C. J. & MAHIDA, Y. R. (1999) Human colonic subepithelial myofibroblasts modulate transepithelial resistance and secretory response. *American Journal of Physiology-Cell Physiology,* 277, C271-C279.

BENEDETTI, E., PANARO, F., HOLTERMAN, M. & ABCARIAN, H. (2003) Surgical approaches and intestinal transplantation. *Best Practice & Research in Clinical Gastroenterology,* 17, 1017-1040.

BENZEEV, A., FARMER, S. R. & PENMAN, S. (1980) Protein-Synthesis Requires Cell-Surface Contact While Nuclear Events Respond to Cell-Shape in Anchorage-Dependent Fibroblasts. *Cell,* 21, 365-372.

BENZEEV, A., ROBINSON, G. S., BUCHER, N. L. R. & FARMER, S. R. (1988) Cell Cell and Cell Matrix Interactions Differentially Regulate the Expression of Hepatic and Cytoskeletal Genes in Primary Cultures of Rat Hepatocytes. *Proceedings of the National Academy of Sciences of the United States of America,* 85, 2161-2165.

BERRY, C. C., CAMPBELL, G., SPADICCINO, A., ROBERTSON, M. & CURTIS, A. S. G. (2004) The influence of microscale topography on fibroblast attachment and motility. *Biomaterials,* 25, 5781-5788.

BIEDERMAN, H. (2004) *Plasma Polymer Films,* London, Imperial College Press, pp 386.

BOATENG, S. Y., LATEEF, S. S., MOSLEY, W., HARTMAN, T. J., HANLEY, L. & RUSSELL, B. (2005) RGD and YIGSR synthetic peptides facilitate cellular adhesion identical to that of laminin and fibronectin but alter the physiology of neonatal cardiac myocytes. *American Journal of Physiology-Cell Physiology,* 288, C30-C38.

CAI, Q., SHI, G., BEI, J. & WANG, S. (2003) Enzymatic degradation behavior and mechanism of Poly(lactide-co-glycolide) foams by trypsin. *Biomaterials,* 24, 629-638.

CANAVAN, H. E., CHENG, X. H., GRAHAM, D. J., RATNER, B. D. & CASTNER, D. G. (2005) Cell sheet detachment affects the extracellular matrix: A surface science study comparing thermal liftoff, enzymatic, and mechanical methods. *Journal of Biomedical Materials Research Part A,* 75A, 1-13.

CASTNER, D. G. & RATNER, B. D. (2002) Biomedical surface science: Foundations to frontiers. *Surface Science,* 500, 28-60.

CHATELIER, R. C., XIE, X. M., GENGENBACH, T. R. & GRIESSER, H. J. (1995) Effects of Plasma Modification Conditions on Surface Restructuring. *Langmuir,* 11, 2585-2591

CHAN, C. M., KO, T. M. & HIRAOKA, H. (1996) Polymer surface modification by plasmas and photons. *Surface Science Reports,* 24, 3-54.

CHEN, C. S., MRKSICH, M., HUANG, S., WHITESIDES, G. M. & INGBER, D. E. (1997) Geometric control of cell life and death. *Science,* 276, 1425-1428.

CHOI, R. S., RIEGLER, M., POTHOULAKIS, C., KIM, B. S., MOONEY, D., VACANTI, M. & VACANTI, J. P. (1998) Studies of brush border enzymes, basement membrane components, and electrophysiology of tissue-engineered neointestine. *Journal of Pediatric Surgery,* 33, 991-996.

CHOI, R. S. & VACANTI, J. P. (1997) Preliminary studies of tissue-engineered intestine using isolated epithelial organoid units on tubular synthetic biodegradable scaffolds. *Transplantation Proceedings*, 29, 848-851.

CHU, P. K., CHEN, J. Y., WANG, L. P. & HUANG, N. (2002) Plasma-surface modification of biomaterials. *Materials Science & Engineering R-Reports*, 36, 143-206.

CIMA, L. G., INGBER, D. E., VACANTI, J. P. & LANGER, R. (1991) Hepatocyte Culture on Biodegradable Polymeric Substrates. *Biotechnology and Bioengineering*, 38, 145-158CUMMINGS, J. H. & MACFARLANE, G. T. (1997) Role of intestinal bacteria in nutrient metabolism (Reprinted from Clinical Nutrition vol 16, pg 3, 1997). *Journal of Parenteral and Enteral Nutrition*, 21, 357-365.

CURTIS, A. & WILKINSON, C. (1997) Topographical control of cells. *Biomaterials*, 18, 1573-1583.

DALBY, M. J., GADEGAARD, N., TARE, R., ANDAR, A., RIEHLE, M. O., HERZYK, P., WILKINSON, C. D. W. & OREFFO, R. O. C. (2007) The control of human mesenchymal cell differentiation using nanoscale symmetry and disorder. *Nature Materials*, 6, 997-1003.

DAW, R., CANDAN, S., BECK, A. J., DEVLIN, A. J., BROOK, I. M., MACNEIL, S., DAWSON, R. A. & SHORT, R. D. (1998) Plasma copolymer surfaces of acrylic acid 1,7 octadiene: Surface characterisation and the attachment of ROS 17/2.8 osteoblast-like cells. *Biomaterials*, 19, 1717-1725.

DE-SOUZA, D. A. & GREENE, L. J. (2005) Intestinal permeability and systemic infections in critically ill patients: Effect of glutamine. *Critical Care Medicine*, 33, 1125-1135.

DELIE, F. & RUBAS, W. (1997) A human colonic cell line sharing similarities with enterocytes as a model to examine oral absorption: Advantages and limitations of the Caco-2 model. *Critical Reviews in Therapeutic Drug Carrier Systems*, 14, 221-286.

DESLOGES, N., BASORA, N., PERREAULT, N., BOUATROUSS, Y., SHEPPARD, D. & BEAULIEU, J. F. (1998) Regulated expression of the integrin alpha 9 beta 1 in the epithelium of the developing human gut and in intestinal cell

lines: Relation with cell proliferation. *Journal of Cellular Biochemistry,* 71, 536-545.

DEWEZ, J. L., SCHNEIDER, Y. J. & ROUXHET, P. G. (1996) Coupled influence of substratum hydrophilicity and surfactant on epithelial cell adhesion. *Journal of Biomedical Materials Research,* 30, 373-383.

DIENER, A., NEBE, B., LUTHEN, F., BECKER, P., BECK, U., NEUMANN, H. G. & RYCHLY, J. (2005) Control of focal adhesion dynamics by material surface characteristics. *Biomaterials,* 26, 383-392.

ENGLE, M. J., GOETZ, G. S. & ALPERS, D. H. (1998) Caco-2 cells express a combination of colonocyte and enterocyte phenotypes. *Journal of Cellular Physiology,* 174, 362-369.

EATON, S. & SIMONS, K. (1995) Apical, Basal, and Lateral Cues for Epithelial Polarization. *Cell,* 82, 5-8.

EVANS, G. S., FLINT, N., SOMERS, A. S., EYDEN, B. & POTTEN, C. S. (1992) The Development of a Method for the Preparation of Rat Intestinal Epithelial-Cell Primary Cultures. *Journal of Cell Science,* 101, 219-231.

FARMER, S. R., BENZEEV, A., BENECKE, B. J. & PENMAN, S. (1978) Altered Translatability of Messenger-Rna from Suspended Anchorage-Dependent Fibroblasts - Reversal Upon Cell Attachment to a Surface. *Cell,* 15, 627-637.

FATH, K. R. & BURGESS, D. R. (1995) Microvillus Assembly: Not actin alone. *Current Biology,* 5, 591-593.

FLEET, J. C., WANG, L. Y., VITEK, O., CRAIG, B. A. & EDENBERG, H. J. (2003) Gene expression profiling of Caco-2 BBe cells suggests a role for specific signaling pathways during intestinal differentiation. *Physiological Genomics,* 13, 57-68.

FOLKMAN, J. & MOSCONA, A. (1978) Role of Cell-Shape in Growth-Control. *Nature,* 273, 345-349.

FRANCE, R. M., SHORT, R. D., DAWSON, R. A. & MACNEIL, S. (1998) Attachment of human keratinocytes to plasma co-polymers of acrylic acid octa-

1,7-diene and allyl amine octa-1,7-diene. *Journal of Materials Chemistry,* 8, 37-42.

FRISCH, S. M. & RUOSLAHTI, E. (1997) Integrins and anoikis. *Current Opinion in Cell Biology,* 9, 701-706.

FRISCH, S. M. & SCREATON, R. A. (2001) Anoikis mechanisms. *Current Opinion in Cell Biology,* 13, 555-562.

GIANCOTTI, F. G. & RUOSLAHTI, E. (1999) Transduction - Integrin signaling. *Science,* 285, 1028-1032.

GOMPERTS B & KRAMER I (2003) *Signal Transduction,* San Diego, Elsevier Academic Press, pp 576

GRIKSCHEIT, T. C., OGILVIE, J. B., OCHOA, E. R., ALSBERG, E., MOONEY, D. & VACANTI, J. P. (2002) Tissue-engineered colon exhibits function in vivo. *Surgery,* 132, 200-204.

GROTH, T. & ALTANKOV, G. (1995) Fibroblast Spreading and Proliferation on Hydrophilic and Hydrophobic Surfaces Is Related to Tyrosine Phosphorylation in Focal Contacts. *Journal of Biomaterials Science-Polymer Edition,* 7, 297-305.

GROTH, T. & ALTANKOV, G. (1996) Studies on cell-biomaterial interaction role of tyrosine phosphorylation during fibroblast spreading on surfaces varying in wettability. *Biomaterials,* 17, 1227-1234.

HADDOW, D. B., FRANCE, R. M., SHORT, R. D., MACNEIL, S., DAWSON, R. A., LEGGETT, G. J. & COOPER, E. (1999) Comparison of proliferation and growth of human keratinocytes on plasma copolymers of acrylic acid/1,7-octadiene and self-assembled monolayers. *Journal of Biomedical Materials Research,* 47, 379-387.

HADDOW, D. B., MACNEIL, S. & SHORT, R. D. (2006) A cell therapy for chronic wounds based upon a plasma polymer delivery surface. *Plasma Processes and Polymers,* 3, 419-430.

HADDOW, D. B., STEELE, D. A., SHORT, R. D., DAWSON, R. A. & MACNEIL, S. (2003) Plasma-polymerized surfaces for culture of human keratinocytes and

transfer of cells to an in vitro wound-bed model. *Journal of Biomedical Materials Research Part A*, 64A, 80-8

HENCH, L. L. & ETHRIDGE, E. C. (1983) *Biomaterials: An Interfacial Approach* New York, Academic Press Inc, pp 385.

HIDALGO, I. J., RAUB, T. J. & BORCHARDT, R. T. (1989) Characterization of the Human-Colon Carcinoma Cell-Line (Caco-2) as a Model System for Intestinal Epithelial Permeability. *Gastroenterology*, 96, 736-749.

HOLTERMAN, M. J., HOLTERMAN, A. L., CARROL, R., JOHN, E., TESTA, G., SANKARY, H., COHEN, M., GREVIOUS, M., ABCARIAN, H. A. & BENEDETTI, E. (2003) Living-related bowel transplantation to treat short bowel syndrome in a four-year-old child: A case report. *Journal of Pediatric Surgery*, 38, 1763-1765.

HOLY, C. E., CHENG, C., DAVIES, J. E. & SHOICHET, M. S. (2001) Optimizing the sterilization of PLGA scaffolds for use in tissue engineering. *Biomaterials*, 22, 25-31.

HUBATSCH, I., RAGNARSSON, E. G. E. & ARTURSSON, P. (2007) Determination of drug permeability and prediction of drug absorption in Caco-2 monolayers. *Nature Protocols*, 2, 2111-2119.

HUNTER, A., ARCHER, C. W., WALKER, P. S. & BLUNN, G. W. (1995) Attachment and Proliferation of Osteoblasts and Fibroblasts on Biomaterials for Orthopedic Use. *Biomaterials*, 16, 287-295

HUTMACHER, D. W. (2000) Scaffolds in tissue engineering bone and cartilage. *Biomaterials*, 21, 2529-2543.

HUTMACHER, D. W. (2001) Scaffold design and fabrication technologies for engineering tissues - state of the art and future perspectives. *Journal of Biomaterials Science-Polymer Edition*, 12, 107-124.

INAGAKI, N. (1996) *Plasma Surface Modification and Plasma Polymerization*, Basel, Technomic Publishing AG, pp265.

IULIANO, D. J., SAAVEDRA, S. S. & TRUSKEY, G. A. (1993) Effect of the Conformation and Orientation of Adsorbed Fibronectin on Endothelial-Cell

Spreading and the Strength of Adhesion. *Journal of Biomedical Materials Research,* 27, 1103-1113.

JENKINS, H. R. & MILLA, P. J. (1993) The Effect of Colitis on Large-Intestinal Electrolyte Transport in Early-Childhood. *Journal of Pediatric Gastroenterology and Nutrition,* 16, 402-405

KAWAGUCHI, A. L., DUNN, J. C. Y. & FONKALSRUD, E. W. (1998) In vivo growth of transplanted genetically altered intestinal stem cells. *Journal of Pediatric Surgery,* 33, 559-563.

KERR, J. (1999) *Atlas of Functional Histology,* Elsevier Health Sciences.

KESELOWSKY, B. G., COLLARD, D. M. & GARCIA, A. J. (2003) Surface chemistry modulates fibronectin conformation and directs integrin binding and specificity to control cell adhesion. *Journal of Biomedical Materials Research Part A,* 66A, 247-259.

KIM, S. S., PENKALA, R. & ABRAHIMI, P. (2007) A perfusion bioreactor for intestinal tissue engineering. *Journal of Surgical Research,* 142, 327-331.

KJELLEN, L. & LINDAHL, U. (1991) Proteoglycans - Structures and Interactions. *Annual Review of Biochemistry,* 60, 443-475.

KUMAR, P. & CLARK, M. (2002) *Clinical Medicine,* London, Saunders, pp 1446.

L'HEUREUX, N., PAQUET, S., LABBE, R., GERMAIN, L. & AUGER, F. A. (1998) A completely biological tissue-engineered human blood vessel. *Faseb Journal,* 12, 47-56

LAMPIN, M., WAROCQUIERCLEROUT, R., LEGRIS, C., DEGRANGE, M. & SIGOTLUIZARD, M. F. (1997) Correlation between substratum roughness and wettability, cell adhesion, and cell migration. *Journal of Biomedical Materials Research,* 36, 99-108.

LANGER, R. & VACANTI, J. P. (1993) Tissue Engineering. *Science,* 260, 920-926.

LAUFFENBURGER, D. A. & HORWITZ, A. F. (1996) Cell migration: A physically integrated molecular process. *Cell,* 84, 359-369.

LAURENCIN, C. T., AMBROSIO, A. M. A., BORDEN, M. D. & COOPER, J. A. (1999) Tissue engineering: Orthopedic applications. *Annual Review of Biomedical Engineering,* 1, 19-46.

LAURENT, T. C. & FRASER, J. R. E. (1992) Hyaluronan. *Faseb Journal,* 6, 2397-2404.

LEE, J. H., JUNG, H. W., KANG, I. K. & LEE, H. B. (1994) Cell Behavior on Polymer Surfaces with Different Functional-Groups. *Biomaterials,* 15, 705-711.

LEE, M., DUNN, J. C. Y. & WU, B. M. (2005) Scaffold fabrication by indirect three-dimensional printing. *Biomaterials,* 26, 4281-4289.

LI, W. J., LAURENCIN, C. T., CATERSON, E. J., TUAN, R. S. & KO, F. K. (2002) Electrospun nanofibrous structure: A novel scaffold for tissue engineering. *Journal of Biomedical Materials Research,* 60, 613-621.

LIEBERMAN, M. A. & LICHTENBERG, A. J. (2005) *Principles of Plasma Discharges and Materials Processing,* John Wiley & Sons, pp 600.

LINEZ-BATAILLON, P., MONCHAU, F., BIGERELLE, M. & HILDEBRAND, H. F. (2002) In vitro MC3T3 osteoblast adhesion with respect to surface roughness of Ti6A14V substrates. *Biomolecular Engineering,* 19, 133-141.

LIOTTA, L. A. & KOHN, E. (2004) Anoikis - Cancer and the homeless cell. *Nature,* 430, 973-974.

LLOYD, D. A. J., ANSARI, T. I., GUNDABOLU, P., SHUREY, S., MAQUET, V., SIBBONS, P. D., BOCCACCINI, A. R. & GABE, S. M. (2006) A pilot study investigating a novel subcutaneously implanted pre-cellularised scaffold for tissue engineering of intestinal mucosa. *European Cells & Materials,* 11, 27-33.

LOUVARD, D., KEDINGER, M. & HAURI, H. P. (1992) The Differentiating Intestinal Epithelial-Cell - Establishment and Maintenance of Functions through Interactions between Cellular Structures. *Annual Review of Cell Biology,* 8, 157-195.

LU, L., GARCIA, C. A. & MIKOS, A. G. (1999) In vitro degradation of thin poly(DL-lactic-co-glycolic acid) films. *Journal of Biomedical Materials Research,* 46, 236-244.

MACCHIARINI, P., JUNGEBLUTH, P., GO, T., ASNAGHI, M. A., REES, L. E., COGAN, T. A., DODSON, A., MARTORELL, J., BELLINI, S., PARNIGOTTO, P. P., DICKINSON, S. C., HOLLANDER, A. P., MANTERO, S., CONCONI, M. T. & BIRCHALL, M. A. (2008) Clinical transplantation of a tissue-engineered airway. *The Lancet*, 372, 2023-2030.

MADARA, J. L. (1989) Loosening Tight Junctions - Lessons from the Intestine. *Journal of Clinical Investigation*, 83, 1089-1094.

MADARA, J. L. (1998) Regulation of the movement of solutes across tight junctions. *Annual Review of Physiology*, 60, 143-159.

MAHIDA, Y. R., BELTINGER, J., MAKH, S., GOKE, M., GRAY, T., PODOLSKY, D. K. & HAWKEY, C. J. (1997a) Adult human colonic subepithelial myofibroblasts express extracellular matrix proteins and cyclooxygenase-1 and -2. *American Journal of Physiology-Gastrointestinal and Liver Physiology*, 36, G1341-G1348.

MAHIDA, Y. R., GALVIN, A. M., GRAY, T., MAKH, S., MCALINDON, M. E., SEWELL, H. F. & PODOLSKY, D. K. (1997) Migration of human intestinal lamina propria lymphocytes, macrophages and eosinophils following the loss of surface epithelial cells. *Clinical and Experimental Immunology*, 109, 377-386.

MANN, B. K., TSAI, A. T., SCOTT-BURDEN, T. & WEST, J. L. (1999) Modification of surfaces with cell adhesion peptides alters extracellular matrix deposition. *Biomaterials*, 20, 2281-2286.

MARLER, J. J., UPTON, J., LANGER, R. & VACANTI, J. P. (1998) Transplantation of cells in matrices for tissue regeneration. *Advanced Drug Delivery Reviews*, 33, 165-182.

MARSHMAN, E., BOOTH, C. & POTTEN, C. S. (2002) The intestinal epithelial stem cell. *Bioessays*, 24, 91-98.

MATSUDA, N., SHIMIZU, T., YAMATO, M. & OKANO, T. (2007) Tissue engineering based on cell sheet technology. *Advanced Materials*, 19, 3089-3099.

MCKAIG, B. C., MAKH, S. S., HAWKEY, C. J., PODOLSKY, D. K. & MAHIDA, Y. R. (1999) Normal human colonic subepithelial myofibroblasts enhance epithelial migration (restitution) via TGF-beta 3. *American Journal of Physiology-Gastrointestinal and Liver Physiology*, 276, G1087-G1093.

MILLER, D. C., THAPA, A., HABERSTROH, K. M. & WEBSTER, T. J. (2004) Endothelial and vascular smooth muscle cell function on poly(lactic-co-glycolic acid) with nano-structured surface features. *Biomaterials,* 25, 53-61.

MIYAHARA, Y., NAGAYA, N., KATAOKA, M., YANAGAWA, B., TANAKA, K., HAO, H., ISHINO, K., ISHIDA, H., SHIMIZU, T., KANGAWA, K., SANO, S., OKANO, T., KITAMURA, S. & MORI, H. (2006) Monolayered mesenchymal stem cells repair scarred myocardium after myocardial infarction. *Nature Medicine,* 12, 459-465.

MIYAMOTO, S., TERAMOTO, H., COSO, O. A., GUTKIND, J. S., BURBELO, P. D., AKIYAMA, S. K. & YAMADA, K. M. (1995) Integrin Function - Molecular Hierarchies of Cytoskeletal and Signaling Molecules. *Journal of Cell Biology,* 131, 791-805.

MORRA, M., OCCHIELLO, E. & GARBASSI, F. (1990) Surface Characterization of Plasma-Treated Ptfe. *Surface and Interface Analysis,* 16, 412-417.

MOONEY, D. J., ORGAN, G., VACANTI, J. P. & LANGER, R. (1994) Design and Fabrication of Biodegradable Polymer Devices to Engineer Tubular Tissues. *Cell Transplantation,* 3, 203-210.

MOUTOS, F. T., FREED, L. E. & GUILAK, F. (2007) A biomimetic three-dimensional woven composite scaffold for functional tissue engineering of cartilage. *Nature Materials,* 6, 162-167.

NISHIDA, S., LEVI, D., KATO, T., NERY, J. R., MITTAL, N., HADJIS, N., MADARIAGA, J. & TZAKIS, A. G. (2002) Ninety-five cases of intestinal transplantation at the University of Miami. *Journal of Gastrointestinal Surgery,* 6, 233-239.

O'BRIEN, J., WILSON, I., ORTON, T. & POGNAN, F. (2000) Investigation of the Alamar Blue (resazurin) fluorescent dye for the assessment of mammalian cell cytotoxicity. *European Journal of Biochemistry,* 267, 5421-5426.

O'TOOLE, L., BECK, A. J. & SHORT, R. D. (1996) Characterization of plasma polymers of acrylic acid and propanoic acid. *Macromolecules,* 29, 5172-5177.

OKANO, T., YAMADA, N., OKUHARA, M., SAKAI, H. & SAKURAI, Y. (1995)
Mechanism of Cell Detachment from Temperature-Modulated, Hydrophilic-
Hydrophobic Polymer Surfaces. *Biomaterials,* 16, 297-303.

OKANO, T., YAMADA, N., SAKAI, H. & SAKURAI, Y. (1993) A Novel Recovery-
System for Cultured-Cells Using Plasma-Treated Polystyrene Dishes Grafted
with Poly(N-Isopropylacrylamide). *Journal of Biomedical Materials Research,* 27,
1243-1251

PEK, Y. S., WAN, A. C. A., SHEKARAN, A., ZHUO, L. & YING, J. Y. (2008) A
thixotropic nanocomposite gel for three-dimensional cell culture. *Nature
Nanotechnology,* 3, 671-675.

PERREAULT, N. & BEAULIEU, J. F. (1998) Primary cultures of fully
differentiated and pure human intestinal epithelial cells. *Experimental Cell
Research,* 245, 34-42.

PEIFER, M. (2002) Developmental biology - Colon construction. *Nature,* 420,
274-277.

PIERSCHBACHER, M. D. & RUOSLAHTI, E. (1984) Cell Attachment Activity of
Fibronectin Can Be Duplicated by Small Synthetic Fragments of the Molecule.
Nature, 309, 30-33.

PRATOOMSOOT, C., TANIOKA, H., HORI, K., KAWASAKI, S., KINOSHITA, S.,
TIGHE, P. J., DUA, H., SHAKESHEFF, K. M. & ROSE, F. (2008) A
thermoreversible hydrogel as a biosynthetic bandage for corneal *wound repair.*
Biomaterials, 29, 272-281.

RAFATI, H., COOMBES, A. G. A., ADLER, J., HOLLAND, J. & DAVIS, S. S.
(1997) Protein-loaded poly(DL-lactide-co-glycolide) microparticles for oral
administration: Formulation, structural and release characteristics. *Journal of
Controlled Release,* 43, 89-102.

RE, F., ZANETTI, A., SIRONI, M., POLENTARUTTI, N., LANFRANCONE, L.,
DEJANA, E. & COLOTTA, F. (1994) Inhibition of Anchorage-Dependent Cell
Spreading Triggers Apoptosis in Cultured Human Endothelial-Cells. *Journal of
Cell Biology,* 127, 537-546.

REYES, J., BUENO, J., KOCOSHIS, S., GREEN, M., ABU-ELMAGD, K., FURUKAWA, H., BARKSDALE, E. M., STROM, S., FUNG, J. J., TODO, S., IRISH, W. & STARZL, T. E. (1998) Current status of intestinal transplantation in children. *Journal of Pediatric Surgery*, 33, 243-253.

ROCHA, F. G. & WHANG, E. E. (2004) Intestinal tissue engineering: From regenerative medicine to model systems. *Journal of Surgical Research*, 120, 320-325.

RUARDY, T. G., SCHAKENRAAD, J. M., VANDERMEI, H. C. & BUSSCHER, H. J. (1995) Adhesion and Spreading of Human Skin Fibroblasts on Physicochemically Characterized Gradient Surfaces. *Journal of Biomedical Materials Research*, 29, 1415-1423.

RUBAS, W., CROMWELL, M. E. M., SHAHROKH, Z., VILLAGRAN, J., NGUYEN, T. N., WELLTON, M., NGUYEN, T. H. & MRSNY, R. J. (1996) Flux measurements across Caco-2 monolayers may predict transport in human large intestinal tissue. *Journal of Pharmaceutical Sciences*, 85, 165-169.

RUOSLAHTI, E. (1996) RGD and other recognition sequences for integrins. *Annual Review of Cell and Developmental Biology*, 12, 697-715.

SANCHO, E., BATLLE, E. & CLEVERS, H. (2004) Signaling pathways in intestinal development and cancer. *Annual Review of Cell and Developmental Biology*, 20, 695-723.

SCHLAEPFER, D. D., HANKS, S. K., HUNTER, T. & VANDERGEER, P. (1994) Integrin-Mediated Signal-Transduction Linked to Ras Pathway by Grb2 Binding to Focal Adhesion Kinase. *Nature*, 372, 786-791.

SHAO, J. Y., SHENG, G. G., MIFFLIN, R. C., POWELL, D. W. & SHENG, H. M. (2006) Roles of myofibroblasts in prostaglandin E-2-stimulated intestinal epithelial proliferation and angiogenesis. *Cancer Research*, 66, 846-855

SIGAL, G. B., MRKSICH, M. & WHITESIDES, G. M. (1998) Effect of surface wettability on the adsorption of proteins and detergents. *Journal of the American Chemical Society*, 120, 3464-3473.

SIMONASSMANN, P., KEDINGER, M., DEARCANGELIS, A., ROUSSEAU, V. & SIMO, P. (1995) Extracellular-Matrix Components in Intestinal Development. Experientia, 51, 883-900.

SINGHVI, R., STEPHANOPOULOS, G. & WANG, D. I. C. (1994) Effects of Substratum Morphology on Cell Physiology - Review. Biotechnology and Bioengineering, 43, 764-771.

SIOW, K. S., BRITCHER, L., KUMAR, S. & GRIESSER, H. J. (2006) Plasma methods for the generation of chemically reactive surfaces for biomolecule immobilization and cell colonization - A review. Plasma Processes and Polymers, 3, 392-418.

VACHON, P. H., DURAND, J. & BEAULIEU, J. F. (1993) Basement-Membrane Formation and Re-Distribution of the Beta-1 Integrins in a Human Intestinal Coculture System. Anatomical Record, 235, 567-576.

VASILEV, K., BRITCHER, L., CASANAL, A. & GRIESSER, H. J. (2008) Solvent-induced porosity in ultrathin amine plasma polymer coatings. Journal of Physical Chemistry B, 112, 10915-10921.

VIHOLA, H., LAUKKANEN, A., VALTOLA, L., TENHU, H. & HIRVONEN, J. (2005) Cytotoxicity of thermosensitive polymers poly(N-isopropylacrylamide), poly(N-vinylcaprolactam) and amphiphilically modified poly(N-vinylcaprolactam). Biomaterials, 26, 3055-3064.

WAKE, M. C., GUPTA, P. K. & MIKOS, A. G. (1996) Fabrication of pliable biodegradable polymer foams to engineer soft tissues. Cell Transplantation, 5, 465-473.

YANG, J., YAMATO, M., KOHNO, C., NISHIMOTO, A., SEKINE, H., FUKAI, F. & OKANO, T. (2005) Cell sheet engineering: Recreating tissues without biodegradable scaffolds. Biomaterials, 26, 6415-6422.

ZELZER, M. (2009) Plasma Polymer Gradients. School of Pharmacy. Nottingham, The University of Nottingham.

SOLMI, R., LAURIOLA, M., FRANCESCONI, M., MARTINI, D., VOLTATTORNI, M., CECCARELLI, C., UGOLINI, G., ROSATI, G., ZANOTTI, S., MONTRONI, I., MATTEI, G., TAFFURELLI, M., SANTINI, D., PEZZETTI, F., RUGGERI, A., CASTELLANI, G., GUIDOTTI, L., COPPOLA, D. & STRIPPOLI, P. (2008) Displayed correlation between gene expression profiles and submicroscopic alterations in response to cetuximab, gefitinib and EGF in human colon cancer cell lines. *Bmc Cancer*, 8.

STEELE, J. G., JOHNSON, G., MCLEAN, K. M., BEUMER, G. J. & GRIESSER, H. J. (2000) Effect of porosity and surface *hydrophilicity* on migration of epithelial tissue over synthetic polymer. *Journal of Biomedical Materials Research*, 50, 475-482.

STRATER, J., WEDDING, U., BARTH, T. F. E., KORETZ, K., ELSING, C. & MOLLER, P. (1996) Rapid onset of apoptosis in vitro follows disruption of beta(1)-integrin/matrix interactions in human colonic crypt cells. *Gastroenterology*, 110, 1776-1784.

STUTZMANN, J., BELLISSENT-WAYDELICH, A., FONTAO, L., LAUNAY, J. F. & SIMON-ASSMANN, P. (2000) Adhesion complexes implicated in intestinal epithelial cell-matrix interactions. *Microscopy Research and Technique*, 51, 179-190.

TAMADA, Y. & IKADA, Y. (1993) Effect of Preadsorbed Proteins on Cell-Adhesion to Polymer Surfaces. *Journal of Colloid and Interface Science*, 155, 334-339.

TIMPL, R. & BROWN, J. C. (1996) Supramolecular assembly of basement membranes. *Bioessays*, 18, 123-132.

VACANTI, J. P., MORSE, M. A., SALTZMAN, W. M., DOMB, A. J., PEREZATAYDE, A. & LANGER, R. (1988) Selective Cell Transplantation Using Bioabsorbable Artificial Polymers as Matrices. *Journal of Pediatric Surgery*, 23, 3-9.

VALENTICH, J. D., POPOV, V., SAADA, J. I. & POWELL, D. W. (1997) Phenotypic characterization of an intestinal subepithelial myofibroblast cell line. *American Journal of Physiology-Cell Physiology*, 272, C1513-C1524.

VAN DE WETERING, M., SANCHO, E., VERWEIJ, C., DE LAU, W., OVING, I., HURLSTONE, A., VAN DER HORN, K., BATLLE, E., COUDREUSE, D., HARAMIS, A. P., TION-PON-FONG, M., MOERER, P., VAN DEN BORN, M., SOETE, G., PALS, S., EILERS, M., MEDEMA, R. & CLEVERS, H. (2002) The beta-catenin/TCF-4 complex imposes a crypt progenitor phenotype on colorectal cancer cells. *Cell,* 111, 241-250.

WAKE, M. C., GUPTA, P. K. & MIKOS, A. G. (1996) Fabrication of pliable biodegradable polymer foams to engineer soft tissues. *Cell Transplantation,* 5, 465-473.

WANG, Y. Q., QU, X., LU, J., ZHU, C. F., WAN, L. J., YANG, J. L., BEI, J. Z. & WANG, S. G. (2004) Characterization of surface property of poly(lactide-co-glycolide) after oxygen plasma treatment. *Biomaterials,* 25, 4777-4783.

WASHBURN, N. R., YAMADA, K. M., SIMON, C. G., KENNEDY, S. B. & AMIS, E. J. (2004) High-throughput investigation of osteoblast response to polymer crystallinity: influence of nanometer-scale roughness on proliferation. *Biomaterials,* 25, 1215-1224.

WATERHOUSE, C. C. M., JOSEPH, R. R. & STADNYK, A. W. (2001) Endogenous IL-1 and type IIIL-1 receptor expression modulate anoikis in intestinal epithelial cells. *Experimental Cell Research,* 269, 109-116.

WEBB, K., HLADY, V. & TRESCO, P. A. (1998) Relative importance of surface wettability and charged functional groups on NIH 3T3 fibroblast attachment, spreading, and cytoskeletal organization. *Journal of Biomedical Materials Research,* 41, 422-430.

WEBB, K., HLADY, V. & TRESCO, P. A. (2000) Relationships among cell attachment, spreading, cytoskeletal organization, and migration rate for anchorage-dependent cells on model surfaces. *Journal of Biomedical Materials Research,* 49, 362-368.

WILLIS, N. D., PRZYBORSKI, S. A., HUTCHISON, C. J. & WILSON, R. G. (2008) Colonic and colorectal cancer stem cells: progress in the search for putative biomarkers. *Journal of Anatomy,* 213, 59-65.

WILSON, S. E., HE, Y. G., WENG, J. A., ZIESKE, J. D., JESTER, J. V. & SCHULTZ, G. S. (1994) Effect of Epidermal Growth-Factor, Hepatocyte Growth-

Factor, and Keratinocyte Growth-Factor, on Proliferation, Motility and Differentiation of Human Corneal Epithelial-Cells. *Experimental Eye Research,* 59, 665-678

YAMAKAWA, N., TANAKA, T., SHIGETA, M., HAMANO, M. & USUI, M. (2003) Surface roughness of intraocular lenses and inflammatory cell adhesion to lens surfaces. *Journal of Cataract and Refractive Surgery,* 29, 367-370.

YEE, S. Y. (1997) In vitro permeability across Caco-2 cells (colonic) can predict in vivo (small intestinal) absorption in man - Fact or myth. *Pharmaceutical Research,* 14, 763-766.

ZELZER, M. (2009) Plasma Polymer Gradients. *School of Pharmacy.* Nottingham, The University of Nottingham.

ZELZER, M., MAJANI, R., BRADLEY, J. W., ROSE, F., DAVIES, M. C. & ALEXANDER, M. R. (2008) Investigation of cell-surface interactions using chemical gradients formed from plasma polymers. *Biomaterials,* 29, 172-184.

ZHANG, X. H., CROMWELL, J. W., KUNJUMMEN, D., YEE, D. & GARCIA-AGUILAR, J. (2003) The alpha 2 and alpha 3 integrins are required for morphologic differentiation of an intestinal epithelial cell line. *Surgery,* 133, 429-437.

APPENDICES

APPENDIX 1

MATERIAL	SUPPLIER/ CATOLOGUE NUMBER
CellCrown 24	Scaffdex, Finland C000001N
Poly (ethylene tetraphthalate) filters	BD Biosciences, USA 353096
Poly (DL-lactide—co-glycolide) (75:25 - 140000g/mol and 85:15 - 35000g/mol)	Medisorb, Purasorb, USA
Oxygen	BOC gases
Tetrahydrofuran (THF) HPLC grade	Fisher Chemicals T425SK1
1,4 diazobicyclo-2-2-2-octane (DABCO)	Sigma-Aldrich D2522
alamarBlue solution	Serotech BUF012B
N-Methyl-2-pyrrolidinone	Sigma-Aldrich 242799
Dimethylsulphoxide (DMSO)	Sigma-Aldrich D8418
Dulbecco's modified eagle medium (DMEM)	Sigma-Aldrich D6429
Ethylenediaminetetraacetic acid (EDTA)	Sigma-Aldrich ED2SS
Foetal calf serum (FCS)	Sigma-Aldrich F7524
Hanks balanced salt solution(HBSS) (without phenol red)	Sigma-Aldrich H1387
Non essential amino acid solution (NEAA)	Sigma-Aldrich M7145
Antibiotic/Antimycotic solution	Invitrogen 15240062
Industrial methylated spirits (IMS)	Fisher Chemicals M/4450/17

171

MATERIAL	**SUPPLIER/ CATOLOGUE NUMBER**
Ethanol (99% HPLC grade)	Fisher Chemicals E/0600/17
Osmium tetroxide solution (2%w/v)	TAAB O006
Glutaraldehyde (50%)	TAAB G006
Phosphate buffered saline (PBS)	Oxoid Products BR0014
Hexamethyldisilazane	Sigma-Aldrich H4875
Sodium phosphate dibasic	Sigma-Aldrich S0876
Glycerol	Sigma-Aldrich G7893
Paraformaldehyde	Sigma-Aldrich P6148
Sodium phosphate monobasic	Sigma-Aldrich S8282
Paraffin wax	Sakura, Netherlands 4653Tissue Tek II
Trypsin solution (25g/L in 0.9% NaCl)	Sigma-Aldrich T4549
Hoechst 33258	Sigma- Aldrich B1155
Sodium chloride	Sigma Aldrich S7653
Trizma base	Sigma-Aldrich T6066
CellTrackerTM Green CMFDA (5-chloromethylfluorescein diacetate).	Invitrogen C2925
Live/Dead viability assay	Invitrogen L3224
Acrylic Acid	Sigma-Aldrich 01730

MATERIAL	SUPPLIER/ CATOLOGUE NUMBER
Acetone	Fisher Chemicals A0560
Human adeno-carcinoma cells - Caco-2	ECACC
Human colon fibroblasts – CCD-18Co	ATCC
Monoclonal mouse anti human smooth Muscle Actin	DAKO M0851
Monoclonal mouse anti human E-Cadherin	DAKO M3612
Fluorescein isothiocyanate –FITC anti mouse conjugate	Sigma-Aldrich F5262
ProLong Gold antifade reagent with 4',6-diamidino-2-phenylindole (DAPI).	Invitrogen P36931
Xylene	Fisher Chemicals X0250/15
Gill's haematoxylin	Nustain AS050
Scotts tap water	Nustain AE077
Eosin	Nustain AD046
Distyrene, plasticizer and xylene (DPX)	Nustain AE020
HEPES	Sigma Aldrich H3375
Sucrose	Sigma Aldrich S9378
Magnesium chloride	Sigma Aldrich M8266
Triton X-100	Sigma Aldrich X100
Bovine Serum Albumin (BSA)	Sigma Aldrich A7030

MATERIAL	SUPPLIER/ CATOLOGUE NUMBER
Horse Radish Peroxidase	Sigma Aldrich
3,3',5,5'-Tetramethylbenzidine (TMB) Liquid Substrate for HRP	Sigma Aldrich T0565
Tween- 20	Sigma Aldrich
Poly(vinyl alcohol) PVA	Sigma Aldrich
Polyolefin Plastomer pellets	Affinity, Dow Chemical Company

APPENDIX 2

Solutions

1. Phosphate buffered Saline (PBS)

PBS   1 tablet

Distilled H_2O (dH_2O)   100 mL

2. CCD-18Co medium

FCS   50 mL

DMEM   500 mL

Antibiotic antimycotic solution   5 mL

All supplements were filtered through into the DMEM using a 0.2um filter.

3. CACO-2 medium

FCS   50 mL

DMEM   500 mL

Antibiotic antimycotic solution   5 mL

NEAA   5 mL

4. Trypsin EDTA in PBS

EDTA solution (0.02%w/v in dH_2O)   10 mL

Trypsin solution (25g/L in 0.9% NaCl)   100 mL

PBS   To 1L

5. Freezing Medium

DMSO	2 mL
FCS	18 mL

6. alamarBlue Working Solution

PBS	9mL
alamarBlue solution	1 mL

7. Cell Tracker Solution

DMSO	10 µL
Medium without FCS	10 mL
CellTracker lyophilized product	1 vial

8. Hoechst DNA Assay Solutions

Hoechst Buffer

100 mM Tris base	12.11g
10 mM EDTA	3.72g
2.0 M NaCl	116.89g

The salts above were added to 800mL of water in a volumetric flask and the pH of the solution was adjusted to 7.4 with concentrated hydrochloric acid. The volume was then made up to 1L and filtered through a 0.45-µm filter.

Stock solution of Hoechst 33258

Hoechst 33258 (bisbenzimide)	1mg
Water	1mL

Working solution of Hoechst 33258

Hoechst Buffer	10mL
Water	90mL
Stock solution of Hoechst 33258	100µl

9. Immunostaining Solutions

4% Paraformaldehyde (PFA)

Paraformaldehyde	4g
PBS	100mL

The 4% paraformaldehyde solution was made by heating the mixture above to 60°C until complete dissolution. Once the solution was clear, it was allowed to cool and pH adjusted to 7.2 before use.

1% Bovine Serum Albumin (BSA)

Bovine Serum Albumin	1g
PBS	100mL

The 1% BSA solution was made by stirring the BSA into the PBS for 1 hour. The solution was prepared freshly for each experiment.

Permeabilising Solution

HEPES	0.48g
Sucrose	10.27g
Sodium Chloride	0.29g
Magnesium chloride	0.06g
Triton X-100	0.5mL
Distilled Water	100mL

All the components listed above were dissolved at room temperature to prepare the

permeabilising solution